Development of 3-D Conceptual Hydrogeological Model for Lake Naivasha area

Based on the Integration of Geology, Hydrochemistry, Isotopic Analysis, and Boundary Conditions

Isah Kiti Nabide

April, 2002

INTERNATIONAL INSTITUTE FOR GEOINFORMATION SCIENCES AND EARTH OBSERVATION

Development of 3-D Conceptual Hydrogeological Model for Lake Naivasha area

Based on the Integration of Geology, Hydrochemistry, Isotopic Analysis and Boundary Conditions

By

Isah Kiti NABIDE

Thesis submitted to the International Institute for Aerospace Survey and Earth Sciences in Partial Fulfillment of the requirements for the degree of Master of Science in Water Resources and Environmental Management, Groundwater Specialization.

Degree Assessment Board

Prof.	**A. M. J. Meijerink**	**Chairman**
Dr.	**Drs. D. Kovacs**	**External Examiner**
Dr.	**R. Betch**	**Supervisor**
Dr.	**M. W. Lubczinsky**	**Member**

INTERNATIONAL INSTITUTE FOR GEOINFORMATION SCIENCES AND EARTH OBSERVATIONS
ENSCHEDE, THE NETHERLANDS

April, 2002

Disclaimer

Dedication

To all those who have contributed to My Education
To the Departed Souls of Loved Ones
And to those whom this will motivate to Aspire Higher

Acknowledgement

This study would not have been realized without the help of a number of selfless individuals and organizations.

I thank the Dutch government through NFP who shouldered the financial burden of my study.

I am grateful to the administration of the Directorate of Water Development for the support they offered during the pursuit of this study. I appreciate the assistance and continual guidance I have received from my Boss, Eng. Moses Gava.

I feel indebted to my supervisor who tirelessly guided me during the fieldwork, data analyses and the write-up of the thesis. I acknowledge the support and guidance from the entire Administration and staff of WRES. Prof. A. M. Meijerink, Dr. Arno Lieshout, Dr. Lubczynsky, Prof. Chris Mannaerts, Dr. Ambro Gieske, Ir. Remco Dost, Dr. Parodi, Dr. V. Zoltan. Wim Tammerman, Dr. Donker, Mr. M. Sparviolla, Ms. B. Casentini. I say thank you very much. I also express my gratitudes to Mr. Polman and Mr. Duim for their selfless services. I appreciate the assistance received from brother Mohammed Said during the entire process of writing of this thesis. Please know that your assistance was a lamp in the tunnel.

I appreciate the contribution of the Management and Staff of Three Point Farm, Delamera Estates, Kijabe Farms and other individuals who provided me with the valuable data and information to accomplish my thesis. Mr. Chinue and Mr. Mark Lidonde, you were wonderfully useful in the field.

During my study, there were moments when I was really down. Its usually short messages that kept me going. Maama Kyazze, W. Kiiza, Mohammed Badaza, J A Kitakarugire, Patrick Lutaya, Paul Kibwika, JS Kintu, Charles, Eng. Omoit, Wakooli, C. Tindimugaya, Anthony, Olet, Ali Chemisto, Walakira, Hassan, Mowor, Paul, Leah, Ester, Lydia, Aminah…………I am afraid the list might be too long for me to remember right away. Please know that mentioned or not, I benefited a lot from the words of encouragement that you offered.

WREM MSc. 2000 was such a wonderful group: Lily, Fred, Victor, Lysste, Stans, Harsha, Carolina, Dawit, Diana, Rupa, Suthakar, Tsefay and Sharamo, I thank you all for the confidence you had in me having elected me as your representative on the students' board. Your cooperation was wonderful. Please know that having served you was more of an honor than a responsibility. I will always have fond memories of the same. To the members of the WREM 2000 Students' family who left earlier, brother: Akorio Ibrahim, Stanslaus Tombe-The Big Brother, Charles Shindaile and the others, it was really fun having you around.

To my family away from home, the entire Ugandese community in Enschede, you gave me the motivation and company that I badly needed. My *kid brother* Yazidhi, thank you very much for the wake up calls.

Aunt Edna Sserwambala, Uncle Lumala and Uncle Ibanda, please know that I am glad you are always there for me.

AND above all, Praise be to the Merciful God who enabled me to accomplish this hectic course in sound health. THANK YOU.

Abstract

The aim of the study was to develop a 3-D conceptual Hydrogeological model on the basis of integration of geology, hydrochemistry, isotopic analysis, and boundary condition.

The area of study is around lake Naivasha in Kenya Rift Valley where recent explosion in the economic activities has increased the demand for water and hence the necessity to understand the resource further for its better management.

The general groundwater flow pattern in the study area is laterally towards the lake from the eastern and western escarpments and axially northwards and southwards away from the Lake.

The gradient of change in water chemistry as water flows in the study is great and cannot be accounted for solely by ordinary dissolution of ions from the rocks along its flow path. There has also been a temporal deterioration of water quality especially in the Northeastern part of the area but it is neither related to yield nor to depth.

Lacustrine sediments are thickest in the northeastern portion of the study area where their thickness is about 120m. Kinangop and Mau plateaus tilt away from the valley bottom. Consequently, rainfall on the plateaus plays minimal role in the regional groundwater recharge with respect to the Valley bottom.

The model is still course and needs refinement as more information becomes available. It, however, give a general pattern of distribution of hydrogeological properties of the geological formation.

Contents

Tables

Figures

Chapter 1 Introduction

1.1 Background of the Study and Problem Statement

Recently, the area around lake Naivasha has become industrially significant as a consequence of development of flower production, horticultural production, tourist industries and other human activities around the shores of the lake. Flower and horticulture production employs more than 20,000 people directly and many others indirectly, while the number of tourists visiting Hell's Gate National Park which is near Lake Naivasha increased by more than 600% between 1985 and 1992 (LNROA, 1995). The population of the Naivasha area is about 250,000 people (LNROA, 1995). As much as the populations of most countries are growing, it is likely the total use of water will increase, even with conservation measures (Fetter, 1994). Similarly, the population explosion caused by increased activities around the lake has definitely translated into a correspondingly high increase in the demand for portable water for agricultural, recreational purposes, and domestic supply to the ever-increasing population in the area, an occurrence that necessitates better management of the water resources if it is to be used sustainably. It is a common practice that wherever pressure on water resources mounts, the groundwater resources bear some or all of it. For sustainable use of any type of water resource, there is a need for its proper management.

How best water resources can be managed depends primarily on how much the resource is understood. In the quest for improved understanding of groundwater resources in the area, a number of studies have been done. Owor (2000) used a numerical simulation model to study the long-term interaction of groundwater with the Lake to determine the long-term water budget for the lake and estimate water abstraction from both the surface and groundwater resources. This was an extension of the earlier work of Mmbui (1999) who used a spreadsheet to numerically model the long-term water balance for lake. Kibona (2000) sought to understand the variation of groundwater levels in space and time by setting up both transient and steady state numerical models of the area. Morgan (1998) examined the groundwater chemistry and quality as the basis to ascertain the relationship between the groundwater chemistry and rock weathering, classify the groundwater type and to understand effect of groundwater flow and evapotranspiration on groundwater chemistry as well as to gain an insight into the impact of groundwater chemistry on the environment. While Salah (1991), estimated the annual economic return per hectare of different agricultural activities to come up with the most economically viable activity, Hoaccho (1998) estimated the irrigated area under different crops types and tried to ascertain their respective irrigational water requirements with the aid of Cropwat Software. Sayed (2001), integrated the work by these two to derive the cost of production on the basis of water requirements of different crop types

The movement and chemistry of groundwater is heavily dependant upon geology, (Fetter, 1994) However, up-to-date, the understanding of the flow system of Naivasha area has been approached either solely or principally using piezometric levels as the determinant for the flow pattern of groundwater. In few studies when geology has been considered, it has been handled two dimensionally, disregarding vertical flow and multiple aquifers have not been addressed sufficiently (Kibona, 2000, Mbui, 1999). This study intends to integrate the information on the groundwater flow, hydrochemistry, and boundary as a basis to construct a conceptual hydrogeological model- taking geology as the prime factor. Emphasis will be focussed on constructing a 3-D model of the distribution of the hydraulic properties. There is no single tool that is strong enough to explain the complex hydrogeology of this area in isolation. As such, other than geology, the study uses other aspects like hydrochemistry and Isotopes to understand the hydrogeology of the area. The flow pattern as studied using hydrochemistry, piezometric levels and stable isotopes is reviewed. The insight of the influence of geology on hydrogeology is improved by studying the geological map of the area and information gathered from the drillers' logs of the numerous wells drilled in the area. This is reinforced with observations made at different outcrops in the field. This information is then used as input into the 3-D hydrogeological Model. The study is expected to result improved understanding of the hydrogeology of the area. How the geology of the area dictates the boundary condition, and how this influences the hydrogeology of the area.

1.2 Objective

- Analyze the influence of Geology on the hydrogeology of the area
- Demonstrate the use of Hydrochemistry in explaining the flow pattern and/ or direction
- Demonstrate the use of stable isotopes in explaining the flow pattern and/or direction.
- Define the boundary conditions of Lake Naivasha area and analyze their influence on the groundwater flow
- Develop 3-D conceptual model of the groundwater flow system of the area

Chapter 2 Methodology

2.1 Introduction

The methodology followed in this study was based on the objectives of the study as stated in section 1.2. The aspects of the study area deemed necessary to attain the set objective are: Geology, Hydrogeology, Ionic Chemistry, and Isotopic analysis. In this chapter, the layout of the key stages/phases and the activities under them are presented. Besides, the major source of information and materials used are stated. Also presented in this chapter is the lay out of the Thesis and the diagrammatic representation of the Methodology.

Due to the diversity of the aspects involved in the study, procedures followed for the different individual aspects are explained in separate sections of this chapter. Other than the activities undertaken, the theoretic basis of the different aspects are presented in their respective sections.

2.2 Outlay of Major Activities in the Studies

- ❖ Pre-Fieldwork Activities
- o Literature review of the work done already in the area
- o Data mining for and Processing of already available Data
- o Studying of Drilling Logs
- o Acquisition of Equipment for field work
- ❖ Field work
- o Collection of Water sample for water chemical analysis
- o Collection for Water samples for Isotopic Analysis
- o Colorations of geological outcrops with geological map
- o Collection of geological samples, analysis of well cuttings
- o Collection of Drillers Logs for recently drilled boreholes
- ❖ Post Fieldwork
- o Data Processing and Analysis
- o Analysis and interpretation of water Chemistry
- o Analysis and interpretation of Isotopic Ratios
- o Set up a 3D model of the aquifer system of the place
- o Report Writing

2.3 Materials Used and Key Sources of Information

- Drillers logs for boreholes in Nakuru District
- Groundwater analysis of boreholes and wells by the University of Leicester 1996
- Groundwater analysis of boreholes and wells from Ministry of Land Reclamation, Regional and Water Development-Water Resources Division, Nairobi 1943-2001
- Isotope data analysis by Oppong-Boateng, 2000
- Isotope data analysis of Lake Naivasha, geothermal well and Boreholes by the British Geological Survey
- Isotope data analysis by Ojambo (1992, 1996)
- Land sat image: Bands 1-7 taken June 1996
- Geological Map 1:10000
- Topographical Maps

2.4 Geology

The geological information was extracted from the studies of previous workers who have mapped the area both from a regional point of view (Thompson and Dodson, 1962, Clark et al, 1990) and from detailed mapping (Naylor, 1927:Odongo, 1986). Besides, information has been gathered from the Geology Map of the study Area (Clark et al, 1988) and drillers' logs for 60 wells. During the fieldwork, geological observations were made at points. Their locations were taken using GPS handset and they were plotted on the map of the study area. They observations were then compared with the published outcrops.

Fault lines in the study area were digitized from official Geological Map. They were than edited to include more faults using on screen digitization of LandSat images (Band 1-7) taken in June 1996.

To understand 3-D geology of the area, the geology of the area was drawn on topographic profiles of the area. ILWIS GIS software was used to analyze the topographic profile of along 11 sections in the study area. Map calculations were used to constitute scripts for these operations. Details of the script of operations are shown in Annex 1

2.5 Hydrochemistry

2.5.1 Introduction

The purpose of this chapter is to use hydro chemistry as a tool to explain the origin and flow direction of ground water in the area of study. Water chemistry will improve the insight of the relative age and direction of flow of the water in the area. The ions used in the study are

Mg^{2+}, Na^{+}, K^{+}, Ca^{2+}, Cl^{-} and F^{-} . Please refer to Appendix 5.1 for the results of the chemical analysis of the samples.

Besides, the temporal trend of the change of the water chemistry in the area is also sought after. This will aide in the detection of any deterioration or improvement in the water quality in the area of study with time.

2.5.2 Theoretic Background

As groundwater moves along the flow paths in the saturated zones, an increase in the total dissolved solids occurs. Generally, shallow groundwater in the recharge areas is lower in dissolved solids than the water deeper in the same system and lower in the dissolved solids than the water in discharge areas.

On basis of over 10000 chemical analysis of well samples from Australia, Chebotarev (1955) concluded that groundwater tend to evolve chemically towards the composition of seawater. He also observed that this evolution is accompanied with changes in dominant anions.

Travel Along Flow Path →

$HCO_3^- \rightarrow HCO_3^- + SO_4^{2-} \rightarrow SO_4^{2-} + HCO_3^- \rightarrow SO_4^{2-} + Cl^- \rightarrow Cl- + SO_4^{2-} \rightarrow Cl^-$

Increasing Age →

These changes occur as water moves from shallow zones of active flushing through intermediate zones into zones where the flow is sluggish and water is old.

For sedimentary environment, the above anionic sequence can be described in terms of two variables: mineral availability and mineral solubility. The HCO_3^- content in the groundwater is normally delivered from soil zone CO_2 and from dissolution of calcite and dolomite that occurs in most sedimentary basins. Besides, calcites and dolomites dissolve rapidly when in contact with CO_2 -charged groundwater making HCO_3^- almost invariably the dominant anion in recharge areas.

However, once this water meets a formation with SO_4^{2-} such as gypsum ($CaSO_4.2H_2O$) and/or anhydrite ($CaSO_4$), the HCO_3^- is displaced as a result of which SO_4^{2-} becomes the dominant anion. In deep groundwater flow systems in sedimentary basins and in some shallow systems, groundwater may evolve past the stage where SO_4^{2-} is the dominant anion to a Cl^- rich brine which is the case if water comes into contact with a very soluble chloride mineral such as halite or sylvite which can occur as salt strata.

Crystalline rocks of igneous origin contain appreciable amounts of quartz and aluminosilicates minerals such as feldspars and micas that are formed at temperatures and pressures far greater than those occurring at or near the earth's surface. These minerals are thermodynamically unstable on earth's surface, in the soil zone and in the groundwater zone to depths of many hundreds of meters as a result of which, they tend to dissolve when in contact with water. This process causes water to acquire dissolved constituents and the rock to become mineralogically altered. (Freeze and Cherry, 1979).

When CO_2 charged waters low in dissolved solids encounters silicates high in cations, aluminium and silica, cations and silica is leached out leaving an aluminosilicate residue of a clay mineral such as kaolinite, illite or montmorillonite. The cations released to the water are normally Na^+, K^+, Mg^{2+} and Ca^{2+}. The concentration of the cations increases as the water moves away from the recharge area. Consequently, the concentrations can generally be spatially related to the distance and direction of flow.

In the study area, volcanic mineralogy is reflected in the groundwater. The rhyolitic composition indicated reflects the composition of the comendites and pantellerites which form the pumice and trachytes in the area of study (Morgan, 1998)

2.5.3 Fieldwork

33 samples were collected from different locations in the study area. As the southern part of the lake had samples taken from most of the wells found there, the sampling was concentrated in the northern, western, and eastern sides of the lake. The location of the wells from which samples were taken are as shown in the map in Figure 2.5. Their locations were chosen in such a manner that in the different direction, the locations were approximately parallel to the postulated flow direction: towards the lake.

The waters had their EC measured in the field before being shipped to ITC where the rest of the tests were conducted. The locations of the well were the samples were ascertained with aide of Garmin GPS handset.

Other than the collection of water sample for chemical analysis, hydro chemical data was gathered from different boreholes records of Delamera farm and Three Point Farms. These will aide in ascertaining the trend of change of water chemistry with time.

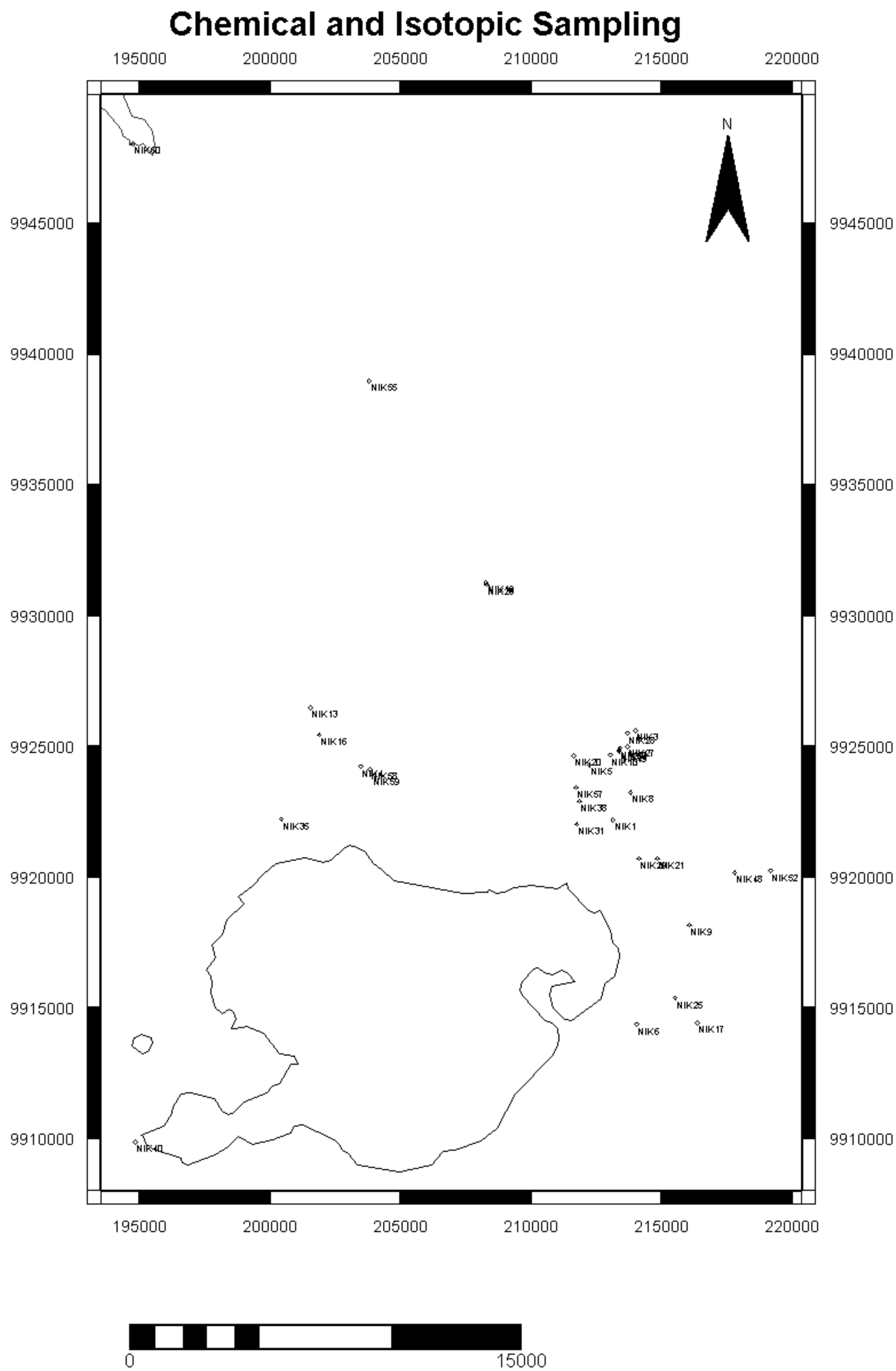

Figure 2.5: Location of Sampled Wells. Most them were concentrated in the Northern Part of the Study area.

2.5.4 Linearity Analysis

The purpose of the linearity analysis is to check on the accuracy of the instrument used in the analysis of the samples. It is not a measure of accuracy of the results. It is intended to check weather the reading as taken by the instrument increases linearly with increasing concentration of the sample. Of the parameters analyzed from the water samples, F^-, and Cl^-, was analyzed with the DR/2001 Spectrophotometer while all the cat ions were analyzed using ICP method. The results of the linearity tests of both the instruments used in the analysis are as shown in Appendix 1.2. The analysis was done for each of the individual species for which the instrument was used to analyze.

2.5.5 Interpretation of Results

To use the water chemistry as a tool to explain the water flow direction, water chemistry was studied along some sections shown in figure 6.4.

EC of 8 wells were plotted against the sampling time to study the temporal variation of the water chemistry. Due to the random nature of the sampling time, absence of consistent data on most well, and varying probes used for measuring of the parameter, the implication of some of the trends are not obvious. Besides, their EC values were also plotted against yield and depth for 7 wells to understand the correlation between EC and each of them.

2.5.6 Basis of Interpretation

The water in the study area can be traced from three possible origins and hence classified as such.

Direct recharge from rainfall,
Surface water mainly from the lake
Geothermal water from geothermal aquifers

High $NaCl^-$ concentration and Li^+ are indices of geothermal influence as geothermal water in this area is characterized by high concentration of the same while $NaHCO_3$ and $NaSO_4$ is indicative of dissolution of evaporates from surrounding sediments. Direct recharge and water from lake is characterized by very low concentration of dissolved salts.

2.6 Isotopic Analysis

2.6.1 Theoretic Background

Isotopes of an element have the same number of protons and electrons but differing number of neutrons, thus having the same chemical behaviours but differ in atomic weight. Some isotopes are radioactive and decay naturally to other atomic forms at a characteristic rate while others are stable. For purposes of this study, the interest lies in the stable isotopes of Hydrogen and oxygen.

The table below shows the different isotopes of oxygen and Hydrogen and their relative abundance.

Isotope	Natural Abundance (%)	Stability
H	99.985	Stable
^{2}H (deuterium)	0.015	Stable
^{3}H (tritium)	Trace	Radioactive
^{16}O	99.76	Stable
^{17}O	0.04	Stable
^{18}O	0.2	Stable

Table 2.6.1 Isotopes of Hydrogen and Oxygen

The ratios $^{2}H/^{1}H$ and $^{18}O/^{16}O$ of the main isotopes that comprise water molecules are of special interest to hydro geologist. These ratios are expressed in delta (δ) units as per mille (parts per thousands, $^{o}/_{oo}$ difference relative to an arbitrary standard known as Standard Mean Ocean Water (SMOW)

$$\delta^{o}/_{oo} = [(R-R_{standard})/R_{standard}] \times 1000$$

Where R and $R_{standard}$ are the isotopes ratios $^{2}H/1H$ or $^{18}O/^{16}O$ of samples and standard respectively which gives:

$$\delta\, ^{2}H\ ^{o}/_{oo} = [((^{2}H/^{1}H)_{Sample}-(^{2}H/^{1}H)_{SMOW})/(^{2}H/^{1}H)_{SMOW}] \times 1000$$

$$\delta\, ^{18}O\ ^{o}/_{oo} = [((^{18}O/^{16}O)_{Sample}-(^{18}O/^{16}O)_{SMOW})/(^{18}O/^{16}O)_{SMOW}] \times 1000$$

Water with less ^{2}H than SMOW has a negative $\delta\, ^{2}H\ ^{o}/_{oo}$ while water with more ^{2}H than SMOW has a positive $\delta\, ^{2}H\ ^{o}/_{oo}$, the same applies to $\delta^{18}O\ ^{o}/_{oo}$.

Stable isotope studies are based on the tendency of some pairs of Isotopes to separate into light and heavy fractions, a process referred to as fractionation. Various isotopic forms of water have slightly different vapor pressures and freezing temperatures. This causes a difference in the ^{18}O and ^{2}H concentrations in water in various parts of hydrologic cycle. The process whereby the isotope content of a substance changes as a result of evaporation, condensation, freezing, melting, chemical reaction or biological processes is known as Isotopic Fractionation. This phenomenon is the basis of studies of Stable Isotope of ^{18}O and ^{2}H in hydrogeology because the relative concentration of these isotopes can be used in some hydro geological situations to identify the source of water in glaciers, aquifers or streams.

During evaporation, the water vapor produced is depleted in ^{18}O and ^{2}H relative to the water body. In contrast, the residual water phase becomes relatively more enriched in the heavy isotopes. When the water condenses, however, the opposite happens. The rain or snow that falls has a higher ^{18}O and ^{2}H relative to the water body. With subsequent events of evaporations and precipitation, as water vapor moves farther from the water body as part of regional or continental atmospheric circulation system, rain or snow becomes characterized by low concentrations of heavy isotopes ^{18}O and ^{2}H. The ^{18}O and ^{2}H content of precipitation at a given locality at a particular time depends in a general way on the location within the continental land mass and more specifically on the condensation-precipitation history of the atmospheric water vapor. Since these depend on temperature, isotopic composition of precipitation is also Temperature Dependent.

The combined effects of these are:

- Strong continental trend in the average annual isotopic composition of precipitation
- Strong seasonal variation in the time-averaged isotopic composition of precipitation at a given location.
- The isotopic composition of rain or snow during an individual precipitation event is very variable and unpredictable. Because of temperature changes or isotopic depletion effects, large variations can even occur during an individual rainfall event. Changes can also occur in the raindrop during its fall, especially at the beginning of a rainstorm and in arid or semiarid regions.

In deep subsurface zones where temperatures are above 50-100^{o}C, the ^{18}O and ^{2}H content of the groundwater can be significantly altered as a result of chemical interaction with the host rocks. However, in shallower groundwater systems, where temperatures are below 50^{o}C, the concentration of ^{18}O and ^{2}H isotopes is negligibly, if at all, affected by chemical processes, as the isotopes are non-reactive. Their concentration is determined by the isotopic composition of the precipitation that falls on the ground and the amount of evaporation that occurs before the water penetrates below the upper part of the soils. Once below the upper part of the soil, the concentration of ^{18}O and ^{2}H becomes a characteristic property of the subsurface water mass, which in many hydro geological settings enables the source areas and mixing patterns to be determined by sampling and analysis for these Isotopes.

^{18}O and ^{2}H concentrations obtained from global precipitation surveys correlate according to the relation (Dansgaard, 1964)

$\delta^{2}H^{o}/_{oo} = 8\delta^{18}O^{o}/_{oo}+10$

Which is known as Global Meteoric Water Line. Linear correlations with coefficients different are obtained from studies of local precipitation and are known as Local Meteoric Water Lines. The departure of ^{18}O and ^{2}H concentrations from the Meteoric Water Line can be used in a variety of hydrologic investigations. For example, $d^{18}O/ d^{2}H$ for precipitation that has partially evaporated is greater than the ratio for normal precipitation.

2.6.2 Field Work, Handling and Analysis of the Samples

To ensure that the sample bottle conformed to the desired standards, the same institutions also provided Glass brown sample bottles, which were used for the sample collection. The volume of each individual sample bottles was 30 ml.

To sample, each bottle was first thoroughly rinsed with the individual samples to be analysed. The bottles were then each totally filled with the respective water samples and carefully closed and was then dispatched to the laboratory for analysis. The bottles were completely filled so as to prevent any fractionation process from taking place in the sample bottle during transit, a process that would affect the analysis results. The samples were sent for analysis to the laboratory.

A total of 26 samples were collected from different locations in the area of study. Figure 2.5. Indicates the map of study area showing points were the samples were collected for the isotopic analysis. To guide against ambiguity, each sample was assigned a unique code to act as a unique identifier-Isotope Samples (IS1…IS26). The coordinates of the locations of wells were the samples were collected was got using a Garmin GPS handsets.

To ease the compilation of results, the list of the samples together with the location of well from which they were collected was also compiled and submitted to the laboratory where the analysis was to be done. Where the EC values of the water and the altitude of the well location were ascertained, the information was also indicated on the list and consequently forwarded to the laboratory of The University of Groningen, Center for Isotope Research were the analysis was done.

In the Laboratory, 1ml of the water sample was degassed special vacuum system and then brought into isotopic equilibrium with CO_2 at 25^{o}C for a period of 24 hours. After the equilibrium exchange, a fraction of the CO_2 is sampled for $^{18}O/^{16}O$ analysis. Since all samples, the standard V-SMOW included, are submitted to this treatment, the fractionation between CO_2 and H_2O is irrelevant.

The $^{18}O/^{16}O$ ratio of CO_2 of the sample is compared with a reference (pdb), measured in a special isotope ratio mass spectrometer, and expressed in $^{\mathbf{o}}/_{\mathbf{oo}}$. One analysis takes about 10 minutes. Within every series of samples, laboratory references are included. The analysis precision of $^{18}\delta$ is about $\pm$0.1 $^{\mathbf{o}}/_{\mathbf{oo}}$ Results of analysis are shown in appendix 2.

2.6.3 Basis of interpretation

Interpretation of the Isotopic Signatures is based on the assumption that samples lie along the Direct Recharge_ Lake Water Mixing line. Consequently, all samples are a mixture of these two end members, which are Direct Recharge water and Lake Water with d 18 O values of –5.75 $^o/_{oo}$ and 6.5 $^o/_{oo}$ respectively. Therefore, the $\delta^{18}O$ values of all the samples fall between –5.75 $^o/_{oo}$ and 6.5 $^o/_{oo}$.

For a sample with $\delta^{18}O$ value v, its ratio of composition can arithmetically be derivered as shown below:

If X is the ratio of rainwater in the sample, then the ratio of lake water will be (1-x)

$V= \delta^{18}O_{sample} = (X^* \delta^{18}O_{rain}) + ((1-X)^* \delta^{18}O_{lake})$

$=(\delta^{18}O_{rain}X+ \delta^{18}O_{lake}- \delta^{18}O_{lake} X$

From which,

$X=(\delta^{18}O_{sample}- \delta^{18}O_{lake})/(\delta^{18}O_{rain}- \delta^{18}O_{lake})$

2.7 Hydrogeology

Drillers' logs were studied for 60 boreholes to understand the aquifer material in the area of study. These together with the published geological map of the area were used to derive the distribution of hydraulic properties of material encountered during the borehole drilling.

The an approximation of historic flow pattern as of 1980 was attained by drawing lines perpendicular to piezometric contour lines drawn by Owor (2000).

Ground elevations for 11 wells were geodetically levelled to get their accurate altitude above sea level, besides, 14 wells had been geodetically levelled earlier. For wells that were not geodetically levelled, the altitude was got from DEM of the area of study. To up date the map, and hence the flow pattern, modifications were effected on basis of the data from geodetically surveyed wells. The locations of newly drilled wells were got with the aid of Garmin GPS handset. Water level for geodetically levelled wells and the newly drilled wells were taken by lowering a probe attached to an electric cable calibrated in millimetres.

Transect used in the study of geology were also used in the study of hydrogeology along the same section. Long these section, the geology, hydro chemistry and isotopic data was studied to understand the flow pattern in the respective directions.

2.8 Model

Modeling was done using the GMS. Using Excel spreadsheet, data gathered from interpretation of drilling logs together with the data from the hydrogeology was used to prepare three input data files for GMS software. The input data files prepared for data input into GMS software were a project file which contained all the files in which the data was located, a material files that described the different formations encountered in the study area together with their codes and a borehole file which contained information about the individual information on the boreholes. To be accepted by the GMS software, files were saved with extensions <*.grp>, <*.mat> and <*.bor> respectively. The formats of the input data files are as shown in appendices 5A-8. The data was then imported to GMS software were the modeling was done.

Once in the GMS, similar contact of different wells were used to generate TINS that were in turn used to generate the solids to represent the different formation.

2.9 Layout of the Thesis

The structure of the final report is presented as follows as follows:

Chapter 1: An introduction to the research problem and research objective

Chapter 2: Methodology is presented in this chapter. The materials used and briefly on the key sources of information are also presented.

Chapter3: Previous works related to the subject is dealt with in this chapter.

Chapter 4: Introduction to the study area. An overview of different aspects that characterize the project area is given here. Given the enormous amount of work already done in the area, this chapter has been adapted from the work of Oppong-Boateng (2001) and Pastor(2000)

Chapter 5: The geology of area is analyzed. A verification and correction of the earlier made geological map is included. The influence of the geology on the flow is considered here.

Chapter 6: Hydrogeology. Here the Piezometric Heads, stable isotope, hydrochemistry as tool to understand the flow direction and geology are integrated to explain the hydrogeology. Any trend of the change in water chemistry in time and space is sought after.

Chapter 7: Model. Using information from the two previous chapters, a 3-D geological model is constituted using GMS.

Chapter 8: Conclusions and Recommendations.

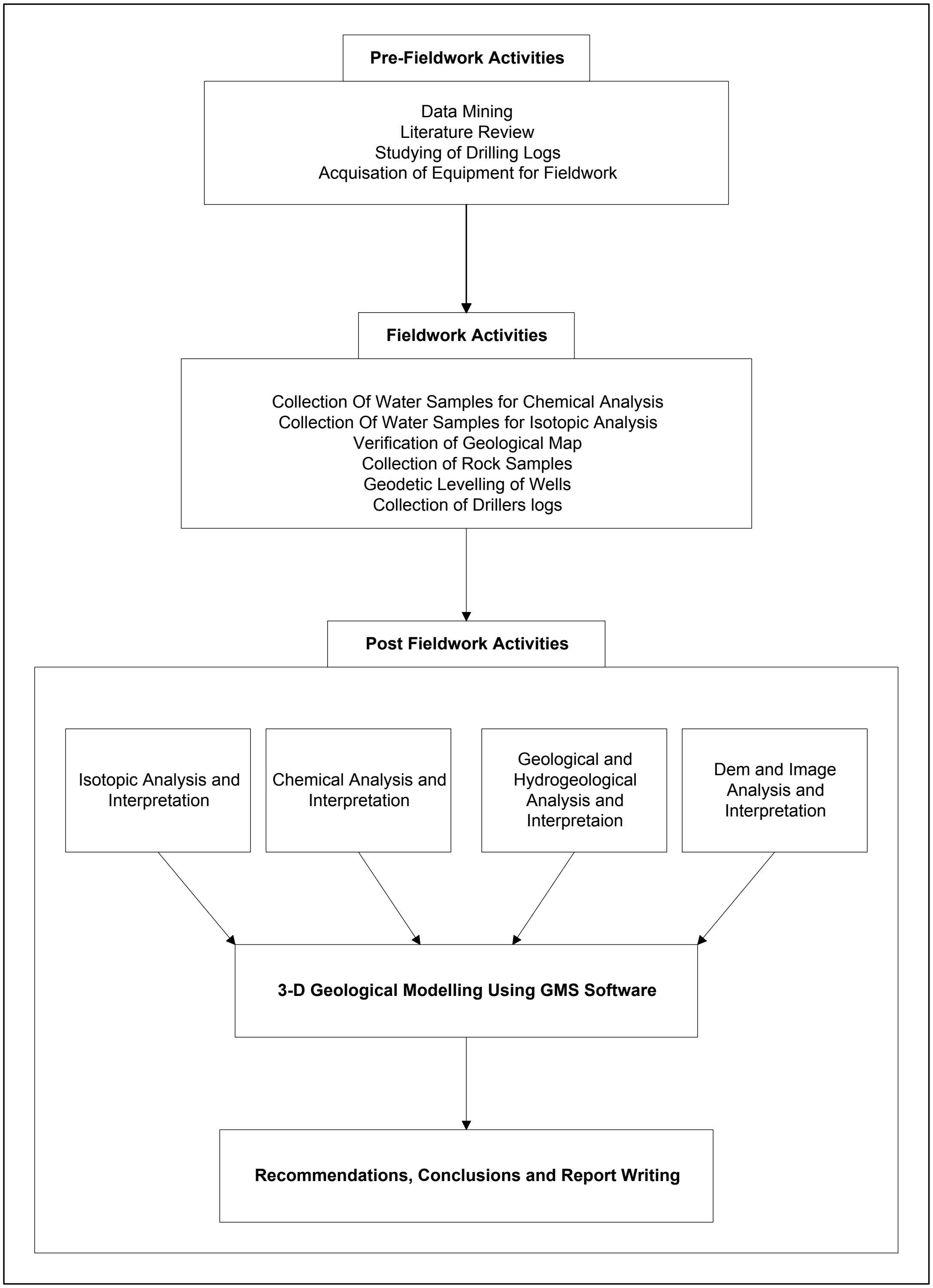

Figure 1.1 Flowchart of Methodology.

Chapter 3 Previous Work

MacCann (1974) observed that due to extensive faulting, fracturing and weathering, virtually all-volcanic rocks in the area have some capacity to yield water to boreholes. Groundwater also occurred in the quaternary alluvium and lake deposits. He noted the occurrence of a multi layered aquifer system, the top one being unconfined while the bottom one(s) was either confined or semi confined but not artesian. After what appeared as adequate water supply could be obtained from the borehole, drilling would be discontinued. Consequently, it is usually not possible to determine the total aquifer thickness of the deeper water bearing zones on the basis of drilling logs.

Generally, ground water obtained from the lacustrine deposits in the lake Naivasha catchment occurs under unconfined or free water table conditions and their yields were generally higher than the yields of boreholes penetrating most volcanic rocks and commonly exceed 4 cubic meters per hour. Some of the shallow wells around Lake Naivasha have a specific capacity greater than 1 liters per second per meter which is higher than the yields of boreholes penetrating most rocks that are not located near zones of faulting (MacCann, 1974). MacCann (1974) observed that due to extensive faulting, fracturing and weathering, virtually all-volcanic rocks in the area have some capacity to yield water to boreholes.

McCann also realized that the very intense faulting within the Rift valley played a significant role in the movement of groundwater and that groundwater basin boundaries did not always conform to catchment drainage divides. Groundwater generally flowed towards the lake from the Mau and Aberdare escarpments, although it was diverted locally by the presence of faults that formed either barriers or conduits. There appeared to be some flows southwards the Kedong Valley but this condition could not be confirmed because of the absence of wells in the valley and effluent flow did not occur in Hell’s Gate.

Chemically, Lake Naivasha is the only fresh water lake in the Rift valley catchment, despite the relatively high rates of potential evaporation that prevailed in the catchment. It is generally Bicarbonate in nature but contained about equal concentrations of calcium and sodium. He interpreted this to indicate occurrence of effluent seepage.

Allen et al., (1989) found out that on a regional scale, the Rift Valley between Lakes Nakuru and Magadi, Naivasha inclusive broadly exhibited the hydro geological features expected of a valley-interfluve's system with lateral groundwater flows from the rift escarpments to discharge areas on the rift floor culminations at Lake Naivasha. This model was modified by the presence of the major rift faults, which acted as barriers to lateral flow, leading to longer, deeper, flow paths and by the grid faulting in the rift floor which tended to align flow paths within the rift along its axis.

They appreciated that the permeabilities of the volcanic rocks underlying the Rift valley are generally low, although there was some considerable local variation. Aquifers were found in fractured or reworked volcanics or along weathered contacts between different lithological units with the highest permeability being found in reworked volcanics composing sediments of the Naivasha area, where specific capacities of the wells often exceeded 3 liter/second/ meter and hydraulic conductivities of greater than 10m/day were common.

Using stable isotopes, they were able to find an approximate correlation of isotopic composition with height. It suggested that much of the groundwater in the Naivasha-Nakuru area was relatively local in origin. This implied that deep component of flow are not important in the shallow hydrology of the rift floor, and therefore supports the contention that permeability at depth are very low.

It has been consistently postulated by numerous researchers that the lake has a subsurface outflow from it's southern shores which help to keep fresh and that this surface flow also recharges the Olkaria geothermal reservoir about 5km to the south (Thompson and Dodson, 1963; McCann, 1972 &1974: Gaudet and Melack, 1981; Ase et al., 1986; Darling, et al., 1990; Clarke, et al., 1990).

Ojiambo (1996) studied the hydrogeologic parameters of the aquifers and found out that that the groundwater hydraulic gradients in the south range from 0.1 to 0.005 from Oloidien bay to the east. The Hydraulic conductivity ranged from 10^{-3} to 8.6×10^{-3} m/s with transmissivities ranging from 3 to over 10000 m^2/day. The subsurface outflow fluxes was calculated for a range of hydraulic conductivities assuming a 30m aquifer thickness; fluxes of $18 \times 10^6 m^3$/yr to 50×10^6 m^3/yr were obtained in conformity with other workers.

With the help of transects drawn to South and North of the Lake, Ojiambo (1996) further realized that the water levels in both the Northern and Southern part of the Lake were below the lake level. Consequently, the water flowed northwards and southwards from the Lake. Just like Ase et al (1986), Ojiambo (1990), pointed out the irregular fluctuation of the lake levels. He postulated that besides the natural tendency to do so, this could also be attributed to intensive pumping of water for agricultural activities. Earlier, McCann (1972) had showed higher water levels in the North and lower ones in the south, which implied subsurface flow of water from the north southwards into the lake and flow southwards from the lake to the south. Ojiambo (1996) also pointed out that while the southward flow of water from the lake had been consistent over time, the was a reversal in the direction of flow in the northern part of the lake- while originally flowing southwards into the lake, it later started flowing northwards away from the lake.

With the aide of chemistry and isotopic strontium concentration, Ojiambo (1996), confirmed that the lake lost water through subsurface outflow to the south. He pointed out that the surface and groundwater in the study area could be classified into three geochemical groups: mixed Ca-Na-HCO_3-Cl-SO_4 waters north of the Lake Naivasha and on the eastern escarpment of the rift valley; Na-HCO_3 water for the rest of the groundwater, river and Lake waters; and Na-Cl for geothermal waters. He observed that the concentrations of major ions in the water south of the Lake Naivasha increased southwards an observation that further confirmed that the water moved southwards from the lake. Gaudet and Melack (1981) pointed out that a large portion of K^+, Ca^{2+}, and Mg^{2+} entering the lake was lost in sediments as the water flowed out of the lake while Na^+ and Cl^- behaved conservatively.

Oppong-Boateng (2001) proposed that the long residence time for reaction of groundwater with underlying aquifers materials from the shallow wells to the Geothermal field might be the cause of changes in groundwater chemistry from predominantly Na-HCO3 and Ca-Na-HCO3 into Na-Cl water types. These Na-HCO3 and Na-Cl waters might therefore have evolved from different bedrock aquifers, as the geology is diverse in the study area. He pointed out the possibility that they might not necessarily be evolutionary but independently formed during and after recharge process.

Using $^{87}Sr/^{86}Sr$ ratios, Davies and Macdonald (1987), also demonstrated that the ground water south of the lake flowed southwards. They realized that the $^{87}Sr/^{86}Sr$ ratio of the ground water increased southward away from the lake. Ojiambo (1996), used δD and $\delta^{18}O$ to further corroborate the hypothesis that the southern water were formed by mixing recharge water from eastern Rift flanks and with Lake Naivasha water and that the lake had a subsurface outflow from its southern shores.

While all researcher until now agree on the existence of subsurface effluent seepage from the lake, most of them postulated that all if not most of the outflow was from the southern shore and flowed southward to Olkaria. Owor (2000) modeled the Long Term Interaction of Groundwater with the Lake and postulated that 63% of the subsurface outflow was to the north and only 37% was to the South.

Oppong-Boateng (2001) carried out source-rock analysis tests. He realized that the concentration of Na^+ exceeded that of Cl^- an observation from which he concluded that besides halites, additional Na^+ originated from dissolution of weathering products. He further observed that the concentration of the Na^+ and Cl^- was low in shallow waters but increased towards deep geothermal wells. Oppong-Boateng also recognized that shallow water composed of mainly NaHCO3 while NaCl was predominant in deep geothermal water. However, the deep geothermal waters were depleted in $Ca^{2+}$and Mg^{2+}. He inferred that water chemistry was greatly influenced by the rock types in the area. By plotting the water chemistry on trilinear diagrams, he also deduced that the shallow waters in the study area are predominantly of alkaline carbonates (Na^+ and K^+) while deep geothermal waters are NaCl. Considering the relative concentration of the different ions and anions, Oppong-Boateng (2001) postulated that the relative concentration of ions was $Na^+>K^+>Ca^{2+}>Mg^{2+}$ and $HCO_3^- > Cl^- > SO_4^{2-} > F^-$. He grouped the water into three major groups: $Na\text{-}HCO_3$, Na-Cl, and $Ca\text{-}Na\text{-}HCO_3$.

Oppong-Boateng (2001) proposed that the long residence time for reaction of groundwater with underlying aquifers materials from the shallow wells to the Geothermal field might be the cause of changes in groundwater chemistry from predominantly Na-HCO3 and Ca-Na-HCO3 into Na-Cl water types. These Na-HCO3 and Na-Cl waters might therefore have evolved from different bedrock aquifers, as the geology is diverse in the study area. He pointed out the possibility that they might not necessarily be evolutionary but independently formed during and after recharge process.

Morgan (1998) classified the water in the study area and concluded that it was predominantly NaHCO3 in nature. He attributed the high Na^+ and low Mg^{2+} to rhyolite, which is widely distributed in the study area. Rhyolite manifests granitic weathering because it is the volcanic equivalent of granite. He pointed out that in the study area, volcanic mineralogy was reflected in the groundwater. The rhyolitic composition indicated reflected the composition of the comendites and pantellerites which form the pumice and trachytes in the area of study. Using Leicester University data set, Morgan realized that though F^- and SiO_2 were considered minor element in study of water chemistry, they were significant in the study area. He attributed this to the weathering of silicates and Fluoride bearing micas and amphiboles in the study area.

Appelo et al. (1996), pointed out that concentrations of F^- beyond 3mg/l caused dental fluorosis (tooth mottling) evident among the local people and more seriously skeletal fluorisis (bone deformation and painful brittle joints in old people). He asserted that the origin of high F^- was due to leaching from minerals in the rocks, in particular volcanic rocks. These constitute the bulk of the rocks in the study area. Appelo et al. (1996) also illustrated that groundwater with high concentration of Ca^{2+} contains low concentrations of F^- while that with low concentration of Ca^{2+} contained high concentrations of F^-.
Ojiambo (1992) analyzed water chemistry data of different water types in the Lake Naivasha area. He realized that the major ionic chemical compositions show enrichment

Oppong-Boateng (2001) used stable and radioactive isotopes to investigate the extent of mixing of water and the flow direction of groundwater in south of the lake. Using stable isotopes ^{18}O and ^{2}H of water, he observed that Lake Naivasha and groundwater in the area had similar isotopic signatures. With the aide of $\delta^{18}O$-δD plots, he showed that the groundwater in the southern part of the lake was a mixture of recharge waters from the flanks and Lake Naivasha. He also postulated that the waters of wells in Sulmac and Kedong C210 which had isotopic signatures similar to the lake was quite young water (about 1000 years) and thus could have been recharged from the lake or was a mixture with quite old groundwater. However, there was no isotopic resemblance between 3-point farm borehole M and the lake. It was older water (about 3000 years), which implied that it consisted of old groundwater or a mixture of modern direct recharge and old groundwater.

Reviews of the previous works in the study area (Thompson and Dodson, 1963; McCann, 1972,1974; Gaudet and Melack, 1981; Ase et al., 1986; Darling, et al., 1990; Clarke, et al., 1990, Ojambo 1992,1996; Owor, 2000; Boateng, 2001; Kibona, 2000; Morgan, 2000) indicate vast discussions on the geology, hydrochemistry, hydrogeology and stable isotopes. This study consequently integrates the various studies in addition to fieldwork in order to improve the understanding of the hydrogeology of the area.

Chapter 4 Description Of Study Area

4.1 Local Setting

4.1.1 Location Of Study Area

The study area lies in the Eastern Kenyan rift valley province in Naivasha Division of Nakuru District approximately 100km from Nairobi, the capital city of Kenya. It lies within the UTM zone 37 and coordinates:

X_{max} =240000, Xmin=170000

Y_{max}=9950000, Y_{min}=9890000

Thus, it is bounded by latitude 0°15′ S and 1°00′ S and longitude36°00′E and 36°45′E. The study area is located in the central portion of the rift floor at a mean altitude of 1885m above mean sea level. It is surrounded by the Lake Nakuru-Naivasha highlands, with decreasing altitude from the North towards the South. The location of study area is depicted in Figure 2.1

Figure 2.1: Location maps of the study area

4.1.2 Rainfall Pattern

There are primarily two rainfall seasons a year and the pattern is similar to other parts of the country. Long-term average annual rainfall shows variation in descending order from 1279mm/year in the first period (March-May) to 598mm/yr in the second one (October-November). Annual values of precipitation in the hilly areas are high, ranging from 1250mm to 1500mm with similar or lower rates of evapo-transpiration while the lower rainfall values average 430mm at Magadi and 930mm at Nakuru for the valley floor (Clarke et al 1990).

The highlands surrounding the drainage basin receive more rain than the lake and valley floor and provide most of the water that maintains the lake. (Lars-Eric, 1986) and (Wiberg, 1976) estimated mean annual rainfall to be 667mm/year and 650mm/year for the period of 1931-1960 by respectively.

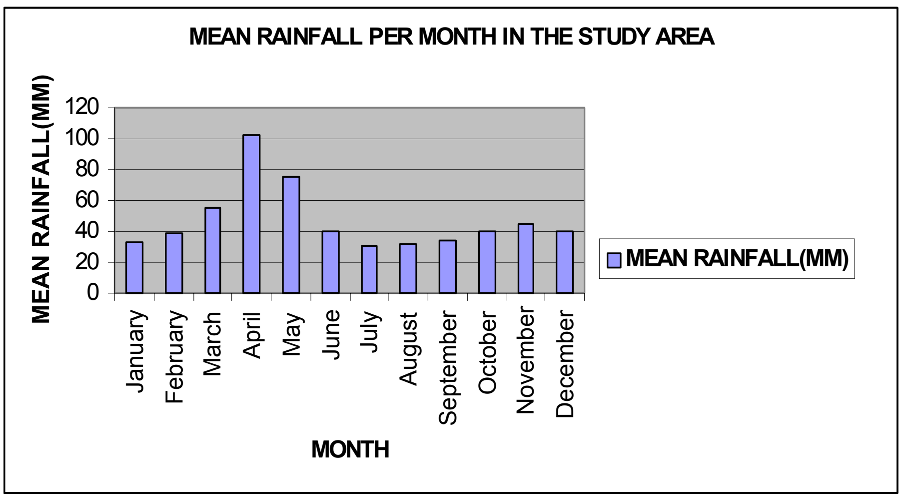

Figure 4.1: Bar chart of Mean Monthly Rainfall in the study area.

4.1.3 Temperature And Evaporation

The temperature in the vicinity of Nakuru is relatively stable, with the mean maximum monthly temperatures varying between 17°C and 20°C. The warmest periods are from January to March with the mean maximum of 29°C recorded in February. The coldest periods are from the months of July to August and the mean minimum temperature of 10°C recorded in January. The mean annual temperature of 18°C is often recorded.

Due to hot, dry and windy climate in the Naivasha section of the Gregory rift, rains and evaporation increases each month after April. This is responsible for the annual evaporation loss exceeding the rainfall by a factor of two. Low relative humidity and an average daily maximum temperature of 25°C tend to cause annual potential evaporation of 1500-1900mm/yr (Ase et al., 1986) far in excess of rainfall.

Therefore, there is very little spatial variation. However, there is often a seasonal variation: potential evapotranspiration is highest during the dry periods and lowest in the rainy periods. This is because rainy periods are characterised by high relative humidity.

Evapotranspiration is notably higher in areas where there is little soil cover and low rainfall, and less in dense thick vegetation and higher rainfall areas.

Month	Jan	Feb	Mar	Apr	May	Jun	Jul	Aug	Sep	Oct	Nov	Dec
Evapo(mm)	188	185	193	138	131	122	123	128	139	131	119	155

Table 1: Monthly evaporation data from 1955-1990 (Nakuru).

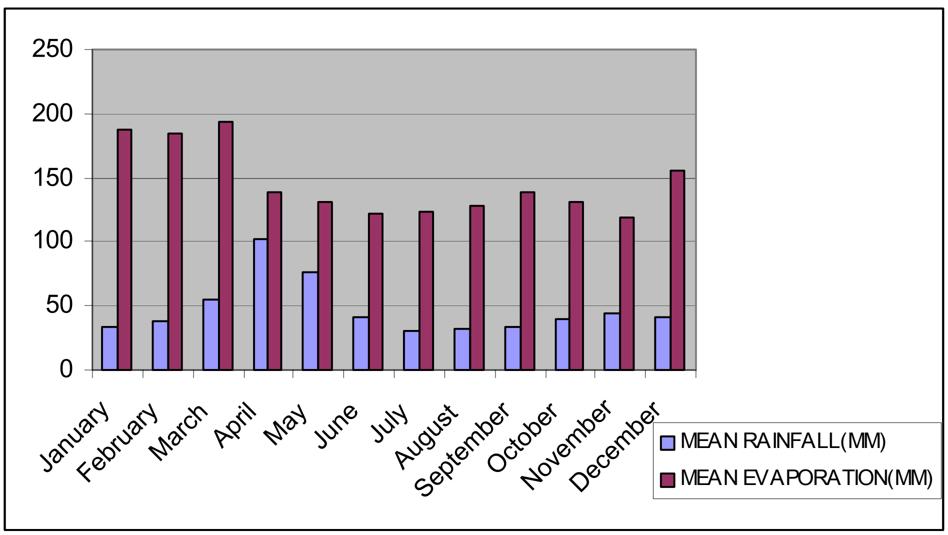

Figure 4.2: Bar chart of Mean Rainfall and Evaporation.

4.1.4 Drainage Network

There are a lot of rivers that discharge into the Naivasha basin. The main rivers are the Gilgil (420km^2 watershed), Karati and Malewa (1750km^2 watershed). The rains on the Aberdare mountains and Kinangop plateau maintains the perennial flow in the Malewa River. The Malewa and Gilgil drain from the northern part of the catchment while Karati River drains from the northeastern part. Flow in the Karati River and other streams are seasonal and often don't reach the lake as surface water.

The Malewa River accounts for about 90% of the river discharge into Lake Naivasha. There are also small streams that flow westwards and develop into four main tributaries, the Mugutyu, Kitiri, Makungi and Turasha. The later is the most important tributary and joins River Malewa at approximately 8km east of Gilgil. Tributaries of the Malewa river form a dense dendritric drainage pattern but have a radial pattern in the Kipipiri area as a result of the conical shape of the volcano in the vicinity. Streams in the western part of the basin disappear in the rift before reaching the Lake.

4.1.4 Vegetation

The vegetation in the flat areas are mainly bushes and savannah. However, due to the diversity within the lake Naivasha basin all sorts of vegetation are found within the vicinity. The northern parts of the basin near the source of the Malewa River are boarded by tropical evergreen forest. Along the slopes of the rift valley is tropical grassland, which ranges into bushland typical of the rift floor.

The vegetation within the rift has a semi-arid character and high potential for grazing purposes. The exceptional case is recognised in mountainous areas where tropical rain forests are prominent. Engulfing the lake Naivasha are acacia trees, woodland with trees, which are as high as 35m tall and the drainage basin serve as polders for grazing.

4.1.5 Soils

Soil surveys have extensively been carried out in the area with each having fairly different level of detail. The soils are derived basically from weathered volcanic and basement rock system and occupy the floor of the rift valley in Naivasha as light grey or brown to pinkish non-calcareous soils (Ongweny, 1973).

In the high areas of the catchment, there are non-calcareous black or grey soils overlying yellow-brown compact sub-soils with iron concretion. The soils in the Aberdare Mountains, Kinangop plateau are young with predominantly morillonite clays (Rachillo, 1977). At edges of the lake, the soil is less alkaline and more liable to crack during drying (Gaudet, 1977) whiles those along the north shore above the lake are generally high in exchangeable Na^+ and K^+ (Makin, 1967).

4.2 Geological and Hydrogeological Settings

4.2.3 Geological Setting

The KRV is mostly underlain by volcanics with phonolitic, trachytic and rhyolitic composition and their sedimentary derivatives. The KRV volcanics were erupted nearly continuously from Early Miocene to Holocene times. The geology of the area is generally made of volcanic rocks and lacustrine deposits. In the basin are complex geological structures, which have been subjected to several tectonic processes leading to varying structural features. The volcanic rocks consist of basalt, trachytes, ashes, tuffs, and agglomerates and acid lava.

There are four major periods of volcanic activity (V1-V4) and faulting (F1-F4) which resulted in the present situation (Baker et al, 1988).

EPISODE	ACTIVITY	UNITS	AGE RANGE
V4 D4	Late quaternary to recent salic volcanoes Extensive minor faults of the rift floor	Longonot, Eburru, Olkaria, Clementia, Ndabibi and Alkira Volcanic groups, fluvio and lacustrine sediments	0.4-0 Ma 0.8-0.4Ma
V3 D3	Quaternary flood lava of the rift Renewed faulting of the rift margin	Gilgil trachytes, Kijabe Hill formation	1.65-0.9Ma 1.7Ma
V2 D2	Early Quaternary flood trachytes Formation of steep faults (narrowing of grabens)	Limuru trachyte,karati Basalt formation	2.0-1.8Ma 3.0-2.0Ma
V1 D1	Pliocene volcanic ash flows Major faulting of Eastern rift margin	Kinangop tuff Mau tuff formation	3.7-3.4Ma 4.0-3.0Ma

Table 2: Major volcanic and deformation episode (adopted from Clark et al, 1990).

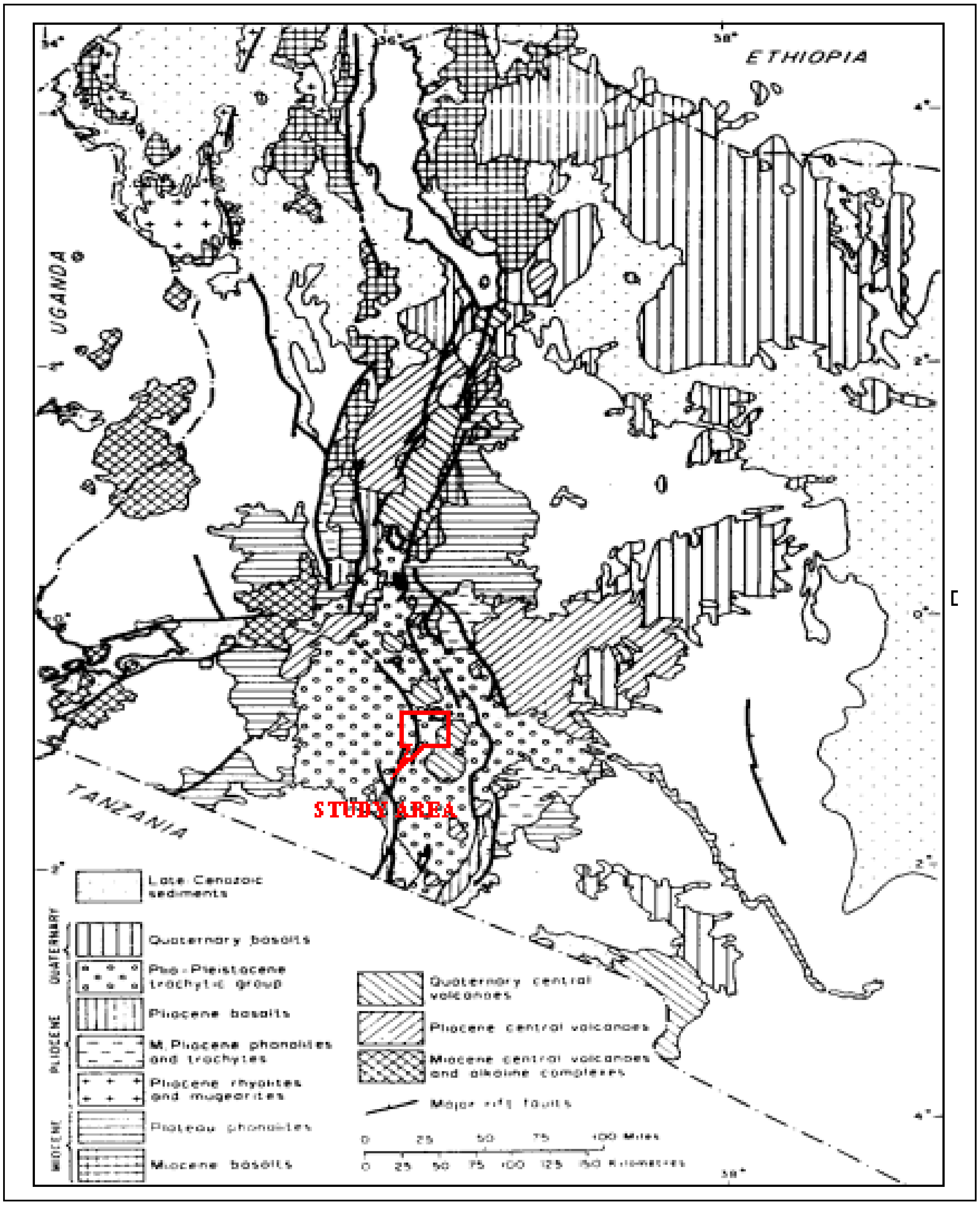

Figure 4.3 Regional Geology of the Kenya Rift taken from Baker, et. al. (1971)

The oldest volcanics are the Miocene Basalts found extensively in Northern Kenya. Overlying them in Central Kenya is an extensive Phonolitic Plateau found on both sides of the rift. These were erupted during a short period of time at the end of Miocene and in Earliest Pliocene Times. The Mid-Pliocene Phonolites and Trachytes include two main formations: the trachytes on the upper part of Kamasia area and the phonolites on the Bahati and Southern Laikipia area. Pliocene rhyolites overlie the Miocene basalts in NW Kenya. These are thick sheets of rhyolites and ignimbrites with intercalated mugearites and trachytes. Pliocene Basalts outcrop on marginal step-fault platforms in the southern part of the rift valley. They also occur beneath a cover of younger volcanics along parts of the floor. Plio-Pleistocene Trachytic lavas and ignimbrites occupy nearly the entire floor of the Central and Southern parts of the rift valley and occurs locally on the marginal plateau. It consists of a lower part of trachytic tuff exposed in Kinangop and Bahati in the east and Mau range on the west of the rift valley. The upper part is represented by the Plateau trachyte series of the Magadi area. Quaternary basalts of Late Pleistocene to Holocene Age occur east of the rift valley. These are composed of numerous basaltic cones with striking linear patterns indicating fissure control.

Miocene Central Volcanoes occur mostly in Western Kenya and Eastern Uganda, Pliocene Central Volcanoes are distributed along the floor and shoulders of the developing rift and Quaternary Central Volcanoes occurred along the central and northern sections of the rift floor. The Quaternary Central Volcanoes are surrounded by well-preserved calderas and the bulk of the volcanics are younger than the Plio-Pleistocene Trachytic Group.

Late Tertiary and Quaternary Volcanics, lacustrine sediments and alluvium principally of reworked volcanic debris generally underlie the study area (Figure 4.5). Most are volcanic rocks that include alkali rhyolites, ashes, pumiceous deposits and trachytes. Lacustrine deposits occur mostly close to Lake Naivasha. The sediments were deposited during the previous high levels of the lake.

The Eastern part of the study area is mainly covered with pyroclastic deposits and lava flows coming from Longonot Volcano. The pyroclastics include ashes, tuff and pumiceous deposits. Lava flow is predominantly of trachytic composition.

The Western part of the study area referred to as the Olkaria Volcanic Complex is also covered with volcanic rocks and lacustrine sediments. Most are volcanic rocks that include alkali rhyolites, ashes, pumiceous deposits and trachytes. The main products of volcanism in the area have been alkali rhyolite and pyroclastics rocks while trachyte and basalts have been minor products. The volcanic centers are structurally controlled and most of the flows are erupted through fault zones. The most recent volcanism is associated with the Ololbutot rhyolite flow. A large fraction of the pyroclastic deposits originated from Longonot Volcano.

Omenda (1998), best describes the geology and structures west of the study area in his report on the Geology and Structural Control of the Olkaria Geothermal System.

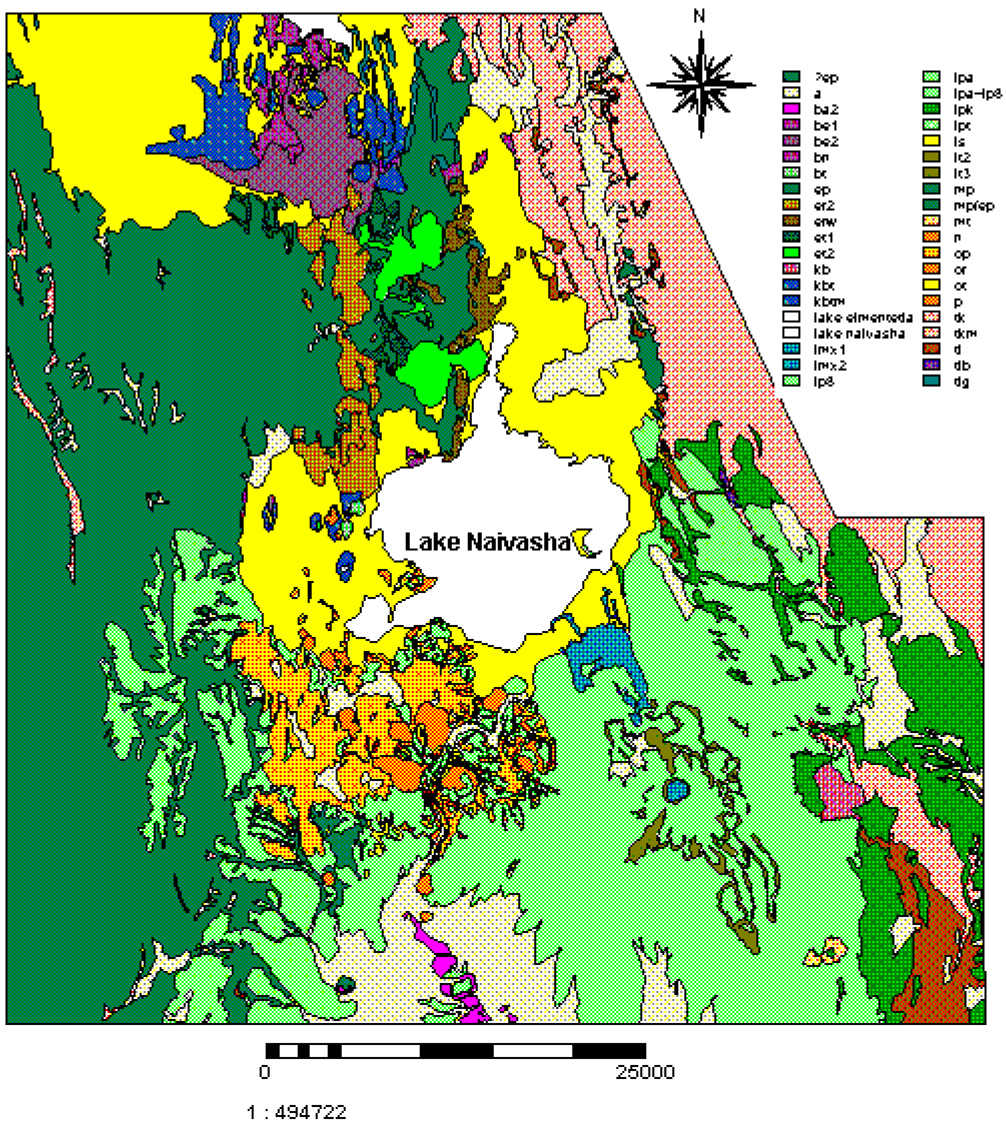

Figure 4.5: Geology map of the study area.

Unit	Description
?ep	Eburru pumice, pantellerite; trachyte pumice, ash fall deposits
a	Alluvial deposit
ba2	Alkaria basalt, basalt and hawaiite lava flows, pyroclastic cones
be1	Older elementetia basalt, hawaiite lava flows, pyroclastic cones
be2	Younger elementetia basalt, basalt, hawaiite and mugearite / benmoreite lava flows and pyroclastic cones
bn	Ndabibi basalt, hawaiite lava flows, pyroclastic cones
bt	Surtseyan / strombolian ash cones
ep	Eburru pumice, pantellerite and trachyte pumice, ash fall deposit
er2	Eastern eburru pantellerite, lava flows, pyroclastic cones
erw	Waterloo ridge pantellerite, welded and unwelded pyroclastics
et1	Older eburru trachyte, lava flows and pyroclastics
et2	Younger eburru trachyte, lava flows and pyroclastic cones
kb	Kijabe hill basalt
kbt	Surtseyan tuff cones
kbtm	Surtseyan tuff cones with laterally equivalent fall tuffs
Imx1	Lower longonot mixed basalt/trachyte lava flows and pyroclastic cones
Imx2	Upper longonot mixed basalt/trachyte lava flows and pyroclastic cones
Ip8	Longonot ash
Ipa	Longonot alkaria pumice
Ipa+ip8	Longonot ash and alkaria pumice
Ipk	Kedong valley tuff, trachyte ingimbrites and associated fall deposit
Ipt	Longonot volcanice, pre-caldera welded pyroclastics and lava flows.
Is	Lacustrine sediments
It2	Lower longonot trachyte, lava flows and pyroclastic cones
It3	Upper longonot trachyte, lava flows and pyroclastic cones
Mp	Maiella pumice, trachyte, pantellerite pumice and ash fall deposits
Mp/ep	Maiella pumice/eburru pumice
Mt	Magaret trachyte, unwelded and welded pyroclastics
N	Ndabibi comendite lava flows, domes and pyroclastics
Op	Olkaria comendite, pyroclastics (include pre-Ipk lacustrine sediments, reworked pyroclastics in ol Njorowa gorge)
Or	Olkaria comendite, lava flows and domes (include ol Njorowa pantellerite lava and welded pyroclastics)
Ot	Olkaria trachyte, lava flows
P	Ndabibi pantellerite lava flows
Tk	Kinangop tuff (eastern rift margin)
Tkm	Mau tuff (western rift valley)
TI	Limuru trachyte
Tlb	Karati and ol mogogo basalt
Tlg	Gilgil trachyte

Table 3: **Description of Legend of Geology map.**

Details of the sub-surface geology were known from cutting and cores of geothermal wells in the area. Omenda (1998) divided them into four (4) broad lithostratigraphic groups namely; 1) Mau Tuff, 2) Plateau Trachytes, 3) Olkaria Basalts and 4) Upper Olkaria Volcanics. He also divided the OVC into east and west sectors wherein the Mau Tuffs predominate in the west sector while Plateau Trachytes and Olkaria Basalts are unique to the east sector.

The Mau Tuff correlates with the tuff of the Mau Ranges on the western escarpment which are Pliocene. They are intersected by all wells drilled in the west sector but not by those in the east. The Pleistocene rocks of the Plateau Trachyte Formation occur mainly in the east sector and are overlain by the Olkaria Basalts.

The structural pattern in the study area trends in an N-S, NW-SE, NNW-SSE and ENE-WSW direction. Faults and fractures are more common in the western part compared to the eastern part where large volumes of pyroclastic deposits are present. The younger N-S faults and fractures are common in the axial region of the rift and represent the latest tectonic activity. Vertical permeability along some of these faults is indicated by the occurrence of strong fumarolic activity. The NW-SE trending faults are mostly inferred from aerial photos and the alignment of volcanic centers. The Mau Escarpment prominently displays the NNW-SSE angle fault trend. The ENE-WSW trending faults called Olkaria Fault Zone cuts through the geothermal area and are the most important permeable structure in the whole Olkaria geothermal area.

The bed of the lake composed mainly of volcanic material and subsequently deposited pyroclastics and organic matter produced locally. The sediments are composed of sand, pebbles as well as gravels made up of rounded pumice clasts (Studdard et. al.1995).The southern part lying within the catchment of the lake falls within the Greater Olkaria volcanic complex that is made up of pyroclastics, which includes lacustrine sediments. Craters, fumaroles, Hot Springs and steam vents are found in several places in the southeastern and southwestern regions.

In the beds of the gorge spring are pumice that have been turned into Chur through geothermal activities. They are the hardest rock types in the study area. There are also Kedong valley tuffs at the slopes of the gorge as well as pronouncement of Lake sediments at the upstream of gorge. Further south of the Gorge is rhyolite but not pumice, which is less than 60,000years old (Martin, 2000).

4.2.2 Hydrogeological Setting

The hydrogeology of Lake Naivasha is complex (Clarke, 1990). Hydrogeology is greatly influence by the geology, topography and climatic factors that pertain in the area. Topography in the vicinity creates two different hydro-geological environments, which affects significantly the Hydrogeology. In the localized highland areas, there exist deep groundwater tables as well as steep groundwater gradient. This environment is often associated with high rainfall values, which are sources of groundwater recharge if all conditions are fulfilled.

Groundwater occurrence is greatly determined by the geological conditions as well as the available water for storage. Fresh volcanic rocks tend to be compact with no primary porosity although secondary porosity may be well developed. These rocks underlying the rift valley therefore have low permeability though there are at times considerable variations where layers with poor hydraulic conductivity may be overlain with layers of good hydraulic properties.

The high hydraulic gradient accounts for the outflow of groundwater from the lake to the south as well as some infinitesimal outflow towards the north. Structural features such as faults often optimise storage, transmissivity and recharge with the significant of these occuring in places that are adjacent to or within a surface drainage system. Shallow groundwater table, low precipitation and low values of recharge characterize the valleys.

The main aquifer is found in sediments covering parts of the rift floor. These, aquifers usually have relatively high permeability and are often unconfined with high specific yield (Stuttard, 1995). . Clark et al (1990) estimated by inventory of boreholes and envisaged that the lake sediments have permeability of 12-148m/d.Besides, aquifers are found in fractured volcanic rocks and at times along weathered contacts between different lithological units and they are often confined or semi-confined with low storage coefficient.. Permeability is generally low in aquifers but there exist some variations locally as a result of some formations

Data from existing boreholes and wells reveal complex hydrogeological conditions and depth to water varies throughout the basin but it is generally ranging from 1.3m to about 240m. Estimated hydraulic conductivity average 10m/d and well yield on average is 3 l/s/m.

While it is lower than the rift escarpments, it lies on the highest elevation of Rift Valley Floor. Ojiambo (1992) recognized two systems operating in the area.

1. The Lake Naivasha subsurface seepage and the cold shallow groundwater system; and

2. The hot highly mineralized deep geothermal systems.

Piezometric plots and isotopic studies show that underground movement of water is occurring both axially along the rift and laterally from the bordering highlands into the rift. Analysis of piezometric map (Figure 4.6) and aquifer properties of the rocks in the area show that much of the subsurface outflow from the Naivasha catchment is to the south, via Olkaria-Longonot towards Suswa. Shallower aquifers may form a significant conduit for southerly flow.

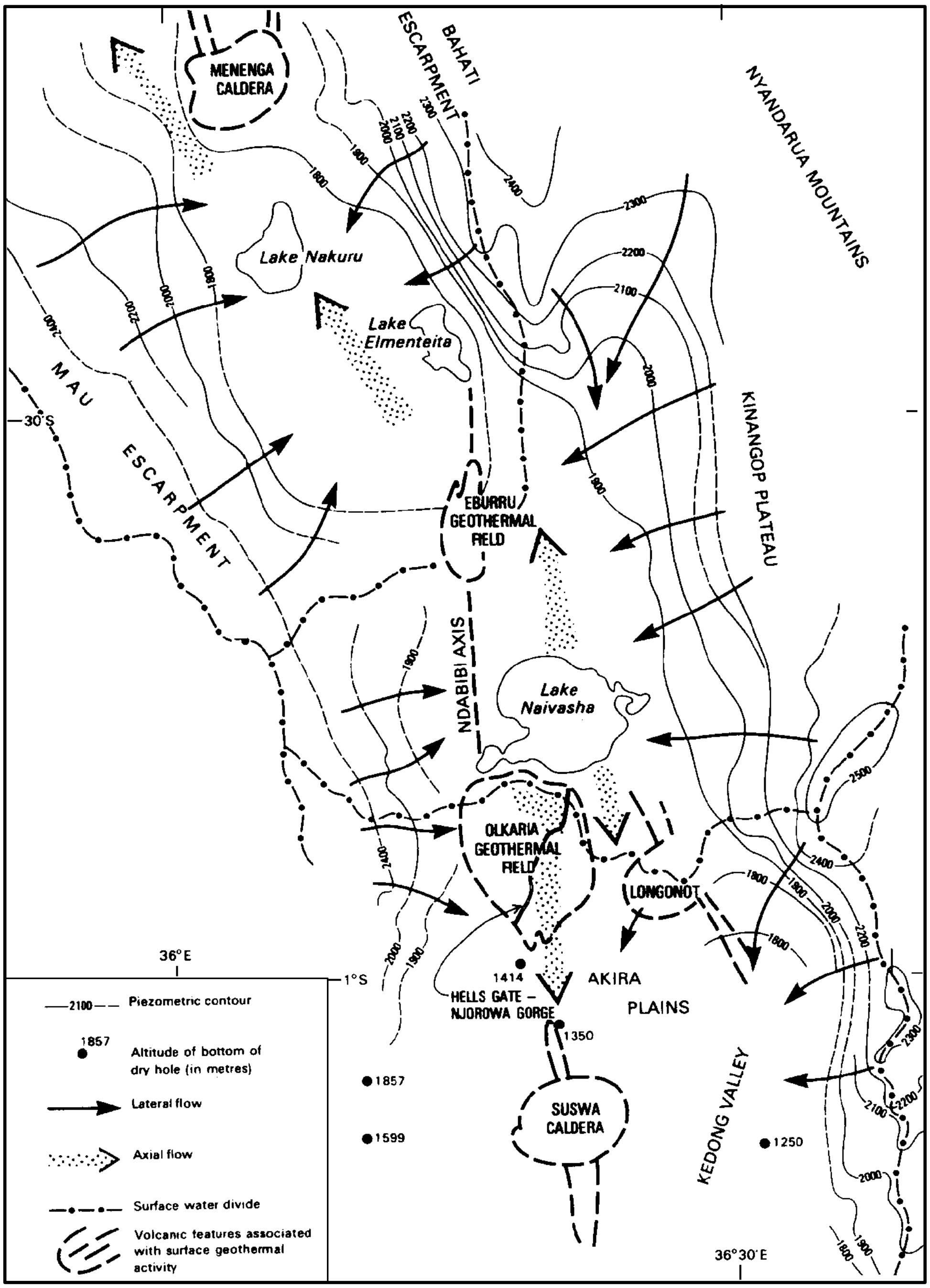

Figure 4.6 Piezometric Map of Lake Naivasha and Vicinities taken from Clarke (1990)

4.3 Hydrology and Morphology of Lake Naivasha

Located at an elevation of 1886m, Lake Naivasha is a freshwater body which is the highest among of all the rift valley lakes. It lies aon the rift valley floor with a mean depth of 4.9m. However, barometric profile of the lake bottom shows the central portion to be flat with the two deepest parts in the Oloidian bay (11.5 meters) and the Crescent Lake (18 meters).

Its size varies between 80-160m^2 in response to climatic inputs. The level of Lake Naivasha has been fluctuating during the past century. Since that time the lake level fluctuated in the order of an incredibly 9.5 meters. This has been attributed to the different use of the lake water for agriculture and domestic water supply to the inhabitants in the Naivasha and its environs. This dynamism has called for a lot of studies to really ascertain the cause of this phenomenon.

Its main tributaries are the Malewa and Gilgil rivers that enter the lake from the north.

4.4 Geomorphology

Three main geomorphologic units are found in the study area. In the western part lies the Mau Escarpment, the Kinangop in the east and the rift valley plain that the lake basin forms a part.

- **Mau Escarpment**

This forms the western part of the rift valley. The maximum elevation is more than 3000 meters above mean sea level and decreases in height in both north and south direction. It consists basically of soft and porous volcanic ashes and tuffs and stretches to a distance of about 36km within the map area. It is drained by river Marmonet and without surface watercourse into the lake except that it recharges the alluvium in the Ndabibi plain.

- **The Kinangop Plateau**

It forms the eastern margin of the study area and rises to an elevation of about 2750 meters above mean sea level. Its western margin has very steep scarp, broad flat plain and ranges in height from an elevation of 100m to 240m but at its extreme portion is buried with young pyroclastic rocks. It is deeply incised deeply by the tributaries of Malewa River. In relative terms, the crest is between 500 and 600meters to the rift floor but it is clearly distinguished from the floor by a lot of faulted basements. The plateau is composed basically of soft volcanic rocks.

- **The Rift floor Plains**

This is an area of moderate altitude that resulted from the time of formation of the rift. The highest elevation is about 2000m and is found in the vicinity of the Naivasha basin. The basin is largely covered with sediments derived from erosion of the surrounding volcanic rocks of the rift margins. They were deposited in the lacustrine environment during the Gamblian stage of the Pleistocene period and are usually referred to as the Gamblian lake sediments.

Surprisingly, the lake sediments are not thick and barely exceed 30meters (Thompson et. al, 1963).

The Naivasha basin is covered partially by quaternary alluvial sediments and composed of mainly sand, pebble beds and gravel having rounded pumice clasts (Stuttard et al, 1995).

Besides, the study area is characterized by various volcanic landforms (Figure 2.2). On the southeast side of the lake is Longonot Volcano while on the southwest side is the Greater Olkaria Volcanic Complex.

- **Longonot Volcano**

Longonot Volcano occupies an area of approximately 350 km^2 and attains a maximum elevation of 2776 masl. Unconsolidated pyroclastic deposits mantle the flanks of the cone. Arcuate lava flow fronts form distinct topographic features on its northern, eastern and southern slopes.

- **Greater Olkaria Volcanic Complex**

Unlike Longonot Volcano, the Greater Olkaria Volcanic Complex is composed of several volcanic centers. Most occur as either steep sided domes or as thick lava flows of restricted lateral extent. Groups of coalesced domes and lava flows form distinct topographic features that include the Gorge Farm-Kikiboni farm group of hills. Individual domes include the Olkaria Hill. East of Olkaria Hill is a fissure system along which there is a series of narrow, deep craters. The Ololbutot lava originates from the southern part of this fissure. Many domes form a topographically distinct arcuate alignment, which is thought to indicate the presence of a buried caldera (Clarke et. al., 1990).

An erosional channel cuts across the volcanic complex. The northern part of which referred to by Clarke, et. al. 1990 as 'Hells Gate' is a sinuous flat-floored feature, which extends southwestwards from the NE side of the volcanic complex. Pinnacles known as Fischer's Tower and Central Tower are volcanic necks exposed by the erosion of the surrounding pyroclastic rocks. The southern part which is referred to by Clarke, et. al. 1990 as Ol Njorowa Gorge is a narrow deeply incised gorge. The Hells Gate-Ol Njorowa Gorge is 16 km in total length and isolates a part of the volcanic complex referred to as East Domes.

4.5 Tectonic Setting

The Kenyan Rift Valley (KRV), as part of the eastern branch of the more extensive East African Rift Valley System (EARS), is linked to the regional dynamics of this system and its structural development (Figure 4.7). Active seismicity, volcanic activity and heat flux defining the edges of lithospheric plates characterize this system.

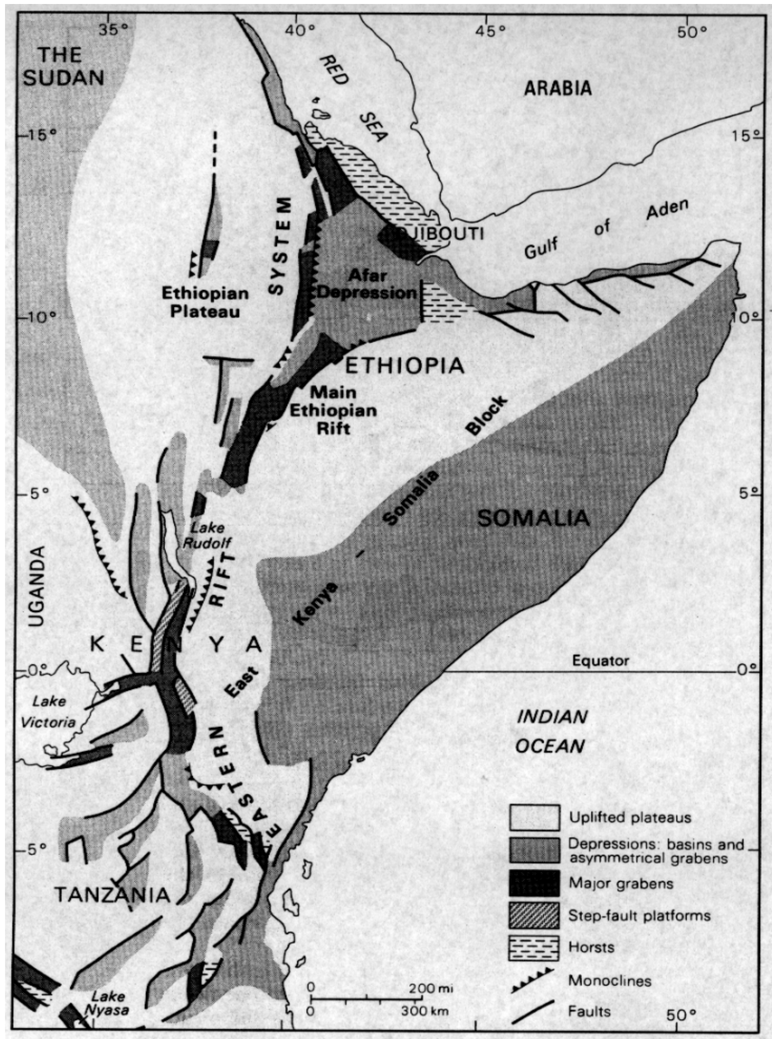

Figure 4.7 Tectonic Setting of East African Rift System (adapted from Baker, B.H., et. al., 1971)

The tectonics and volcanism associated with the Rift System resulted in the formation of the lake basins which include Lake Naivasha, fault scarps, mountain ranges and geothermal activities. The earliest rifting in the KRV started in the Early Miocene followed by updoming and extreme basaltic and phonolitic volcanism. The concept of a broad dome or shield structure has been considered by several authors as an integral stage of the KRV formation. The floor of the rift is highest in the center between Lakes Nakuru and Naivasha and decreases in altitude northwards towards Lake

Turkana and southwards towards Lake Magadi. These early volcanic rocks overlie Late Proterozoic schists and gneisses of the Precambrian Mozambique Belt. Rift faulting started during Late Miocene followed by basaltic, phonolitic and trachytic volcanism and extreme faulting in the Late Pliocene resulting in large volumes of trachytic ignimbrite tuff deposited in the Naivasha Sector. These rocks include the Mau and Kinangop Tuffs. Uplift and graben faulting created the rift structure by the end of the Pliocene. Fissure eruptions of trachytes and basalts on the graben floor occurred during the Early Pleistocene. Extreme rift faulting followed until Mid-Pleistocene, which resulted in the formation of horst and graben structures on the rift floor. Subsequent volcanism occurred in the Late Quaternary. The volcanic materials include Pleistocene-Holocene rhyolites, trachytes, basalts and phonolites.

Chapter 5 Geology

5.1 Introduction

Hydrogeology deals with water in relation to earth's composition. The movement and chemistry of groundwater is heavily dependent upon geology (Fetter, 1994). The geological properties of an area dictate the hydrogeology of that area. In this chapter an over view is given on the geology of the area of study. Attempts are made to discuss the key aspects of the geology. The influence of the different aspect of geology on the hydrogeology of the area has been hypothesized and discussed.

Four aspects that characterize the geology of area of study are:

- The area is geologically young
- The geology of the area is predominantly volcanic
- Other than volcanism, the other geological processes that have been responsible for the current geology of the area are: faulting, erosion and deposition-both lacustrine and fluvial.
- The various processes that operated in the area had limited temporal and spatial extent giving rise to complex geology.

It is these four aspects that characterize the geology of the area of study. In this chapter, I have chosen to postulate how the different aspect of geology of this area influences the groundwater occurrence, its chemistry, its movement and its availability for use in economic activities.

Though later in the chapter an attempt will be made to verify the published geological map in the context of hydrogeology using the limited geological sampling done during field work and data attained from driller's logs, most of the discussions are based on the work done by the numerous previous workers.

5.2 Field work

With the help of TM satellite images, geological maps, and topographical maps of the study area, distinctive features were identified for visitation during the field geological mapping. Geological observations were taken at 44 points. The locations at which observation were taken were ascertained with the aide of hand held Garmin GPS system. The location of observation sites is as shown in the map in figure 5.1 below. The observations made and their implications on the hydrogeology of the area is as shown in the table 3.4 shown below. The geology as discerned from the different out crops agreed with the published geological map of the area.

Geological Observations Points on Published Geological Map

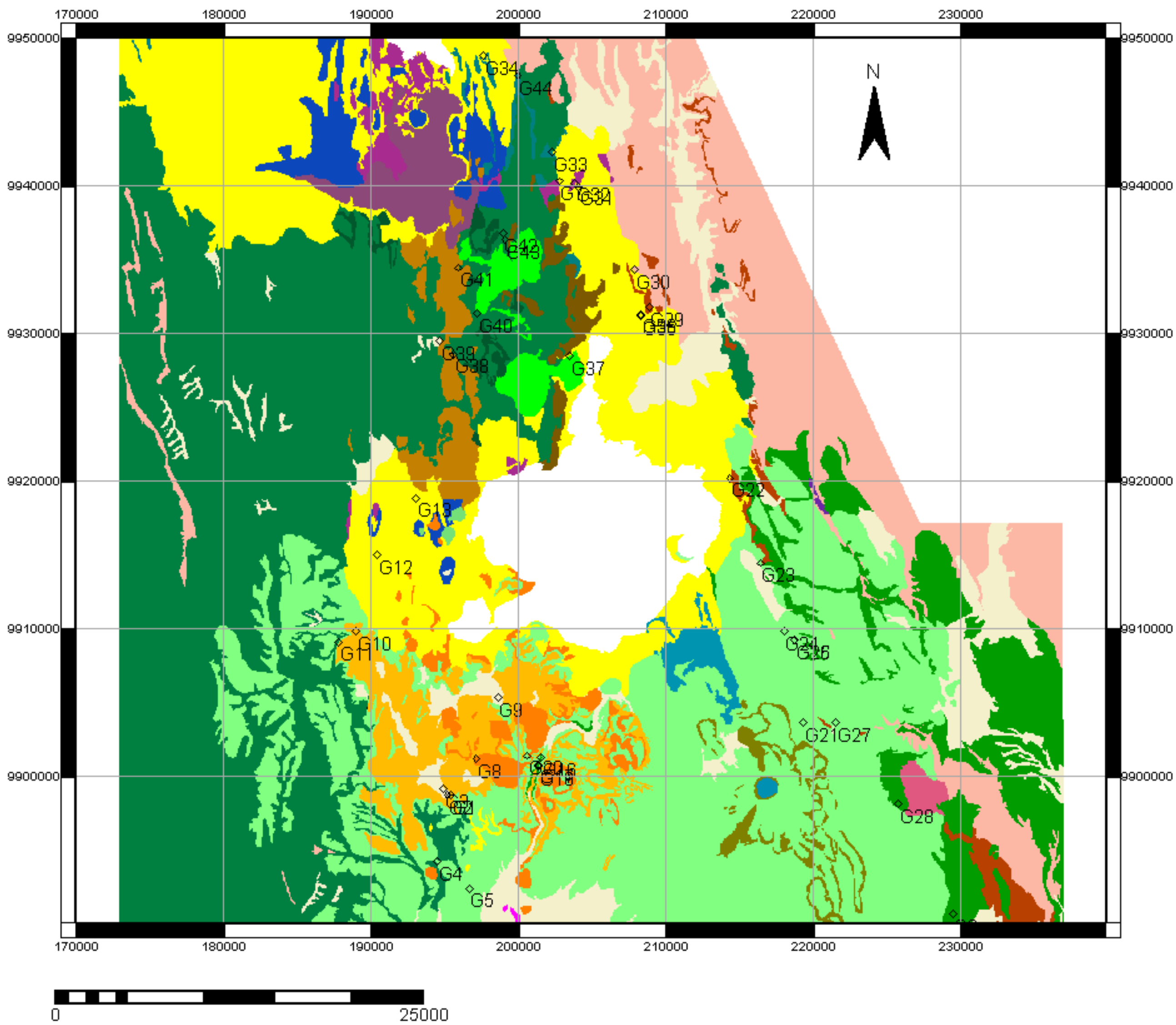

Figure 5.1: Points of Geological Observations. Observations made in the field agree well with the published geological Map of the Area. However, it is not indicative of their role in the Hydrogeology of the area.

5.3 Influence on the Hydrogeology

5.3.1 Influence of Volcanic Geology

Pumice and Lapilli: These are materials with very high porosity and permeability. Where they exist as outcrops, they constitute areas of high infiltration rates. In such cases, except where they are underlain by aquiclude, they never form aquifers but are a source of through flow that recharge aquifers or surface water body. In some places they have been reworked and undergone weathering resulting to formation of layers impervious “cakes” that impede the high infiltration rates.

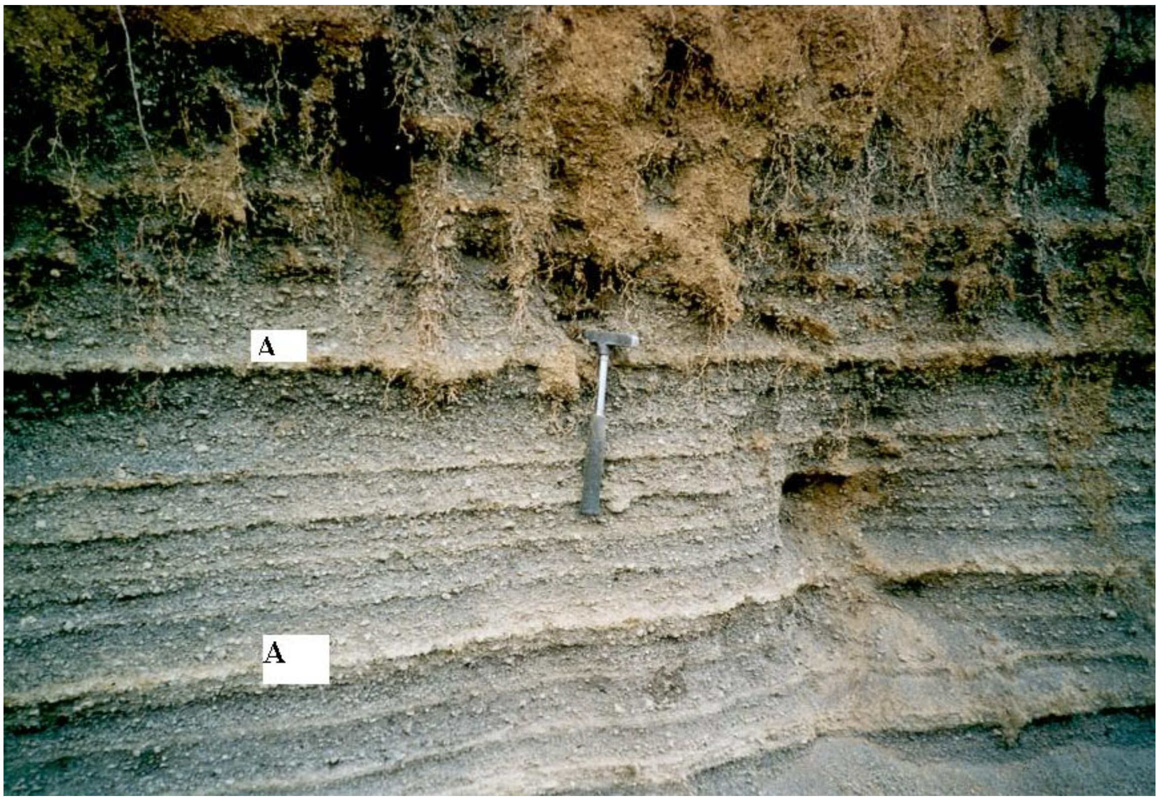

Figure 5.2.1: Deposit of Lapilli and Pumice as observed in the field. Impervious cakes A resulting from reworking of the formations tend to impede infiltration

Trachytes, Basalts and other lava flows: Their primary porosity is as low as 3% (Dingman, 1993). When they are unfractured, or unfaulted, they are characterised by very low primary porosity and hence constitute aquiclude. However, when faulted, fractured and weathered, their porosity and permeability improve tremendously. Under such circumstances, they locally constitute aquifers while at regional scale; they constitute preference flow paths for outflow or inflow

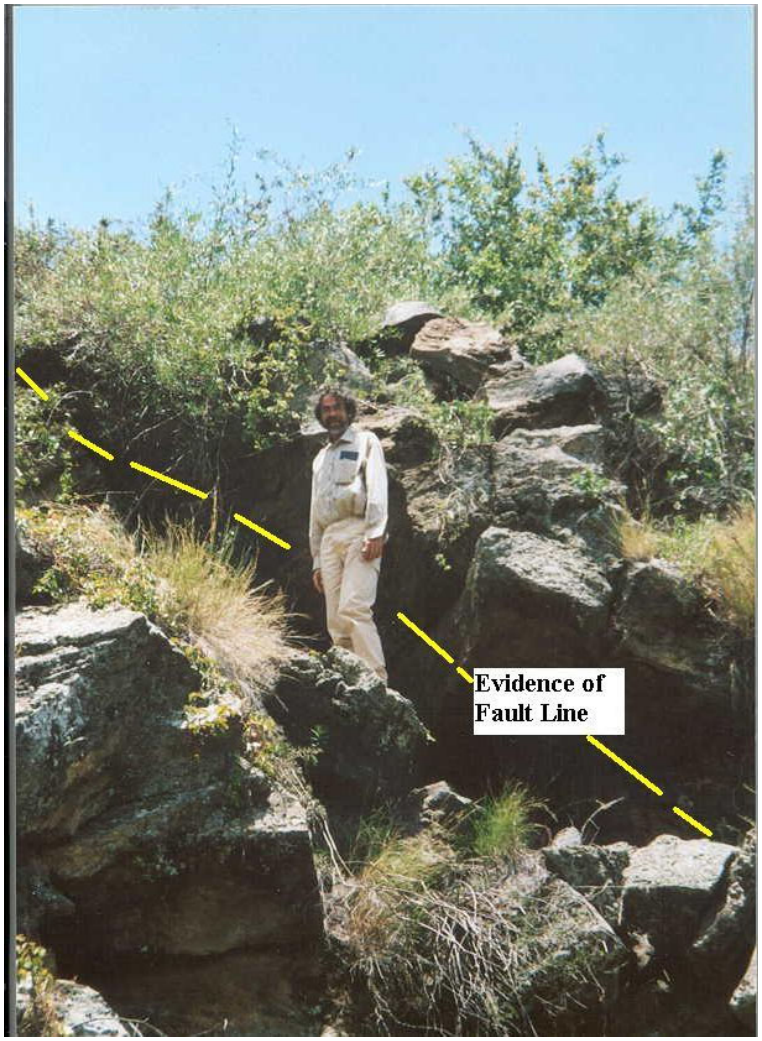

Figure 5.2.2: Faulting in Trachytes as observed at point G41. While due to low primary porosity Trachytes are aquiclude when fresh, they constitute aquifers when faulted and are preferential passages of outflow or inflow that influence regional flow pattern.

Tuffs and welded Pyroclastics: These constitute aquitards with very low conductivities however, once the former are weathered and the latter unwelded, they constitute good aquifers.

Volcanic Ashes: These are constituted of very small particles. Though they have very high primary porosity, their permeability is very low. If laid under water, constitutes an impervious layer, which if on the surface of earth's surface might impedes infiltration. It is because of this property that the water laid ashes and diatomite compose the nature lining for the runoff dams observed at point G2 and G3 in Table 5.1 and shown in Figure 5.2.3 below.

Figure 5.2.3: Volcanic ashes and Diatomites impede infiltration and hence constitute nature lining of surface water dams in the area of study.

5.3.2 Influence of Faulting, Erosion and Deposition (Fluvial and Lacustrine)

Other than volcanism, the other geological processes that have been responsible for the current geology of the area are: faulting, erosion and deposition- both lacustrine and fluvial.

Faults constitute discontinuities in rock sequences and hence control groundwater flow (Mazor, 1991) In massive rocks with no primary porosity; faults contribute heavily to the hydraulic conductivities of the aquifers. In the Naivasha area, it is faulting that accounts for the frequent and often drastic variations of the aquifer properties. McCann (1974) observed that due to extensive faulting, fracturing and weathering, virtually all-volcanic rocks in the area have some capacity to yield water to boreholes. With the help of TM images, a number of faults were delineated in the study area. As shown in the map of faults in the study area in Figure 5.3, most of the faults trend in the Northwest-Southeast direction. Consequently, the regional flow of groundwater is predominantly in the Northwest- southwest Direction.

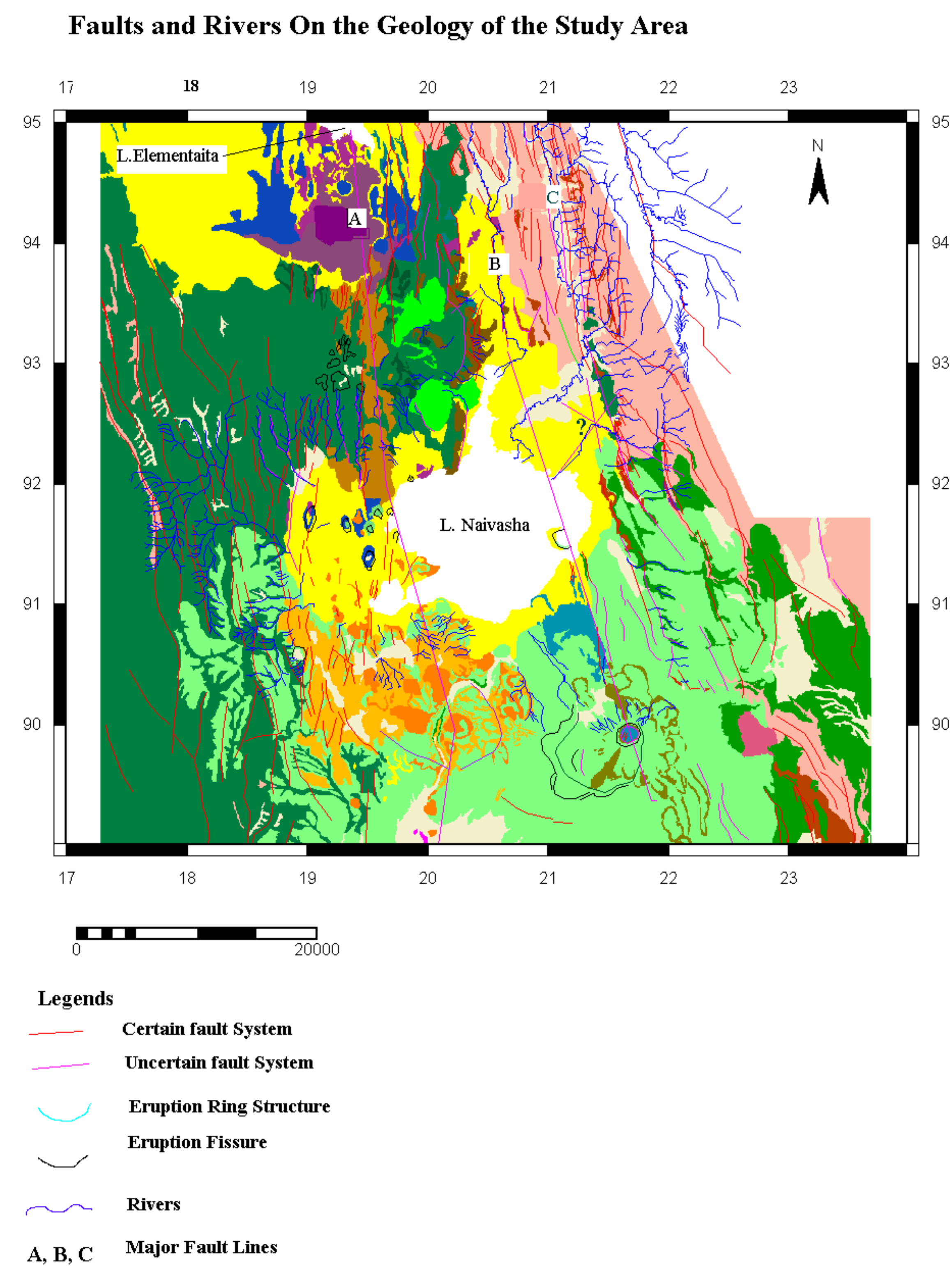

Figure 5.3: Faults drawn on the Geologic Map of the area. Besides, the faults that account for the Mau and Sitama escarpment, there are three major faults (systems) A, B and C that influence (d) the evolution and flow pattern of the study area.

On a large scale, faulting which gave rise to the rift system can influence the groundwater flow in two possible ways as shown by diagrams in figures 5.5.3a and b shown below.

Possibility a would either expose aquifers or place high conducting formation against impervious ones. These situations would both give rise to springs along the rift valley escarpments. However, there was no such springs observed on the Eastern escarpments and there is no documentation of any such springs on the western escarpment.

In scenario b, there is a tilting of blocks way from the fault resulting into reversal of flow direction away from the fault. With no springs observed or reported on the escarpment, it is probable that scenario b holds. `

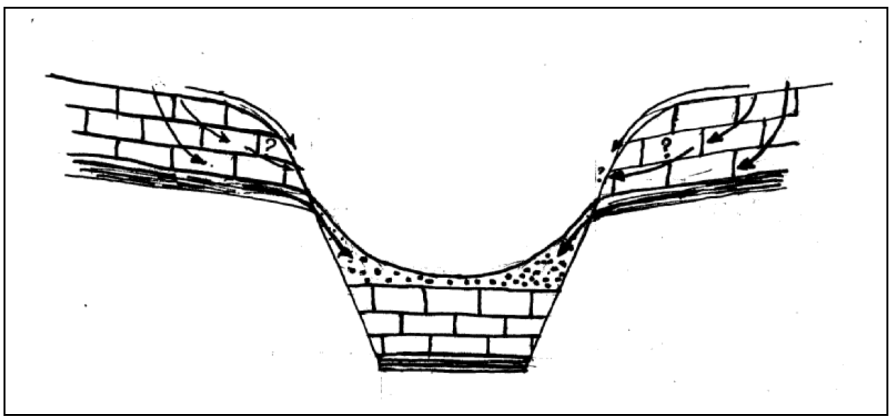

Figure 5.3.3a. Possible influence of Fault, which would give rise to, springs at the escarpments

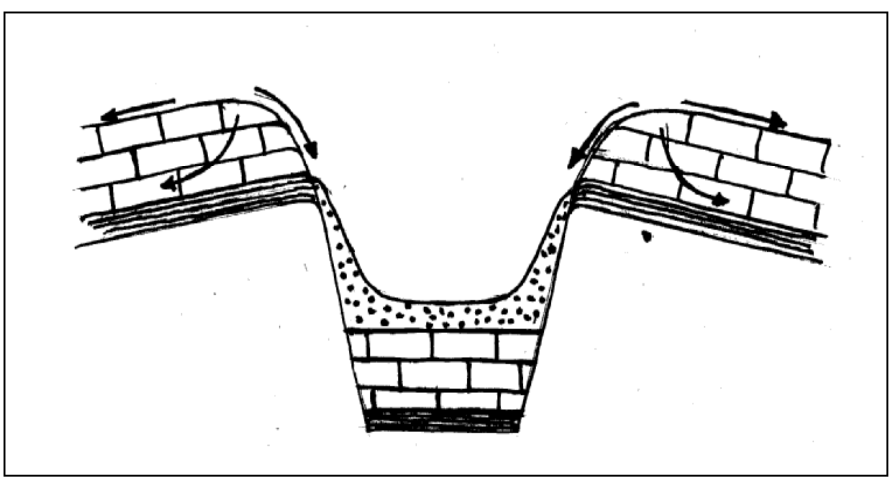

Figure 5.3.3 b Alternative influence of the Faulting which probably hold in the study area.

5.3.3 Influence of Temporal and Spatial Limited Extent of Geological Processes

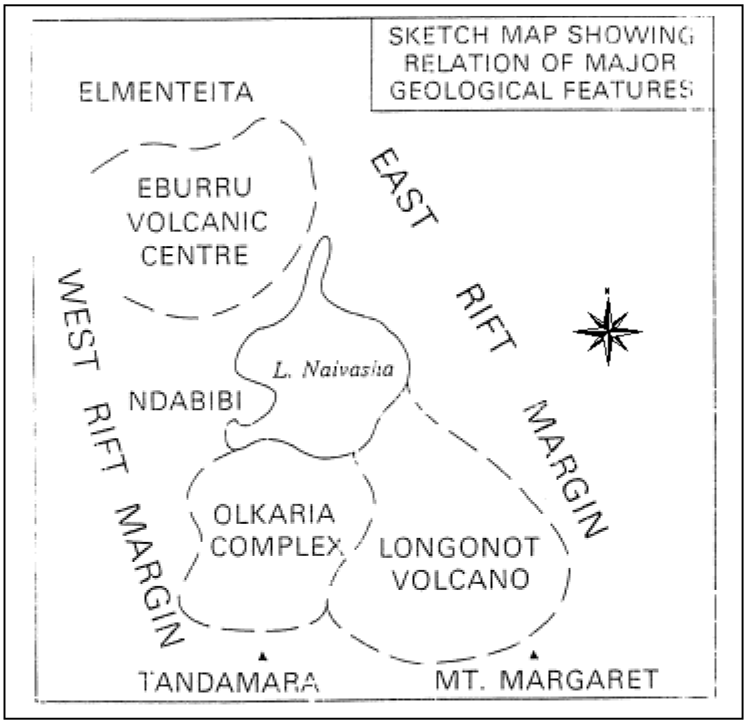

Figure 5.3.4 Map of Study Area Showing Major Volcanic Features and Events (Geological Map of Longonot Valcano, Min of Energy, Gov of Kenya, 1988)

5.4 Definition of boundaries Conditions and Choosing of No flow Boundaries/ Hypothesis Of Boundary Conditions

In this section I postulate a three-layered aquifer system:

- First shallow unconfined aquifer
- Second deep and confined aquifer
- Third confined geothermal aquifer

I hypothesize that the boundary conditions for different aquifers are non-coincident due to varying horizontal extent. See figure 5.4

The aquifer in the immediate surrounding of the lake is unconfined and in hydraulic link with the lake. It could be represented more like a large perched aquifer. From the lakes it extends more to the north than to the south. In the North it extends as far as the escarpments north of the Three Point farm while in the south of the lake it hardly goes beyond Moi South Lake road. It has a very limited extent in the south of the lake. Its boundary is dictated by the extent and thickness of the sedimentary formation, the water levels of the lake and the elevation of the aquiclude at its base Consequently, it varies in space with time depending on the recharge.

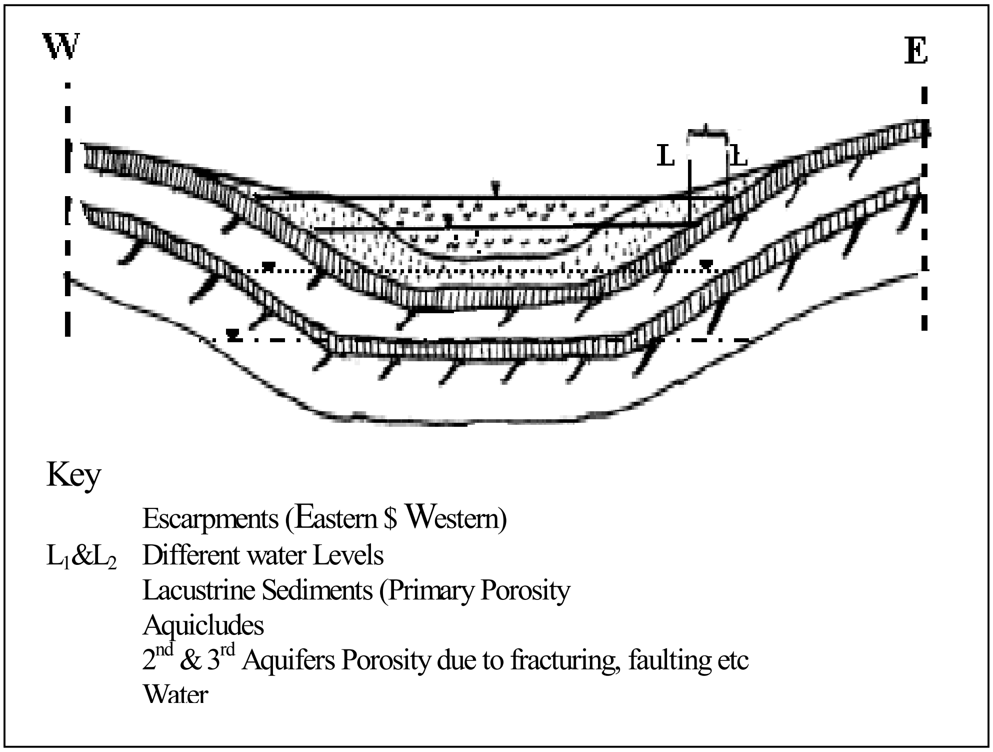

Figure 5.4 Postulation of the E-W Aquifer Section for the area of Study. Aquifer boundary for first aquifer varies from L1 during low water levels of the lake to L2 for high water level

The boundaries of the second aquifer concur with the surface water divides. To the east and west of the rift valley, the Mau escarpment and the prominent escarpments along the Marmanet and Sattima faults form the respective groundwater no flow boundaries. The adjacent respective faults constitute drainage channels boundaries and/or constant head boundary. To the north the boundary is a no flow boundary comprised of the hills south of the Lake Elemeitaita. These hills are composed of the Eburru Trachytes and lava flows. Further to the North Eastern, the boundary is still a no flow boundary composed of hills made of the Kinangop tuffs. In the south the boundary is also a no flow boundary coinciding with surface water divide. It is comprised of the Longonot hills composed of basalt, tranchytes and pyroclastic cones and the Olkaria Hills composed of Olkaria comendites (lava flows and welded pyroclastics

The boundaries of the lowest aquifer (geothermal aquifer) coincide with those of the middle aquifer in the western and the eastern sides of the rift valley. However to the north and to the south, seems beyond the boundaries of the study area.

Station	**x**	**y**	**Altitude**	**Observation**
G1	195422	9898704	2057	Stretch of undulating/ rolling terrain. No evidence of surface runoff.
G2	195178	9898704	2036	Flood Zone, no infiltration as water is reported standing here for over 3 months. The Diatomite are very impervious constituting bases of both man made and nature dams. These diatomites also affect the infilteration rates or stop it totally.
G3	194893	9899174	2028	Here, diatomites and water laid ashes/ tuffs are some of the major impervious layers. Photo of dam was taken.
G4	194518	9894250	1846	Pumice High infiltration rates.
G5	196636	9892388	1704	Epheral river
G45	198990	9889570	1648	Maasai Watering Points Large tranchyte chunks, which appear to have been carried to the location, an occurrence that appears like a geological puzzle. These chunks were covered by volcanic ash, which appear to have been water laid. There seems to have been some river channels which have been time back as evidenced by boulders of rocks which are rounded
G6	229473	9890642	1800	Layers of yellow/cream rock deposits similar to those seen in Kinangop Gorge in hell's gate National Park.
G7	202767	9940318	2016	Boreholes near to the Tranchyte or basaltic rig west of the well
G8	197163	9901180		A lot of Obsidian, a lot of Lava formation
G9	198606	9905368		Hot Spring
G10	188983	9909782		Point with Depression
G11	187795	9909092	2085	Boreholes, 218 m deep. Evidence of alluvial incision, visible 20 m away. Lapilli are observed.
G12	190471	9914988		Suffotion
G13	193033	9918828	1929	Geologically reworked pumice/tuff to a depth of 29.4m
G14	194374	9919312	1933	Ndabibi B's farm swl=42.2
G15	194607	9918648		swl=37.2
G16	201485	9901258		Zoelite=yellow color, Formation is 600000 yrs old
G17	201367	9900804		Sedimentary formation/deposits
G18	201372	9900724		Ignimbrite=100000yrs old
G19	201345	9900676		At bottom of the valley, water lied ashes are seen. They are cemented by li
G20	200609	9901409		Olkaria Power Center
G21	219284	9903640		Suffotion, loose Sands.
G22	214333	9920198		Tuff/tranchyte rig running parallel to Nairobi- Naivasha road until Kijabe, Longonot area.
G23	216386	9914430		Tuff ridge
G24	218002	9909826	2062	Dry well drilled. Cuttings manifest tranchytes.
G25	218698	9909244	2095	Pumice High infiltration rates. It interrupts the tuff/basalt ridge.

G26	218698	9909246		Very deep gully near longonot trading Center. The lithology is made Up of soft intercalation smof reworked Pumice and volcanic dust Covered by recent alluvium deposits. The gully is over 3 meter high.
G27	221490	9903662		Mounts/riles of pumice covered with a layer of decayed pumice. Though The Pumice is highly permeable, in some areas the surface is altered to give a less permeable cake that impedes the infiltration, hence Facilitating run off.
G28	225747	9898150	2073	At the base of Kijabe hills. Tuff covered by pumice
G29	208856	9931824		Sedimentary formation covering pumice which in turn covers Diatomite's
G30	207858	9934308		An outcrop of pyroclastics. Near by, there is a deposit of diatomite.
G31	204025	9939974		Basalts overlaying Paleosoil beneath which pumice lapili overlaying sedimentary formation
G32	203775	9940220		Water Laid sediments overlaid by basalt. A lot of salt observed at this point, this salt could Suggest hydro continuity between this place and the saline Eleimentaita Lake.
G33	202312	9942292		Ebburu Trachytes, moved up and exposed at this point
G34	197612	9948784		Lake sediments, 200m from Diatomite industry.
G35	208314	9931186	1889	Newly drilled well at elevation of 1886m in Beauty line. Sandy l oam soil overlaying yellow sediments. This over lies reworked pumice. SWL=15.05m
G36	208279	9931282	1927	Second well in the beauty line farm
G37	203482	9928460		Maasai Gorge.
G38	195595	9928618	2542	Steam Harvesting
G39	194638	9929486	2571	High infiltration.
G40	197175	9931362	2311	High rates of infiltration zone.
G41	195951	9934470	2162	Junction of fault. Infiltration rates.
G42	198970	9936740	1971	Surface dam with very fresh water
G43	199092	9936336	1991	Approximate Position of form/ old well
G44	199940	9947438		Escarpment. No flow boundary.

Table 5: Geologic Field Observations. The Observations are in agreement with published surface geologic map of the area

Chapter 6 Hydrogeology

6.1 Introduction

In this chapter the groundwater flow pattern is discussed. The use of hydrochemistry and stable isotopes as basis of explaining the flow direction of groundwater is explained. Topographic and geological profiles are drawn in nine directions and discussed as basis to derive the nature of the aquifer material. Temporal variation of water chemistry in 8 different wells is also studied and presented here. Also included is the investigation of the correlation between the depth and water chemistry as well as the correlation between yield and water chemistry.

6.2 Historic Piezometric Heads

In the lake Naivasha Catchment, groundwater generally flows towards the lake from the Mau and Aberdare escarpments, although it is diverted locally by the presence of faults that form either barriers or conduits (McCann, 1974). The congestion of piezometric contours on the eastern side of the lake suggests a high gradient in the piezometric heads, an occurrence that is indicative of low permeability. This coincides with the presence of faults in this place. Consequently, it is probable that here the faults constitute barriers rather than conduits.

Flow direction lines drawn on the historical contour map indicate that the flow is laterally from the eastern and western escarpments towards the Lake, and axially from Lake Naivasha northwards towards lake Elementaita and southwards from towards the Longonot area. The piezometric contour lines around Lake Elementaita as drawn by Gitai (1998) shown in figure 6.2 fits well with the northern portion of those drawn around Lake Naivasha by Owor (2000) shown in figure 6.1 below.

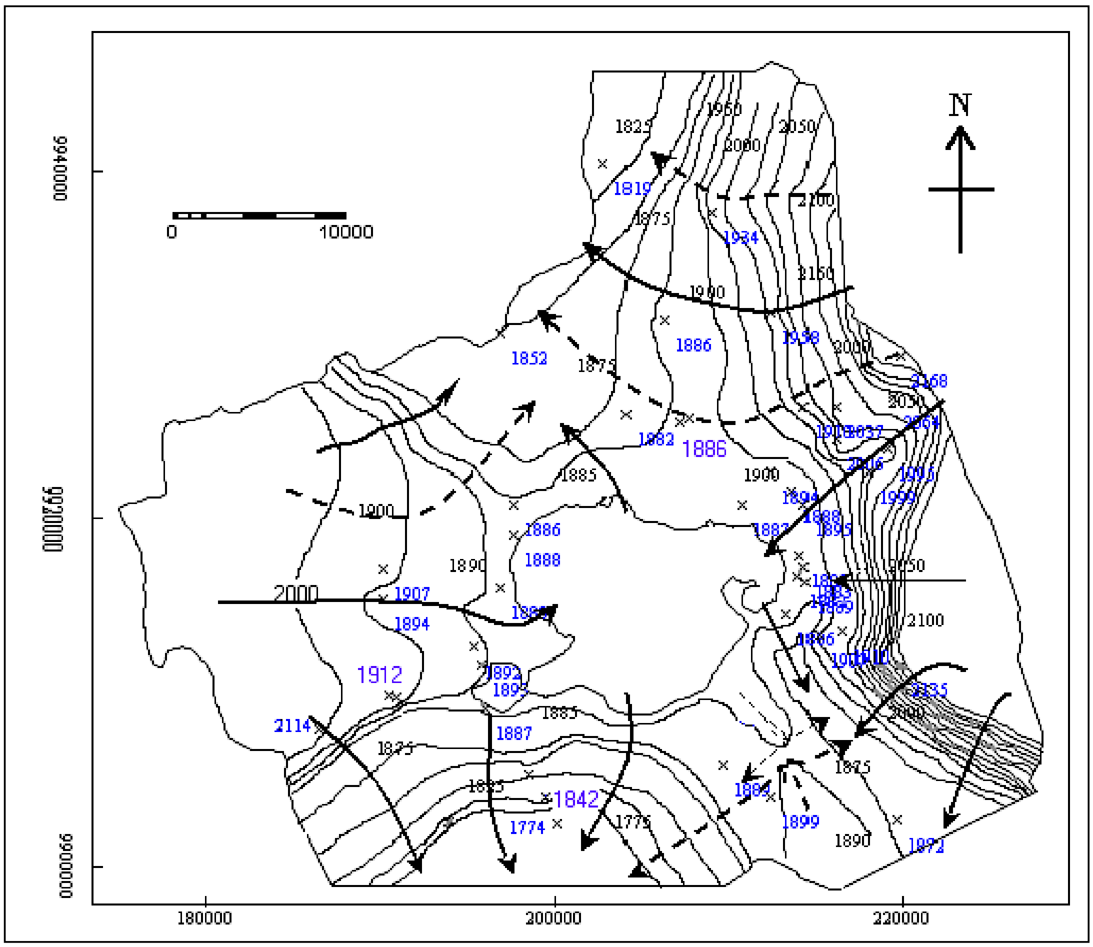

Figure 6.1 Flow Directions as Dictated by Historic Heads of 1980. (Piezometric Map from Owor, 2000)

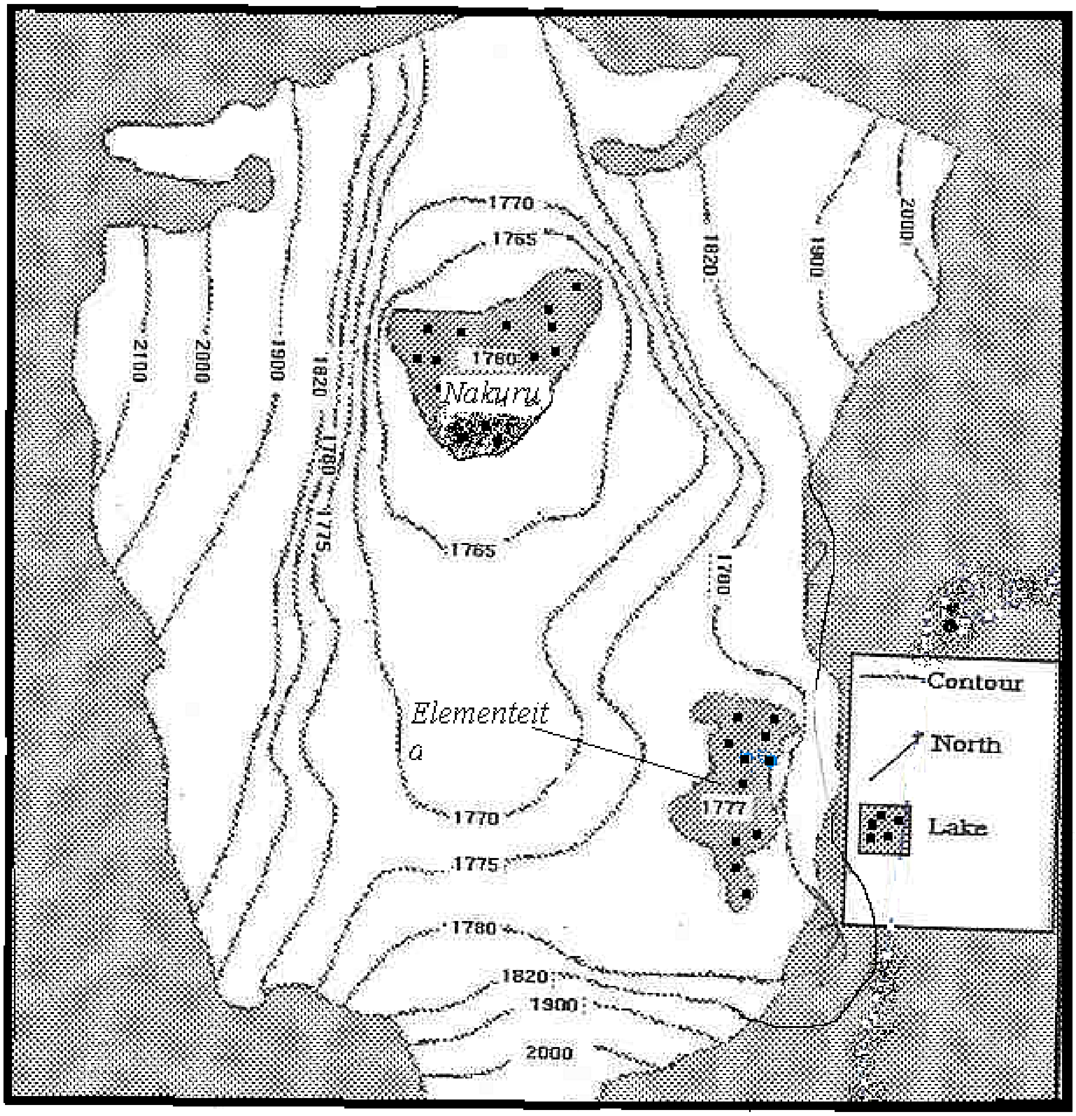

Figure 6.2 Piezometric Contour lines as Drawn by Githaei (1999)

6.3 Modified Piezometric Heads

This is a modification of the piezometric as drawn by Owor in 2000. Adjustments have been effected to reflect corrections based on the knowledge attained from recently drilled wells, newly leveled wells and the wells in which the water levels were measured during fieldwork. Attempts to draw the piezometric map using surfer software proved impropriate as it necessitated high concentration of point, a conditionality that could not be full filled in the entire area of study. To easy the applications of human intuition, the wells were plotted with Ilwis program but the contours were drawn using free hand. The resulting piezometric map is shown on figure 6.3.1. Away from the lake where the gradient was high, a contour interval of 25 m was used. However, close to the lake the interval is reduced to 5 meter.

Though the flow patterns have remained basically the same, there has been a change details. The piezometric contours indicate a development of sink on the Northeastern side of L Naivasha around Three Point Farm and Manera Farms. There has not been a major change in the flow pattern. According to the 1980 peizometric contour map above, there has been a fall in the piezometric heads in the Northwestern part of the study area. Consequently, the area around Three Point Farm and Manera Farm, could account for the change in the flow direction.

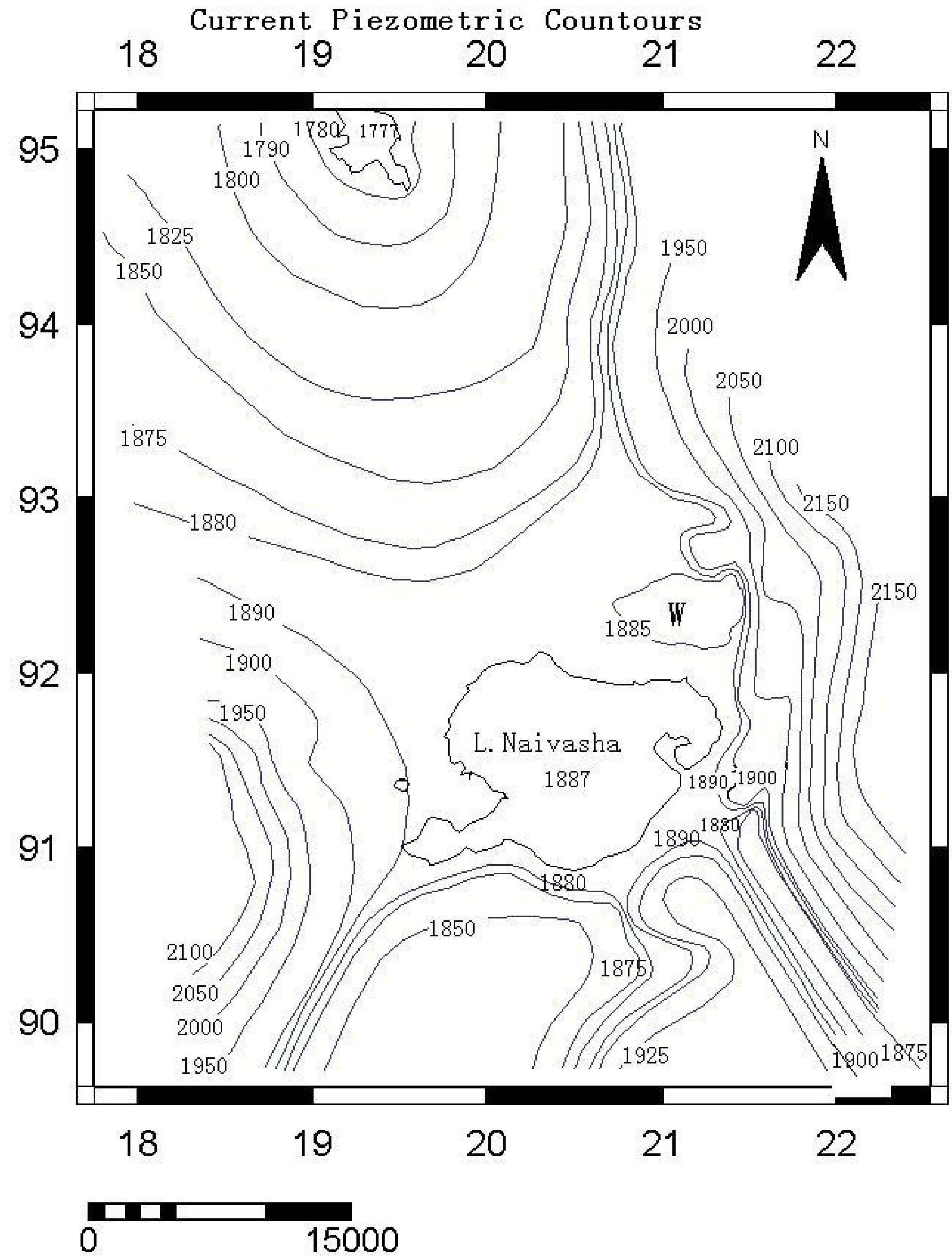

Figure 6.3.1: Current Piezometric Head Contours. W indicates the depression due to extraction from the well field.

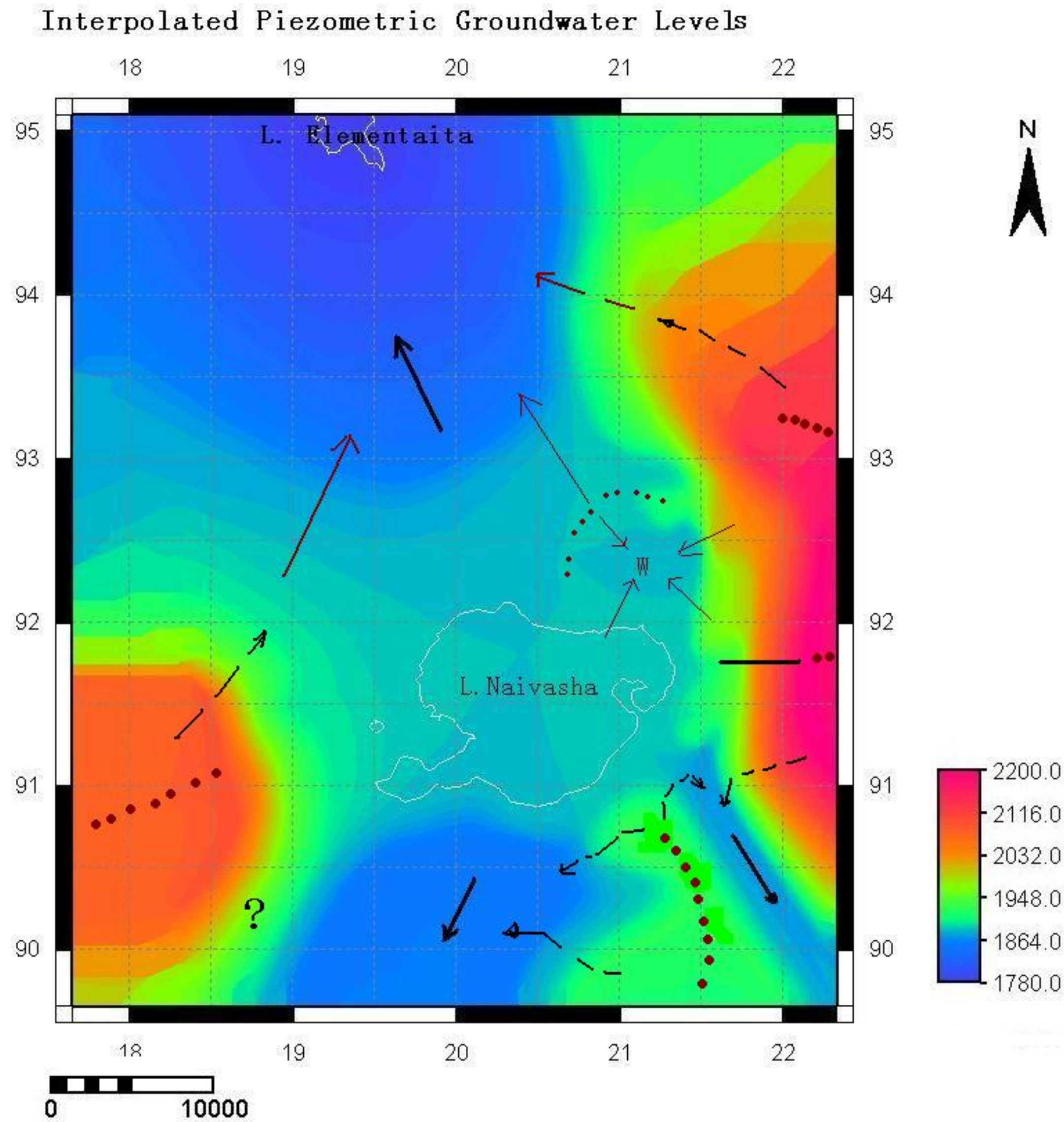

Figure 5.2: Interpolated Piezometric Head Contours. The Arrows indicate directions of flow, broken and thin ones indicating uncertainty. Dots show possible location of no flow areas. The question mark is area with very complex hydrogeology. Though the piezometric map suggests levels near surface, most of the wells drilled here are dry. W is depression in piezometric Heads due to extraction of excessive groundwater northeast of lake Naivasha.

6.4 Integration of Ionic Chemistry, Isotopes, Piezometric Heads, and Geology

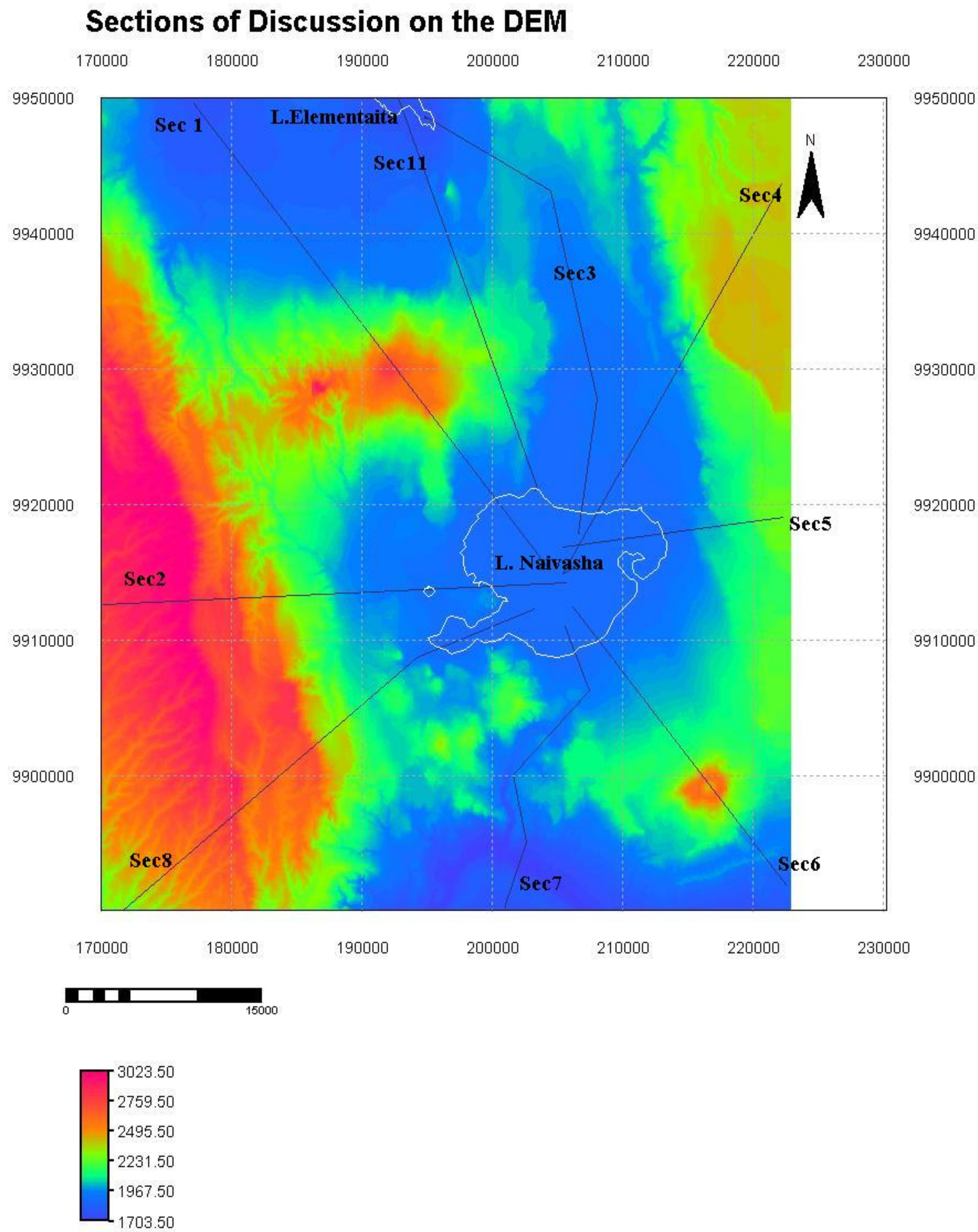

Figure 6.4: Sections along Which Hydrogeology is Discussed

6.4.1 Hydrogeology of Northwestern Part of Study Area

The hydrogeology of the northwestern part of the lake is based on four parameters: piezometric heads, isotopic signatures, ionic chemistry and geology. The sections together with the position of the wells along the section11 are shown in the figure 6.4.1.2 and 6.4.1.3 below.

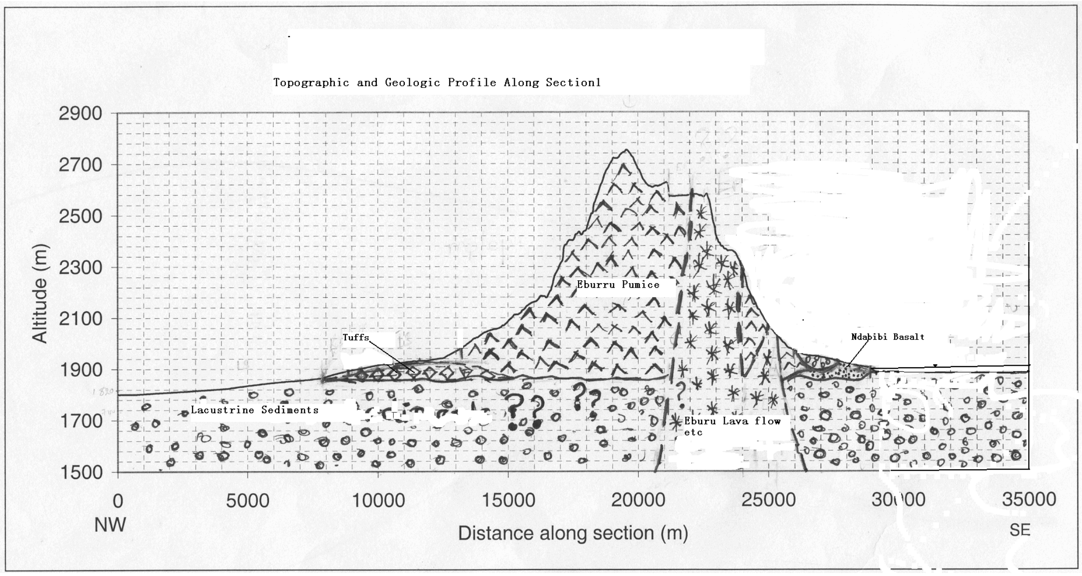

Figure 6.4.1.2: Geological and Topographic Profile Along Section 1. The sediments surrounding Naivasha and those surrounding Elemeitaita Could have been Previous connected

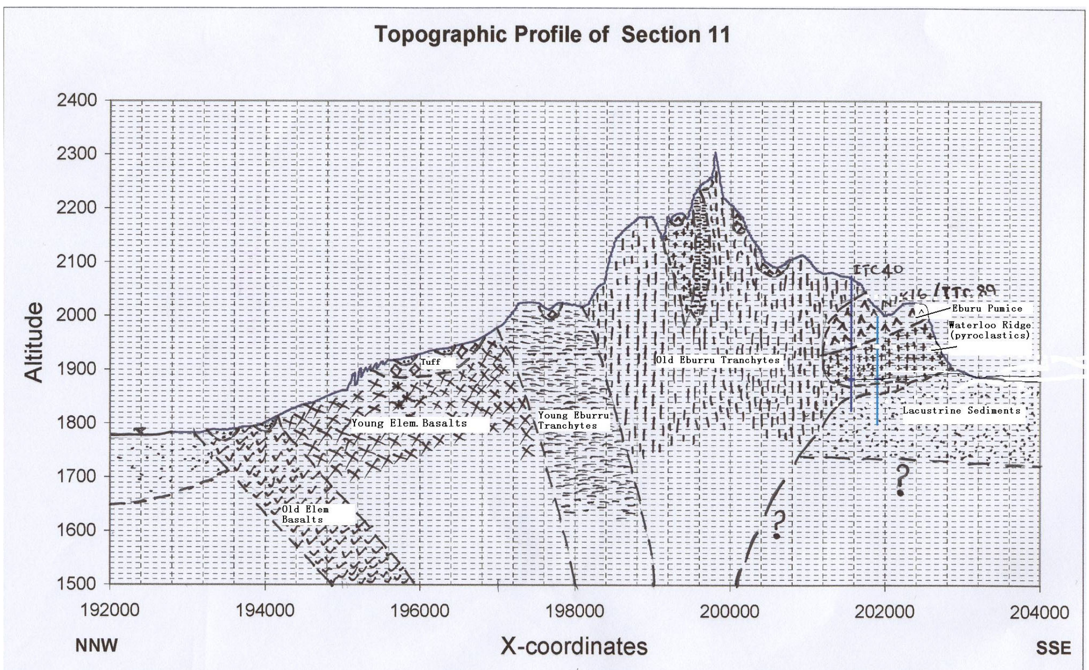

Figure 6.4.1.3: Geological and Topographic Profile Along Section 1. The sediments surrounding Naivasha and those surrounding Elemeitaita Could have been Previous connected

Besides, the topographic profile together with the corresponding geology as postulated from the published geological map and drilling logs is also presented.

The piezometric head of well ITC040 is 1884m a.s.l and that of lake Naivasha is 1886m a.s.l. This suggests that water flows from the lake towards Eburru ranges via Green park area.

The isotopic signatures of the water in wells ITC040 and ITC089 ascertain the assumptions. The mean $\delta^{18}O$ of lake Naivasha water is 6.5 $^{o}/_{oo}$ and that for direct recharge from rainwater is –5.75 $^{o}/_{oo}$ (Boateng, 2001). The value for well ITC089 is 0.05 $^{o}/_{oo}$ (Boateng, 2001) while that of well ITC040 was sampled and its $\delta^{18}O$ value found to be –0.44 $^{o}/_{oo}$. The composition of the water in wells ITC040 and ITC089 can be explained as being a mixture of direct recharge from rainwater and the lake water. The ration of lakw water vs direct recharge from rainfall to well ITC040 and found out that it accounted for 43% of lake water. The well ITC089 has more lake water of 43% and 53 % direct recharge from rainwater.

Assuming the water from well ITC40 has a ratio *x of* lake water and the rest being from direct recharge from rainfall, then:

$$6.5\delta^{18}Ox + \{-5.75\delta^{18}O(1- x)\}= -0.44\delta^{18}O$$
$$12.25\delta^{18}Ox =5.31\delta^{18}O$$
$$x =0.43 \text{ or } 43\%$$

This means that the water in well ITC040 is about 43% lake water and about 57% direct recharge from rainwater. Similarly,

$$6.5\delta^{18}Ox + \{-5.75\delta^{18}O(1- x)\}= 0.05\delta^{18}O$$
$$12.25\delta^{18}Ox =5.8\delta^{18}O$$
$$x =0.47 \text{ or } 47\%$$

Hence this well has about 47% lake water and 53% direct recharge from rainwater.

These mixture ratios indicate that well ITC089 has more of the lake water than well ITC040. This implies that lake water first reaches the former before the later. This occurrence supports the above postulation that that water moves from the lake through Green Park area to Eburru ranges.

The graph in figure 6.4 illustrates the trend in ionic chemistry along the transect. While the average EC of lake water is 330us/cm (Munoz, 2002) that of water from well ITC89 and well ITC40 is 801us/cm and 1160us/cm respectively. Which means that as water flows from the lake to well ITC40 through well ITC089, dissolving solutes on the way resulting to an increment of EC of 830us/cm. Other ionic concentrations also increase in the same direction except for Mg.

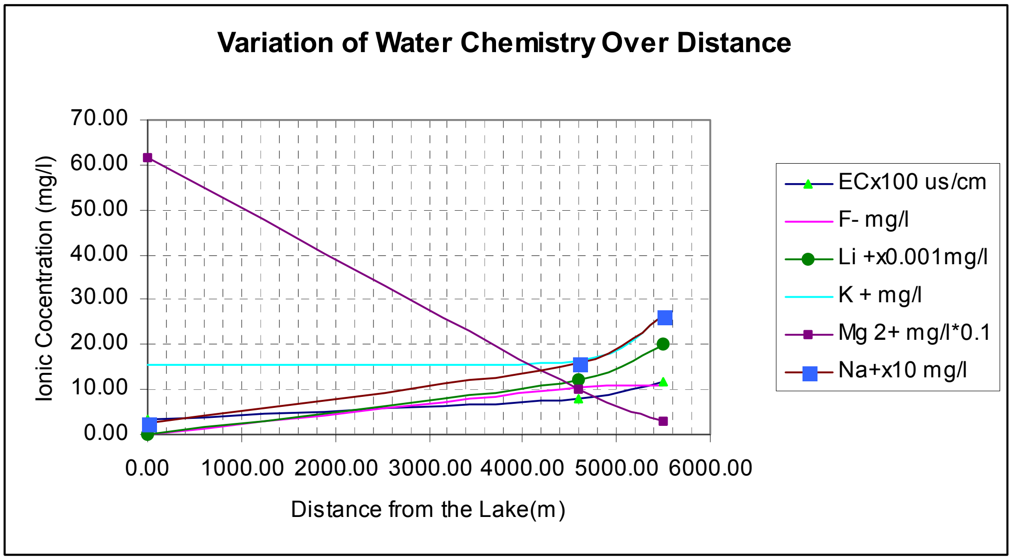

Figure 6.4.1.1: Trend of water chemistry along Section11

From the geological map these well should be drawing water from volcanic rocks. If such is the case, then for the water chemistry to change by such a range, it must interact with the rock for an extremely long period of time.

Based on the assumption the time for water to flow from the lake to well ITC040 was calculated. The effective porosity of aquifer was assumed to be 0.1. The distance between the well and lake was 5500m (based on modeling conducted in GIS using ILWIS. The velocity was calculated based on Darcy's law, $V_e = K\frac{dh}{nedl}$ and further calculated the time. As shown below the result indicate that it will take 14 years

Peizometric head of the lake and well ITC40 are 1888m asl and 1885 respectively From ilwis, the distance between the Well and Lake is 5500m.Transmissivity of aquifer of sedimentary origin in the area = 5960m2/day (Behar, 1999) From drillers logs, the thickness of Aquifer (D)= 25m.

$$Time(t) = \frac{Distance(l)}{Effective Velocity, Ve}$$ -------------------------------- ---- i

From Darcy's law,

$V_e = K \frac{dh}{nedl}$ ---ii

From the hydraulic Heads, dh=1888-1885=2m and from T=KD, K=238m/day, From which, V_e =1 m/day, giving a Time of travel of 13 years.

This is a very short for such a drastic change in the water chemistry to occur! This casts more doubt on the possibility of the aquifer being volcanic in nature.

Consequently, the change in water chemistry cannot be fully explained by the mere dissolution of ions from the rocks as the distance over which it flows from the lake to the well is just over 5km. See graph in figure 6.4 above for the change of water chemistry with distance. It is thus unlikely that the water flows through volcanic rocks and thus draws all the ions from there. Indeed studying the drilling log of well ITC40 reveals that the aquifer is of sedimentary origin. It is thus evident that the aquifer in this portion of the study area is of sedimentary formation. Besides, the change in the ionic concentration of Mg cannot be explained for water flowing through volcanic rocks. However, sediments absorb Mg and hence reduce its concentration in water (Ojambo, 1992). Therefore, it is possible that the Mg is absorbed by the sedimentary aquifer as it flows away from the lake. This provides more support to the assertion that aquifer material is sedimentary.

If such is the case, it is possible that the sedimentary formation contains intercalations of lenses of salt deposits, which are dissolved fast by the water as it flows along. It should be the dissolution of such lenses that accounts for the big increment in the EC of the water over such a small distance.

My interpretation of the geologic profile according to the published geological map (Gov of. Kenya, 1988) as it stands now is also presented on the topographic profile. The boundaries between individual units are a mere approximation as no data could was ascertained on the stratigraphy of the rocks since there are no wells.

There seem to have been a single layer of sedimentary formation that covered the rift flow at one point in the past (approximately middle Pleistocene). The Elementainta

Sediments and Naivasha Sediments could have been separated by eruption of lava, which interrupted the continuity of the sedimentary formation. This volcanic lava constitutes the no flow boundary condition on the northern/ part of the catchment. It is also possible that subsequent episodes of depositions from reworking and erosion of different volcanic materials occurred differently in the two basin. Depending on the mother materials, the products of these subsequent erosion-deposition materials could be different in the different basins. The underlying formation could have undergone faulting. It is through these faults that eruption of lava could have occurred.

There are no wells situated along section 1. The influence of piezometric heads, isotopic signatures, and ionic chemistry cannot be illustrated along this section. However, there is a marked similarity in the stratigraphic setup of section11 along which variations in the various aspects have been used to explain the hydrogeology, and section1 for which explained. It's thus logical to assume that the foregoing explanations also hold for section1.

From the foregoing discussion, it is evident that the aquifer material is sedimentary and the volcanic rocks act as the confining layer. All aspect of groundwater of groundwater support the assertion that water in this portion of the study area flows towards Ebburu ranges.

6.4.2 Hydrogeology of Northern Part of Study Area

The trend of the piezometric heads along section 3 seen in figure 6.4.2.1 below indicates that water flows from lake Naivasha northwards towards Lake Elementaita, which is in conformity with the general piezometric contours discussed in section 6.2 and section 6.3 above.

The drastic increase in the piezometric head immediately north of well ITC026 is indicative of a decrease in transmissivity from that point on. This could be a result of a decrease in the thickness of the aquifer, or/and a change of aquifer type to one of lower decrease in hydraulic conductivity. Well ITC026 is a shallow hand dug well, 13.5m deep drawing its water from lacustrine sediments. While interpretation of the geological cuttings from recently drilled well ITC183 gives the thickness of sand at that location as 8m. This suggests that the thickness of sand decreases northwards away from Lake Naivasha and its hydrogeological relevance as an aquifer ceases after well ITC026 at approximately y-coordinate 9930000 along section 12. There after, its hydro geological role is limited to the facilitation of infiltration. The water rest level of ITC183 is15.05 m below the ground level, a depth is much greater than the thickness of the sedimentary formation at this point. Reworked pumice and tranchytes were identified at the drilling site ad the most predominant cutting and the last cutting to be collected from the well respectively. Hence the aquifer of this well is not sedimentary, it should be the reworked pumice that forms while tranchytes forms the aquiclude in this well. With the aide of the published geological map of the area, the aquifer could be classified as being unwelded pyroclastics from waterloo ridge and the aquiclude as Gilgil tranchyte.

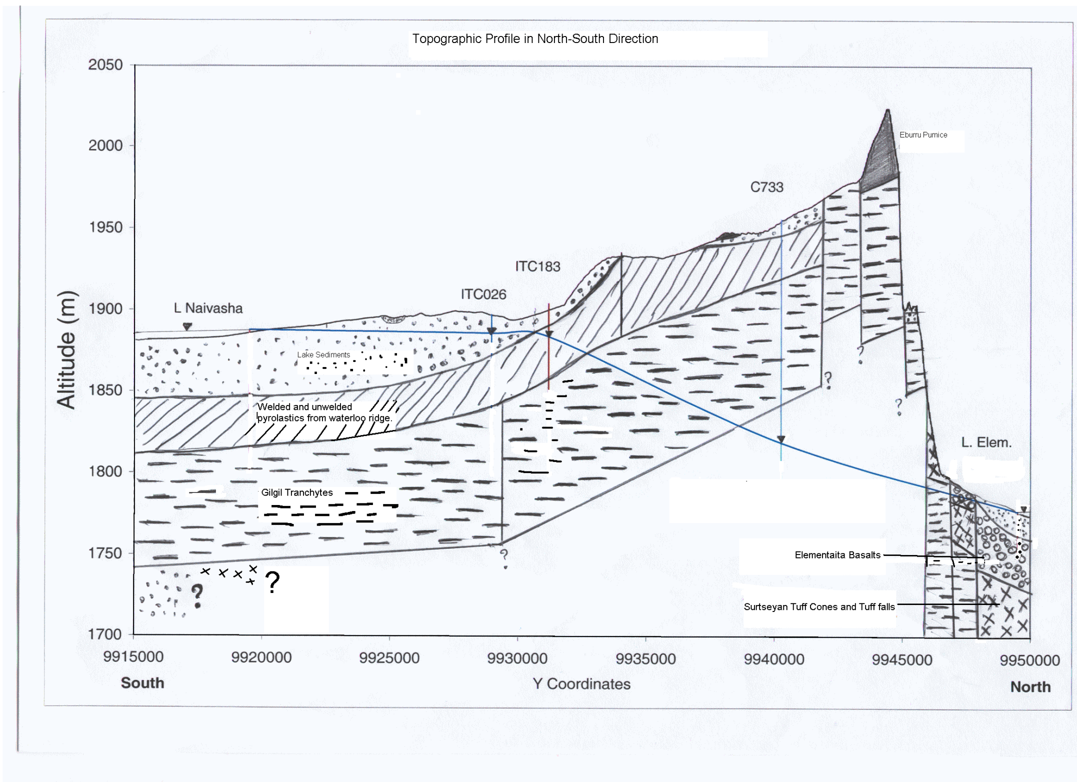

Figure 6.4.2.1 Topographical and Geological Profile along Section 3 in the Study area

The aquifer in well C733 could be of faulted Gilgil tranchyte. It could also be of paleosurface in the contact between the tranchyte and another aquiclude, which could be postulated as Limulu Tranchyte.

Along this transect, the variation in water chemistry is as shown in figure 6.4.2.2 and table 6.4.2.1 shown below. The water quality deteriorates towards well ITC183, improves towards well C733 before deteriorating drastically towards lake Elementaita. As postulated in section 6.4.1, deterioration here can accrues from dissolution of lenses of evaporite and halides intercalated in the sedimentary formation. Improvement of the water towards well C733 could be attributed to dilution effect of direct recharge from rainfall, while the deterioration towards Elementaita is due to dissolution of salt deposits in the area.

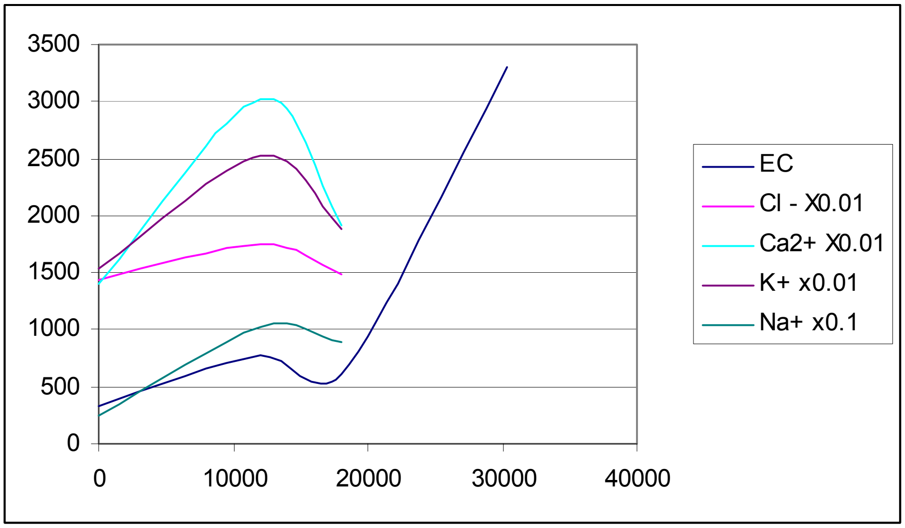

Figure 6.4.2.2:Hydrochemistry along Section 3

Location	Distance (m)	EC	Cl^- X0.01	F^{-x}0.01	Ca^{2+} X0.01	K^+ x0.01	Mg^{2+} x0.01	Na^+ x0.1
ITC044 (L. Naiv)	0	330	1429	0	1400	1537	616	250.4
ITC183	12000	770	1750	330	3024	2526	421	1015.6
C733	18000	613	1480	575	1912	1889	331	892.7
ITC187 (L. Elem)	30400	3300						1996.3

Table 6.4.2.1: Hydrochemistry along Section 3

The δ ^{18}O values for well ITC183, C733 and ITC187 (Lake Elementaita) are -3.35($^o/_{oo}$), -1.02($^o/_{oo}$) and –1.14($^o/_{oo}$) respecvtively, giving respective the content ratio of lake Naivasha water in their water as 20%, 22% and 38%. This suggests that there is more Lake Naivasha water in Lake Elemeintaita than there is in well C733 and more in well C733 than there is in well C733. Isotopic signatures of lake Naivasha waters in these waters contradicts and are inconsistence with evidence from piezometric heads as they seem to suggest that Lake Naivasha is north of Lake Elementaita and the flow is southwards which is not the case. The other possible explaination could be that there is an alternative and faster route through which water flows faster to reach lake elementaita without necessarily flowing through wells ITC183 and C733. This would assume, vertical flow to a lower and highly permeable aquifer, possibly the geothermal aquifer that would then flow northwards to Elementaita. This is very improbable as there is no evidence to that effect.

Sample	δ ^{18}O of Sample($^{o}/_{oo}$)	δ ^{18}O of Lake ($^{o}/_{oo}$)	δ ^{18}O of Rain($^{o}/_{oo}$)	x (%)	y(%)
ITC183	-3.35	6.5	-5.75	80	20
C733	-3.02	6.5	-5.75	78	22
ITC187 (L. Elem)	-1.14	6.5	-5.75	62	38

Table 6.4.2.2: Isotopic ratios of lake water and rain water in the wells. X is the ratio of rain water in the sample while y is the ratio of the lake water in the sample.

Other than Lake Naivasha and direct recharge from water, there are other sources of recharge for the wells along this section. It is probable that there is some infiltration from Gilgil river and other while Lake Elementaita receives water from other sources besides the two-end member on the Lake Naivasha – direct recharge mixing line.

The use of isotopic signature as a tool to trace flow direction is less appropriate along this section it due to interference of other possible sources of water along the way.

6.4.3 Hydrogeology of Northeastern Part of Study Area

While according to the historical piezometric heads of 1980 indicates flow of water towards the lake, situation is different as the current piezometric heads indicate a sink at the location that coincides with the well fields of Manera and Three Point Farm. To explain these possibilities, three hypotheses have been suggested and discussed below. All hypotheses assume a two-groundwater aquifers' system.

Hypothesis 1

This assumes a by-pass flow pattern with the flow in the two aquifers being in opposite direction. The water in the recharge zone (escarpments) is feed predominantly to the deeper aquifer and flows below the shallow towards the lake. Meanwhile lake water flows towards the escarpment. The situation is illustrated schematically in figure 6.4.3.1

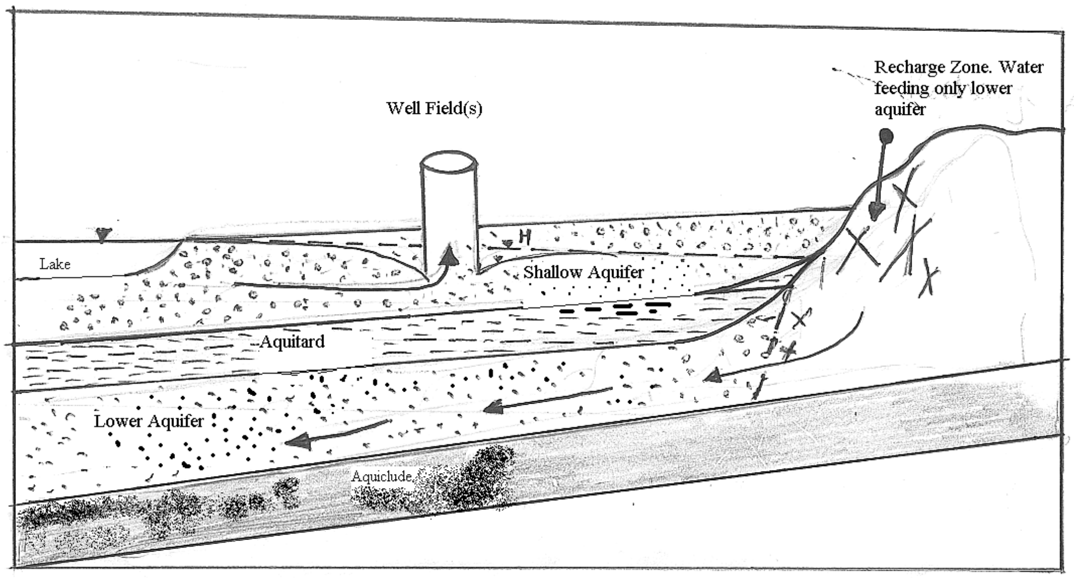

Figure 6.4.3.1: Hypothesis 1. H is the Historic Heads and C is current Head

Hypothesis 2

This assumes a one-aquifer system to which all the recharge is fed and whose historical flow direction is towards the lake. Once extraction begins, however, the flow direction is towards the well field.

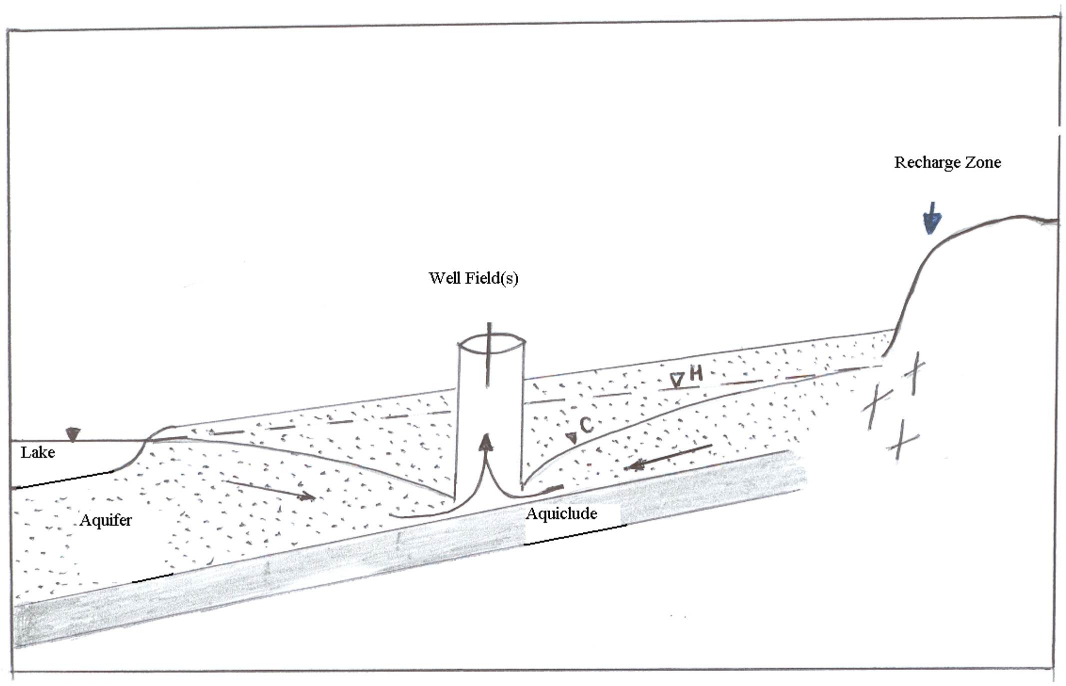

Figure 6.4.3.2: Hypothesis 2. H is the Historic Heads and C is current Head

Hypothesis 3

This assumes two layered aquifer system both of which are feed by the water recharge in the recharge zone and before the well field effect, the flow direction in both was towards the lake. However, with extraction beyond a certain value, the flow in the shallow aquifer is towards the well field. This hypothesis also assumes the existence of a fault system in the area of the well field. Hence, other than the possible leakage through the aquitard, there could be flow between the two aquifers through the fault system, as a result, the fault system work both as a discharge of recharge zone depending on the piezometric pressure differences between the two aquifers.

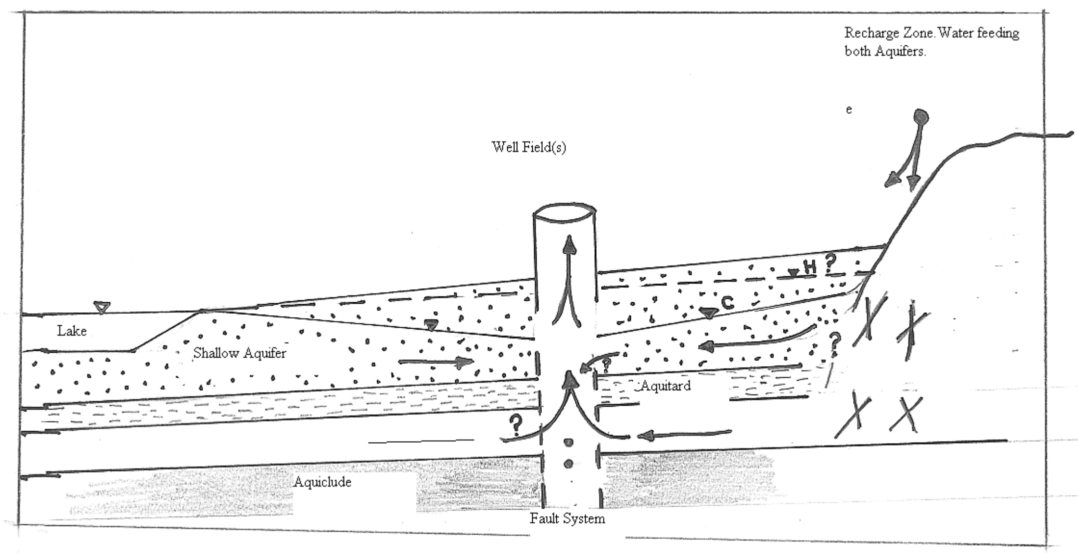

Figure 6.4.3.3: Hypothesis 3. H is the Historic Heads and C is current Head

Discussion of the Hypotheses

If hypothesis 1 holds, then water extracted from the well field should be predominantly lake water. The shortcoming of this hypothesis is that on the basis of isotopic signature, however, there is hardly any lake water in the water from the well fields. The average δ^{18}O value of – 4$^{o}/_{oo}$ for the water in the well field doesn't indicate any significant presence of lake water in the well fields whose δ^{18}O value is 6.4$^{o}/_{oo}$. Hypothesis 1 also fails to account for the fate of the water that flows in the shallow aquifer in case there is no well field.

If hypothesis 2 and 3 are correct, then the isotopic signature should be expected in the well field, which is still not the case. However, this could be explained that the fall of the piezometric heads the well field falling below that of lake is a recent development. The piezometric Heads of 1980 indicated (Owor, 2000) indicate that the even with the extraction then, the flow was still to the lake. This means that the reversal in the flow direction stated less than 20 years ago (after 1980). The distance from the well field as ascertained in GIS environment using Ilwis programme is approximately 5500m. The effective porosity of the aquifer is 20% (Dingman, 1998) and the K value as calculated by in section 6.4.1 is 238 m/day. The average head of the well field is 1885 m while that of the lake is 1888 m.

$$V_e = K \frac{dh}{nedl} \quad \text{---I}$$

From which Ve is 0.65m/day giving the necessary time of travel for water from the lake to reach the well field before Isotopic signature can be detected as being over 23 year, a time span that is yet to pass. This could explain where there is no evident isotopic signature of lake water in the well field.

Hence hypothesis 1 and 2 can hold for the area. However, though most of the wells in the well field were drilled to average depth of 65 meter and draw water from one main aquifer, a driller's log of well C11527, which was drilled to a depth of 130m in the area, clearly indicates the existence of a deeper groundwater aquifer and occurrence that invalidates hypothesis 2, and leaves hypothesis 3 to be tested. See figure 6.4.3.0 below for my interpretation of the drilling log.

Hypothesis 3 also suggests the occurrence of a fault system in the area of the well field. The L bend in Karati river course asserts this assumption further. This bend could be an intersection of two faults. This means that fault system increases the infiltration of water from the Karati River to the well field. If such is the case, then besides Lake water and direct recharge from the rain, Karati River is a major source of recharge to the well field. As to weather Karati River or Lake Naivasha is the bigger source of water is subject to further study.

In conclusion, it is very likely that the aquifer system in the northeastern portion of the study area is two layered. The bend of the Karati River suggests as fault system in the well field. And besides the lake Naivasha and direct recharge from rainfall Karati river contributes appreciably to the recharge of the well field. The depression in piezometric contours in the northeastern direction of the lake, which has resulted to the reversal of the direction of flow of water from, the lake is as a result of water abstraction from the well field. With increased abstraction of water, the hydraulic gradient between the lake and well field will increase over time.

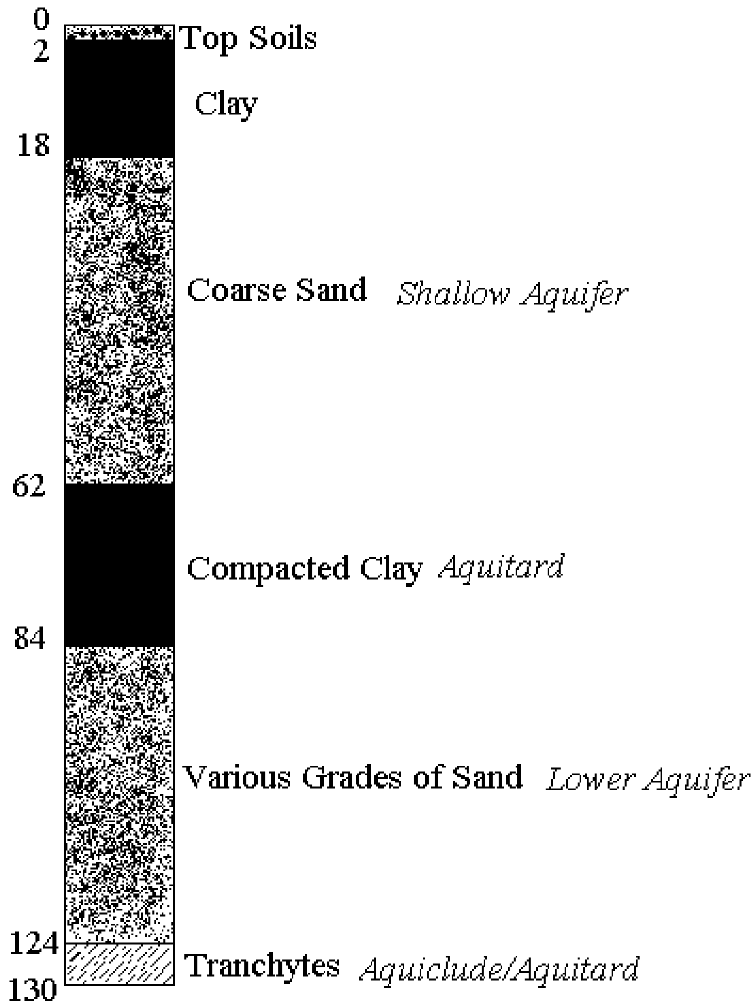

Figure 6.4.3.0: Interpretation of well C11527 Geological Log Clearly Indicates existence of two aquifers

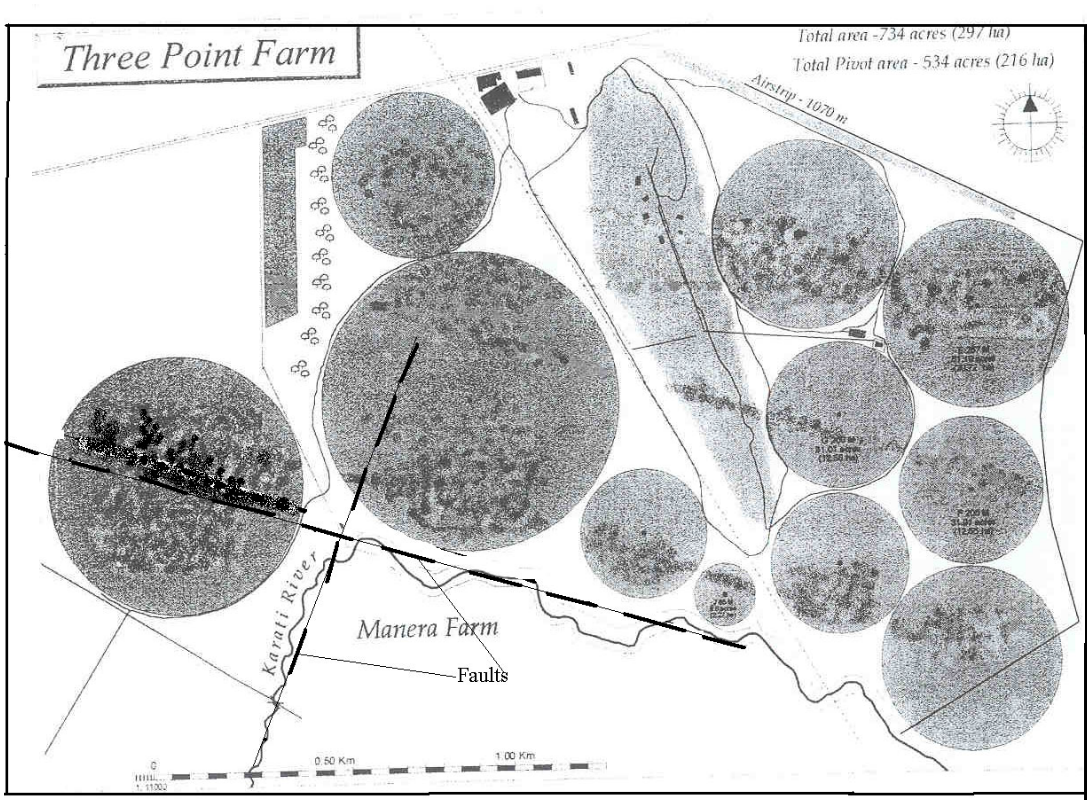

Figure 6.4.3.1: Postulation of the Fault System in the Three Point Farm on the Basis of the L Shape in Karati River.

6.4.3.2 Temporal Variation of EC us/cm for B/H 1

The water chemistry does not change significantly between 1973 and 2000. While the small increment from 550 us/cm in 1973 to 640 us/cm in 2000 could suggest a slight deterioration in the water chemistry, it could also be as a result of the use of different probes being used. The abrupt rise in the EC between 2000 and 2001 indicates a sudden plummet in the water quality in the well.

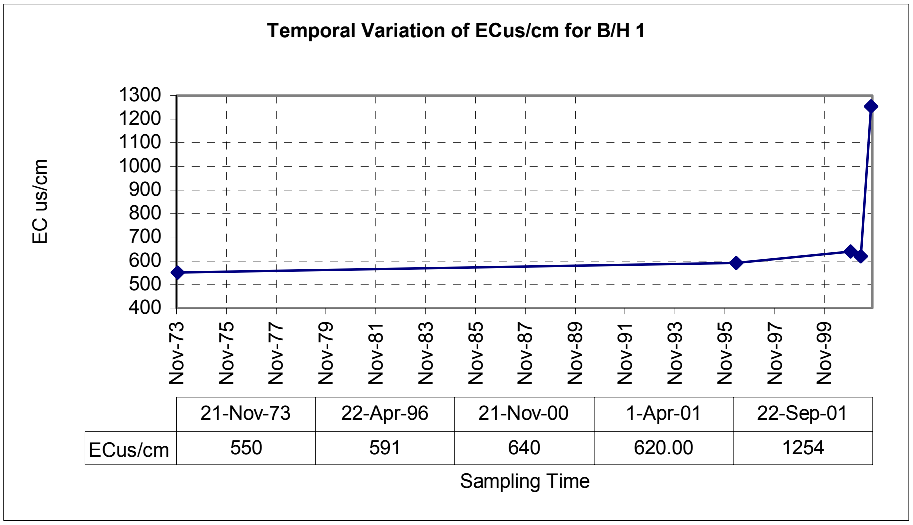

	21-Nov-73	22-Apr-96	21-Nov-00	1-Apr-01	22-Sep-01
ECus/cm	550	591	640	620.00	1254

Figure 6.4.3.2:Temporal variation of water chemistry of well 1

6.4.3.3 Temporal Variation of EC us/cm for B/H 2

The trend of water chemistry as manifested by the temporal variation of the EC of this well indicates a deterioration of water quality. The increment of EC by over 100% from 1973 to 2000 cannot be attributed to differences of used EC probes.

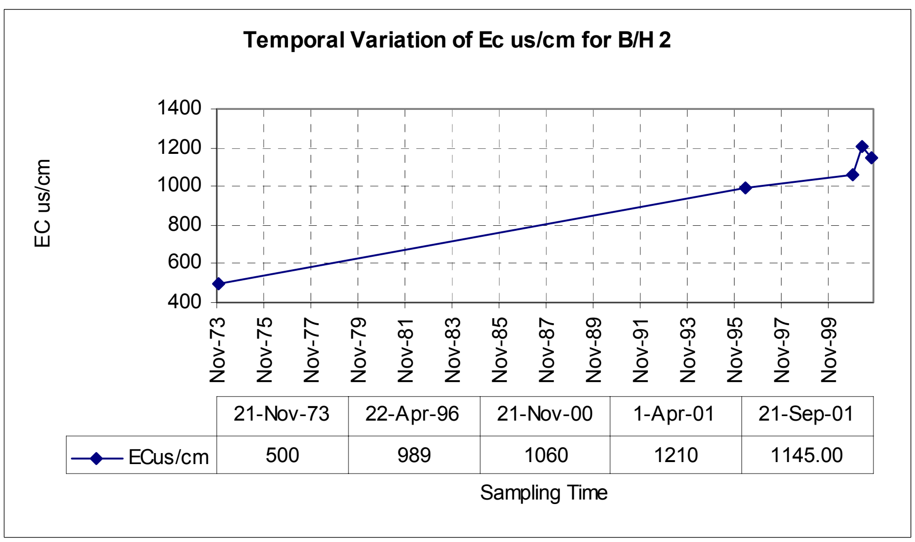

	21-Nov-73	22-Apr-96	21-Nov-00	1-Apr-01	21-Sep-01
ECus/cm	500	989	1060	1210	1145.00

Figure 6.4.3.3:Temporal variation of water chemistry of well 2

6.4.3.4 Temporal Variation of EC us/cm for B/H 3

The trend in the EC values here does not suggest anything definite. The apparent increment in EC values could easily be caused by difference in the used probes.

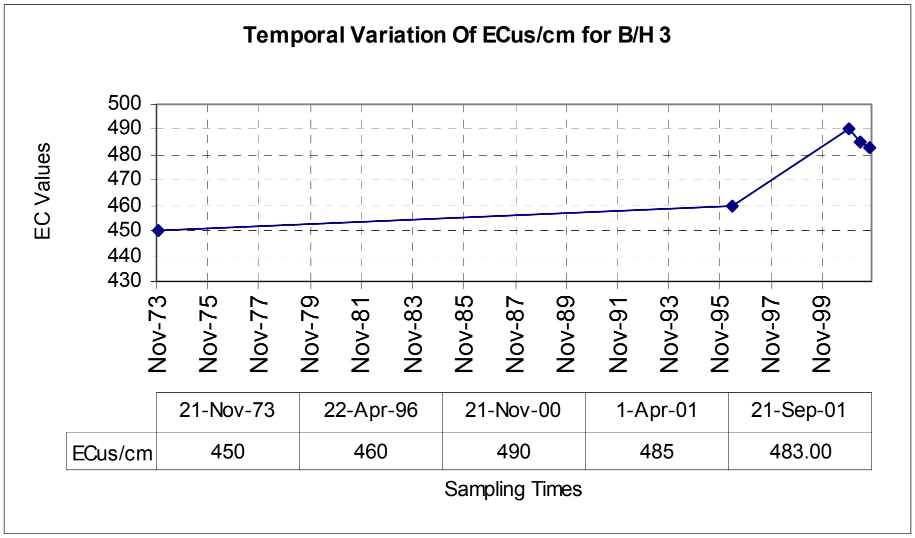

	21-Nov-73	22-Apr-96	21-Nov-00	1-Apr-01	21-Sep-01
ECus/cm	450	460	490	485	483.00

Figure 6.4.3.4:Temporal variation of water chemistry of well 3

6.4.3.5 Temporal Variation of EC us/cm for B/H 4

The increment in the EC values of this well between 1973 and 2000 might signifies deterioration in water quality. The difference of 450 EC units is too significant to be explained by different probes being used.

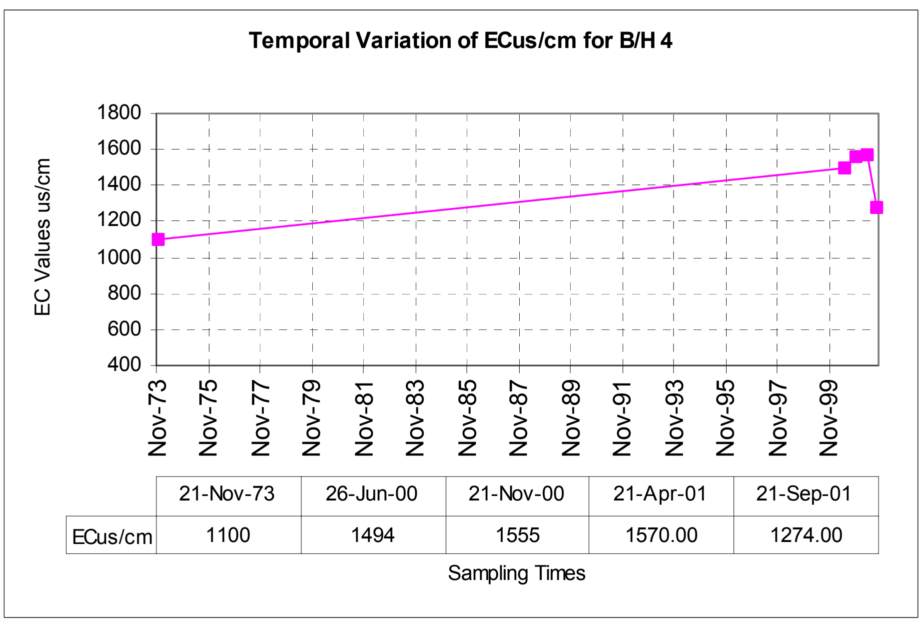

	21-Nov-73	26-Jun-00	21-Nov-00	21-Apr-01	21-Sep-01
ECus/cm	1100	1494	1555	1570.00	1274.00

Figure 6.4.3.5: Temporal variation of water chemistry of well 4

6.4.3.6 Temporal Variation of EC us/cm for B/H 5

The increment in the EC in this case suggests deterioration in water chemistry in that well. Though too significant to be attributed to differences in the type of probe used, it might not necessarily suggest deterioration in the water quality.

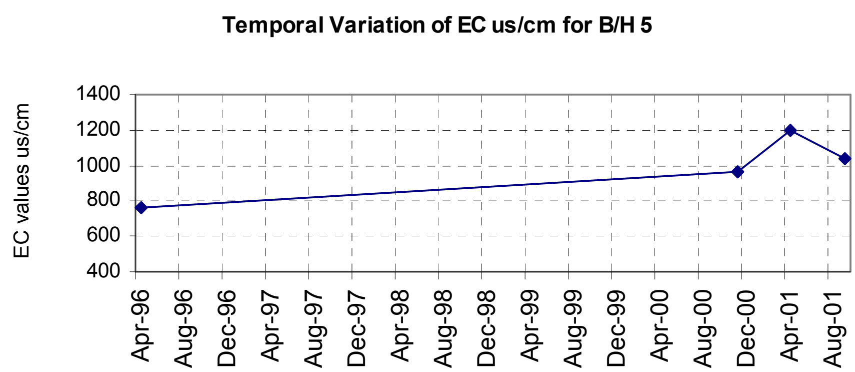

	22-Apr-96	21-Nov-00	1-Apr-01	22-Sep-01
ECus/cm	761	960	1200	1036.00

Sampling Time

Figure 6.4.3.6: Temporal variation of water chemistry of well 5

6.4.3.7 Temporal Variation of EC us/cm for B/H 6

There is a significant increment in the EC of the water from this well over time. It increased by 380 us/cm between 1973 and 2000, which is over 50% of the original EC value. This shows a fall in the water quality over time.

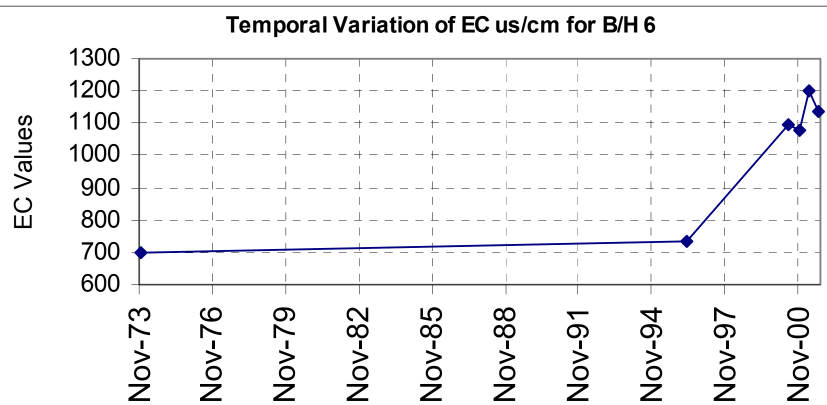

	21-Nov-73	22-Apr-96	26-Jun-00	28-Nov-00	1-Apr-01	21-Sep-01
ECus/cm	700	737	1098	1080	1200	1136.00

Sampling Times

Figure 6.4.3.7:Temporal variation of water chemistry of well 6

6.4.3.8 Temporal Variation of EC us/cm for B/H 7

There is a significant increment in the EC of the water from this well over time by 400 us/cm, 50% of the original EC value, between 1973 and 1999, which indicates a fall in the water quality over time.

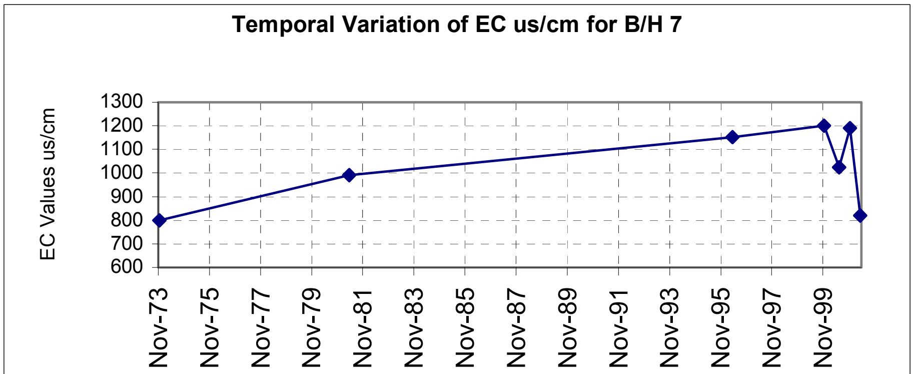

	21-Nov-73	Apr-81	22-Apr-96	1-Nov-99	26-Jun-00	1-Apr-01	21-Nov-00
ECus/cm	800	990	1151	1200	1025	820	1190

Sampling Times

Figure 6.4.3.8:Temporal variation of water chemistry of well 7

6.4.3.9 Temporal Variation of EC us/cm for B/H 10

There is an apparent decrease in the EC values of this well. This doesn't necessarily suggest an appreciation in the water chemistry. It could be attributed to the dilution effect due to new recharge since the sampling was done randomly. It could also be to the use of different EC probes.

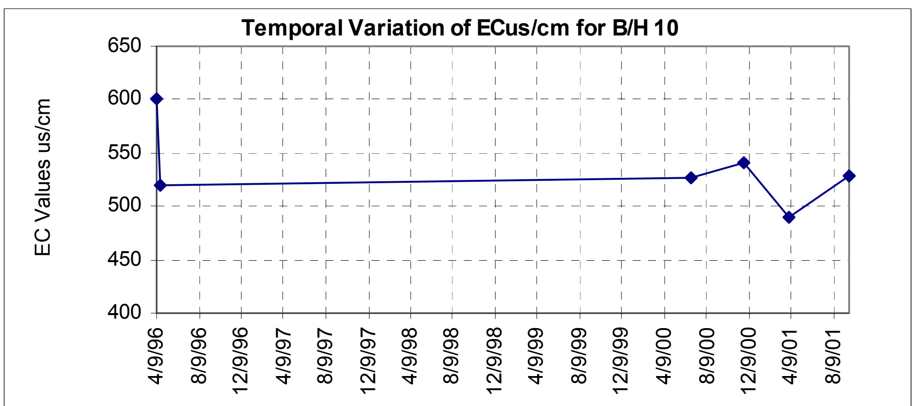

	9-Apr-96	22-Apr-96	26-Jun-00	21-Nov-00	1-Apr-01	21-Sep-01
ECus/cm	600	519	526	540	490	528.00

Sampling Times

Figure 6.4.3.9: Temporal variation of water chemistry of well B/H10

6.4.3.10 Variation of water Chemistry with Depth and Yield

The variation of water chemistry with depth and its variation with yield were studied. Plotting depth and yield of the wells against their respective EC was used to do this. From this graph, it is evident that there is no relationship between the yield and water chemistry or depth and water chemistry in the groundwater aquifer system in the Northeastern portion of the study.

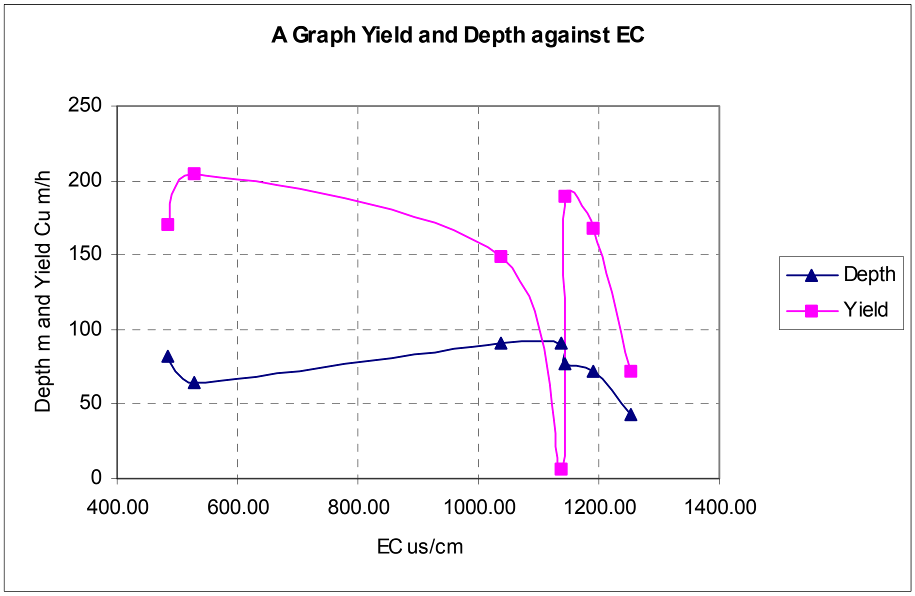

Figure 6.4.3.10: Variation of water chemistry with depth and Yield. There is no correlation been EC and Depth and there is no correlation between EC and Yield.

From the analysis of temporal variation in the water chemistry in the wells above, it can be concluded that the water quality in wells BH2, BH5, and BH6 has fallen over time. There has been an apparent drastic fall in water quality of BH1, which need to be investigated further before a solid conclusion can be drawn. The fall in the water quality in well BH7 also needs further investigation. The trends in wells BH3 and BH4 do not give any evident trend. This necessitates additional investigations if any firm conclusion is to be drawn. Besides, the apparent appreciation in the water quality of well BH10 is also not conclusive and it calls for a systematic sampling and analysis schedule.

6.4.3.11 Topographic, Geologic and Hydrogeologic Profile along Section 4

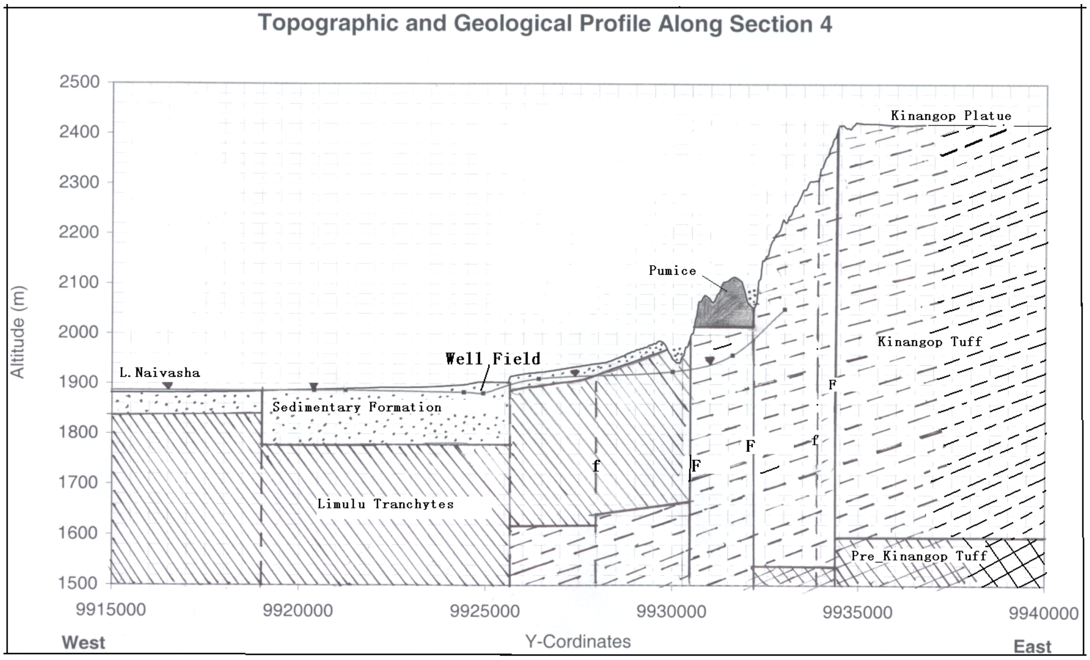

Figure 6.4.3.11: Geologic, Topographic and Hydrogeological Profile along Section 4.Due to low Transmissivity caused by faults, there is a high piezometric gradient at the escarpment.

While the faults can both facilitate or impede flow of water, in the direction along section4 in the study area, they impede it as suggested by the steep piezometric gradient at the escarpment. Going by the piezometric heads, water generally flows from the east to west towards the section. However, there is a sink in the in the piezometric level that coincides with the well field indicated on the section. This implies that water suggests that water flows towards the wellfield from both the escapment and the lake.

Hydrochemistry Along Section 4

Sample Pt	Dist. m	ECx100 us/cm	Li +x0.1mg/l	Mg 2+ mg/l	Cl- mg/l	F- x0.1mg/l	Ca 2+ mg/l	K + mg/l	Na+x10 mg/l
Lake	0	3.3	0	6.16	14.29	0	14	15.37	2.504
NIK 1	3300	12.54	0.4	3.38	33.5	48	21.84	28.24	20.807
NIK 8	4530	5.28	0.8	1.35	7.9	27	20	12.27	7.888
NIK 27	6097	5.6	1.1	1.44	14.3	27	25.03	15.02	7.35
NIK 3	6783	8.1	1.2	0.92	22.2	85.5	15.42	20.17	13.848

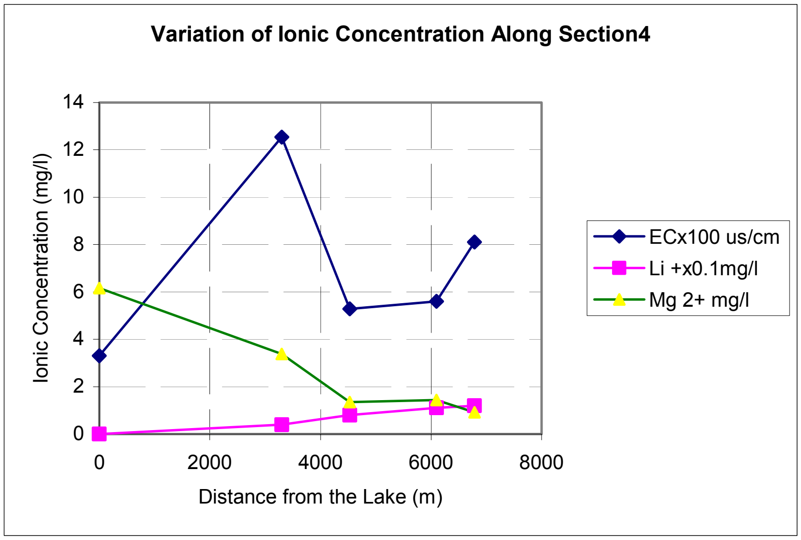

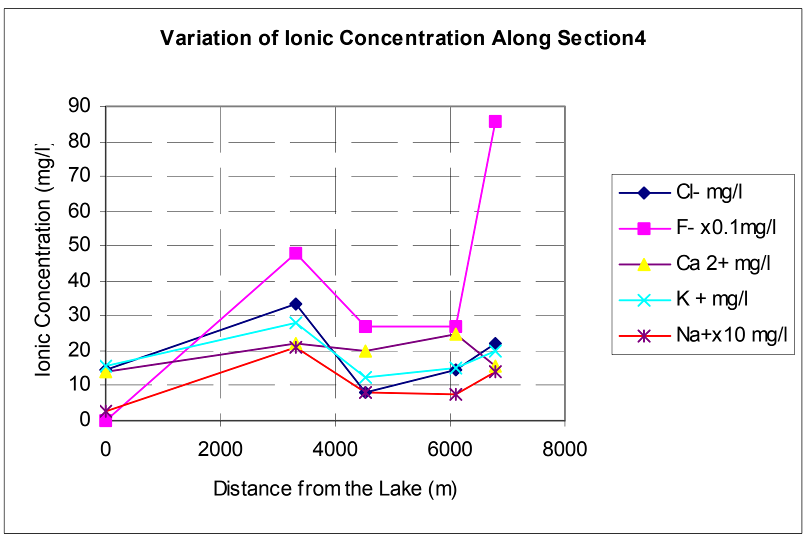

Figure 6.4.3.11b Trend of Water Chemistry along Section4. Along this transect, the ionic concentration of the water decreases as it flows from well NIK3 to well NIK27. and remains low even in well NIK8. However, as water approaches well NIK 1 there is an increase in the ionic concentration. On entering the lake, the ionic concentration of the water falls due to the dilution effect of the surface run off from the Gilgil River and River Malewa. The abrupt fall in the ionic concentration in well NIK27 and NIK8 could be attributed to dilution effect to Karati River, which is very close to this well.

6.4.4 Hydrogeology of Eastern Part of the Study Area

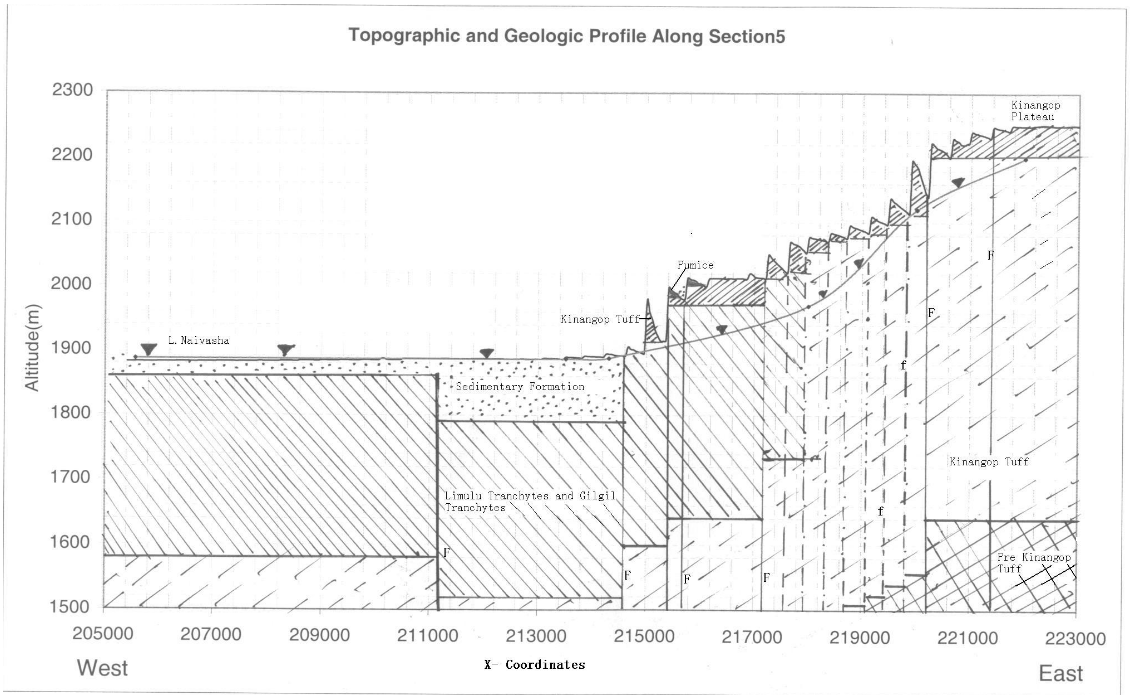

Figure 6.4.4 Geologic, Topographic and Hydrogeological Profile along Section 5.Due to low Transmissivity caused by faults, there is a high piezometric gradient at the escarpment. While at the Valley bottom, the shallow aquifer is composed of sedimentary formation, on the escarpment it is composed of weathered contact between Kedong Valley tuff and Limulu Trachytes and between Kedong Valley tuff and the Kinangop tuff.

Hydrochemistry Along Section 5

Sample Pt	Dist. m	ECx100 us/cm	Li +x0.1mg/l	Mg2+mg/l	Cl- mg/l	F- mg/l	Ca 2+ mg/l	K + mg/l	Na+x10 mg/l
Lake	0	3.3	0	6.16	14.29	0	13	15.37	2.504
NIK 29	3070	11.26	2.2	6.81	113.5	3.7	61.65	60.84	41.038
NIK 21	3820	7.47	1	1.98	44.5	9.1	14.84	25.29	17.26
NIK 48	6500	6.77	0.2	3.15	15.9	6.4	6.13	19.78	12.341
NIK 52	7797	6.63	0.4	1.62	9	6.4	5.61	18.4	12.582

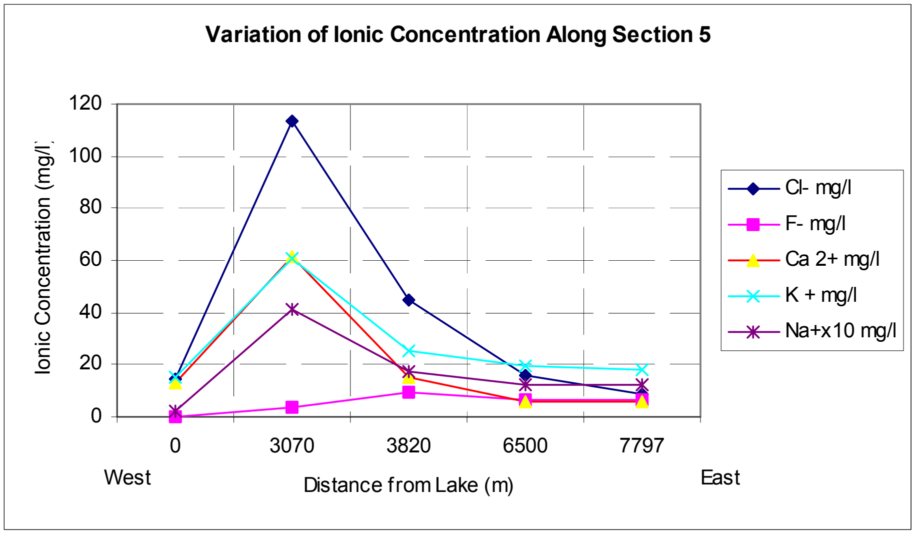

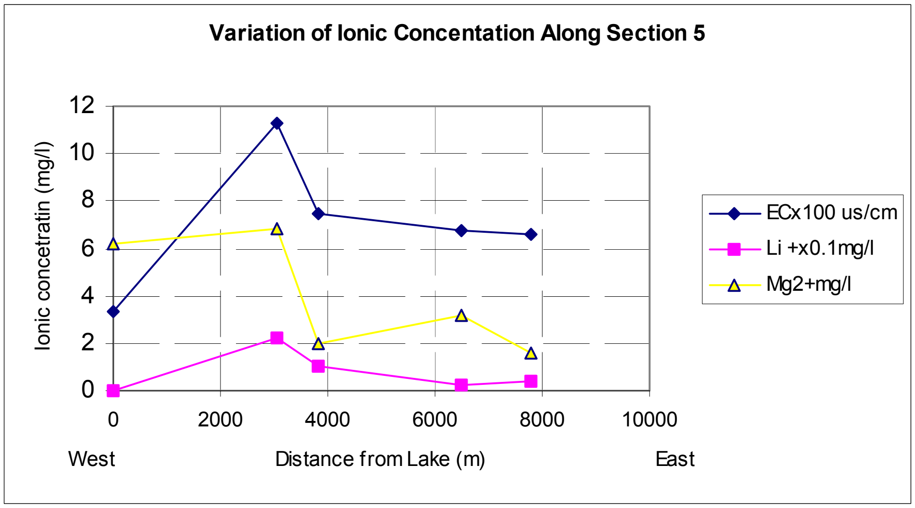

Figure: 6.4.4b: Chemical Trend Along Section 5. The trend of Ionic Concentration along the W-E section5 suggests westward flow of water from well NIK52 through wells NIK48, NIK21and 29 into the lake. In this regards, the areas around well NIK 52 is located more towards the recharge zone than wells NIK 29 and NIK 48. As the water flows from Well 52 to well NIK 48 and later to NIK21 and NIK29, its ionic concentration of $Na^{+,}$ K^{+}, Ca^{+}, Li^{+}, Mg^{2+}, and Cl^{-} increases. However, their concentration in the Lake drops. This is caused by the dilution effect of the water brought in by R. Gilgil and Malewa rivers. While the Concentration of F- is high in well NIK 52, it's concentration drops with increases in Ca^{2+}. This trend confirms a westward movement of water from the plateau into the lake, which suggests a westward movement to the lake.

6.4.5 Hydrogeology of Southeastern Part of the Study Area

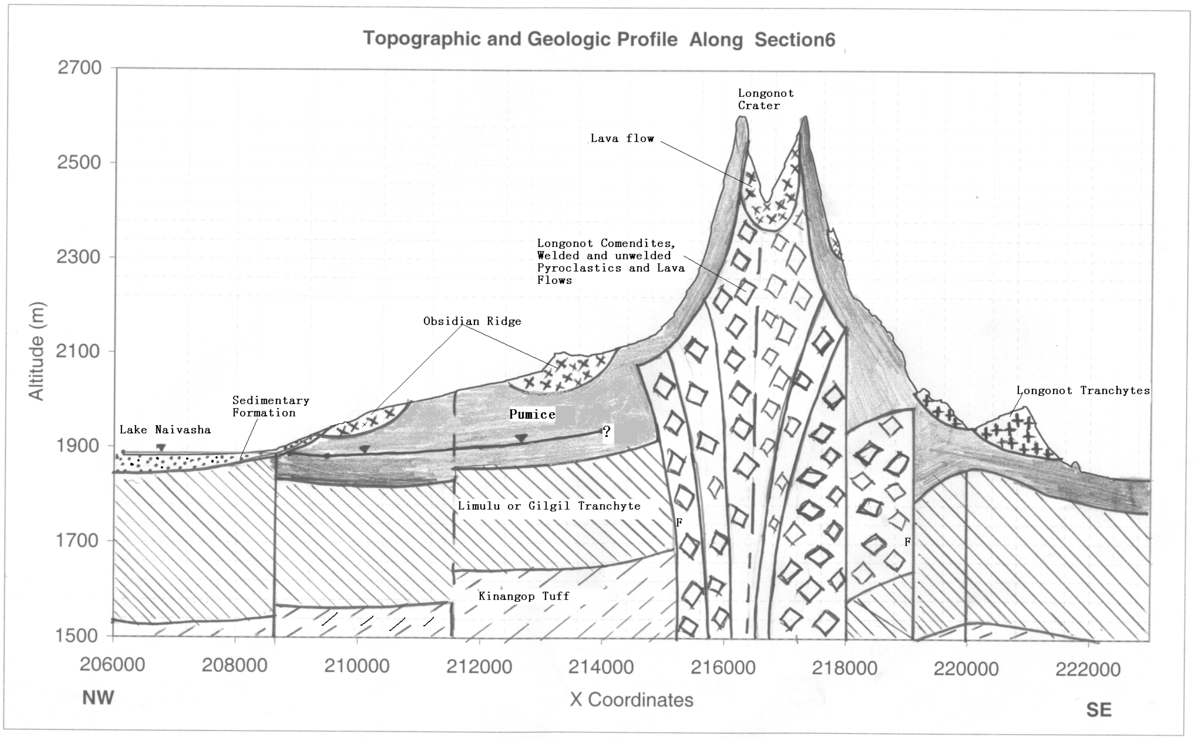

Figure 6.4.5 Geologic, Topographic and Hydrogeological Profile along Section 6. The piezometric Heads show that flow along this section is towards the lake along. The gradient is low, suggesting higher transmissivities than those at the escarpments in the two sections discussed above. Near the lake, shallow aquifer is composed of sedimentary formation; away from the lake it is composed of weathered contact between pumice and Limulu or Gilgil. Towards Longonot Mountain, the trend of the piezometric head is un traceable. It is probable that this water is sourced from the direct recharge from rainfall on the Longonot hills.

6.4.6 Hydrogeology of Southern Part of the Study Area

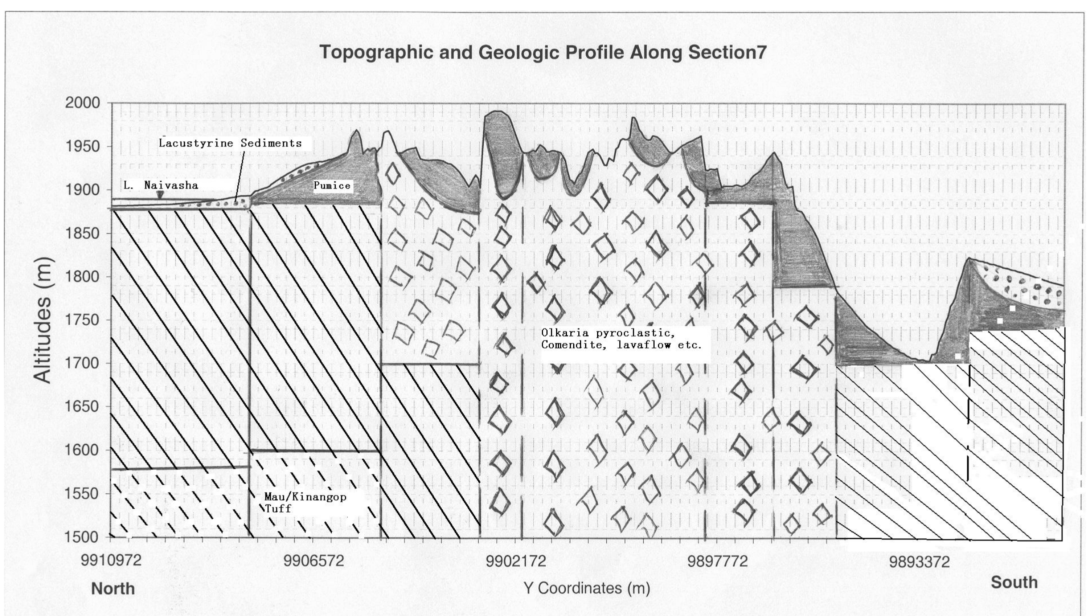

Figure 6.4.6: Topographic and Geological Profile Along Section 7. The hydrogeology along

this section is very complex and needs further investigation. Most of the wells along this section are dry.

6.4.7 Hydrogeology of Southwestern Part of the Study Area

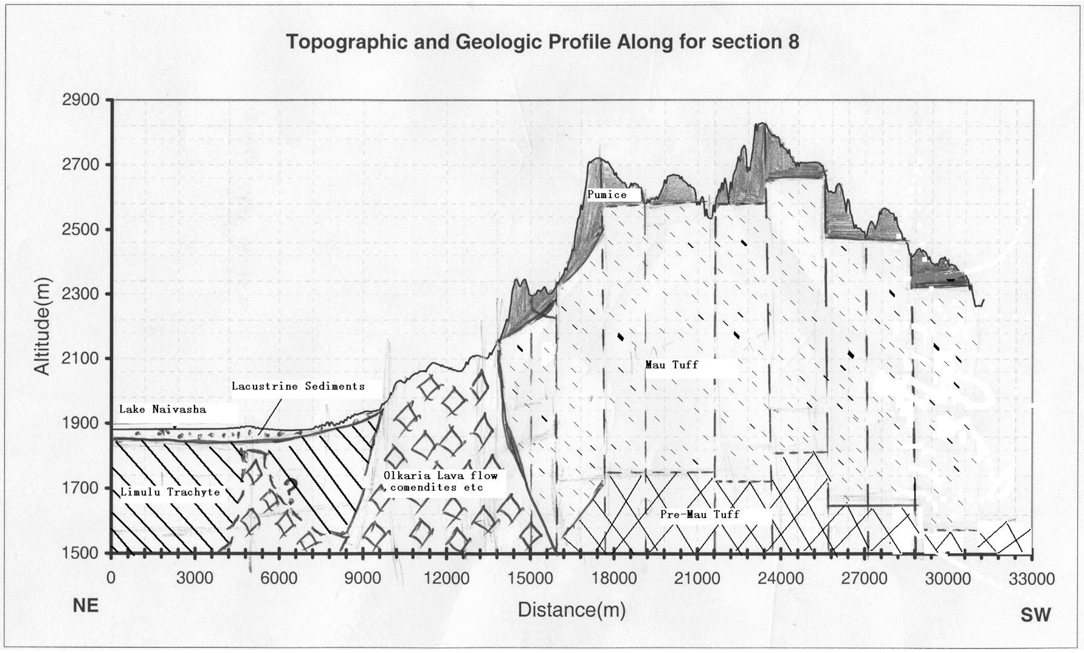

Figure 6.4.7: Topographic and Geologic Profile Along Section 8. Aquifers are Mostly between the pumice and Mau Tuff. Close to the lake they are mostly of weathered Limuli or Gilgil Trachytes

6.4.8 Hydrogeology of Western Part of the Study Area

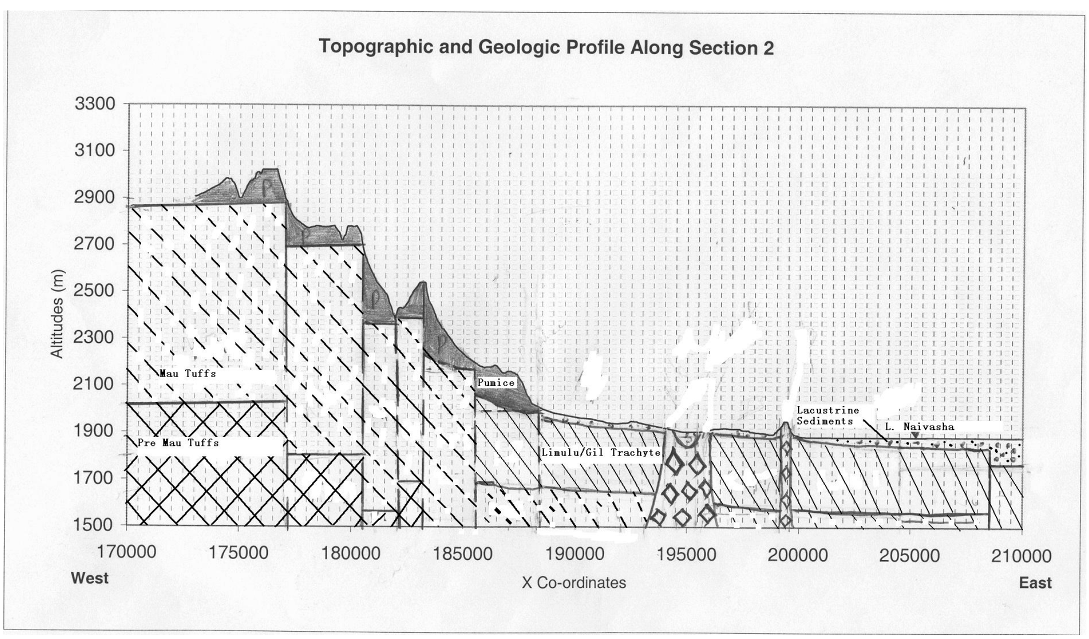

Figure 6.4.8: Topographic and Geologic Profile Along Section2. The Sedimentary Aquifer along this Section barely exists. Aquifers are principally of weathered Limuli Trachytes. Towards Mau Plateau, the aquifers are mainly found at the contact between the pumice and the Mau Tuff.

Chapter 7 Model

7.0 Introduction

A model is any devise that represents an approximation of a field situation (Anderson, and Woessner, 1991). It is a simplified version of reality which enables the study of complex real life situation by representative. Models can be used in prediction, mitigation, and visualization among others and can be classified as numerical, analytical or conceptual models. Regardless of the type and role of model, it must be a simplification of the actual situation on the ground without compromising the basic characteristics of the situation.

The motive of the modeling here in is to understand the influence of geology on the hydrogeology of the area of study through the visualization of 3-D spatial distribution of the key geologic units and consequently the different hydraulic properties of the area. To do this a 3-D conceptual Hydrogeological model is developed. As explained later in section 7.3 the visualization is done at three levels, viz: 3-D Visualization of Topographic Surface, 2.5-D Visualization of Geology, and 3-D Representation of Geology.

Though the boundaries of the catchment have been dually defined in section 5.4, the model is done for the entire area from Lake Elementaita to the North to the area South of Longonot Hills in the south. This was aimed at allowing flexibility for future modeling exercises.

7.1 Previous Works

Owor (2000) used a numerical simulation model to study the long-term interaction of groundwater with the Lake to determine the long-term water budget for the lake and estimate water abstraction from both the surface and groundwater resources. This was an extension of the earlier work of Mmbui (1999) who used a spreadsheet to numerically model the long-term water balance for lake. Kibona (2000) sought to understand the variation of groundwater levels in space and time by setting up both transient and steady state numerical models of the area.

7.2 Model Input Data

In this section, different data types used in the model are explained and their source or method of derivation given.

7.2.1 Surface TIN

Surface TIN was derived from the rasterized DEM <demfinal>of the study area as described below.

- Point map "surface" was created with 2500 points scattered over the entire study area. First they were first evenly distributed evenly over the entire area and later, more points were inserted in areas with drastic topographic contrasts.
- The point map was then opened as a table. A column "elevation was created to retrieve elevation values from "demfinal" for each location of the point in the point map that had been created in the first step indicated above. The mapcalc used is ***elevation=mapvalue(coordinate,demfinal)***
- From the table, x, y, and z for each of the point may were copied into excel from where vertices were prepared and exported GMS.
- The vertices were then triangulated into a TIN representing the topographic surface of the study area.

The format of the vertices file and the TIN files are as shown in appendix 5.

7.2.2 Boreholes

With the aide of 60 well in the study area and published geologic map of the area of study, nine geologic sections shown in on the map in section 6.2 were prepared. These together with the two published sections were used to create 220 fictious wells distributed throughout the study area. These were then entered in excel spreadsheet and served as a text with an extension " ***.bor** ". The file was edited to a form accept able by GMS program in WordPad. These files include the beginning of a particular well, name of the well, and number of contacts in the well and the x, y and z value of all the contacts between different formations. The format of the used file is shown in appendix 6.

7.2.3 Materials

These contain geological formation found in the study area. They contain the names of the different materials in the area of study, their codes as well as their colour. For purposes of this model, 16 materials were used. Attempts were made were possible to assign each formation the same colour in the model as that assigned to it on the published geologic map of the area. The materials were entered in excel spread sheet and saved as text with an extension " ***.mat** ". Addition changes were effected in WordPad to a format accepted by GMS as shown in appendix 7.

7.2.4 Geologic Map

Digital format of geological map of the study area is ascertainable in the ITC database. This was rasterized and imported from ILWIS file as an image with extension " ***.img** " and was used as explained in section 7.3.2 below.

7.2.5 Faults

These were prepared as explained in section 5.3.2 and were to be used after section 7.3.3.2 below but could not be used.

7.3 Procedure of Model Setup

7.3.1 3-D Visualization of Topographic Surface

The vertices on the topographic surface in the area of study were triangulated to constitute a TIN representing the topography of the area. This was then extruded into a solid to an elevation of 1500m above sea level to give a 3-D topographic impression of the study area. A section was then cut across the Rift Valley in the West-East direction from Mau Plateau to Kinangop Plateau through Lake Naivasha to ascertain that direction of tilting of the Mau and Kinangop plateaus in order to check the validity of the assumptions made in section 5.3.2. Figures 7.3.1a and 7.3.1b below show the 3D topographic expression and the Cross section of the area.

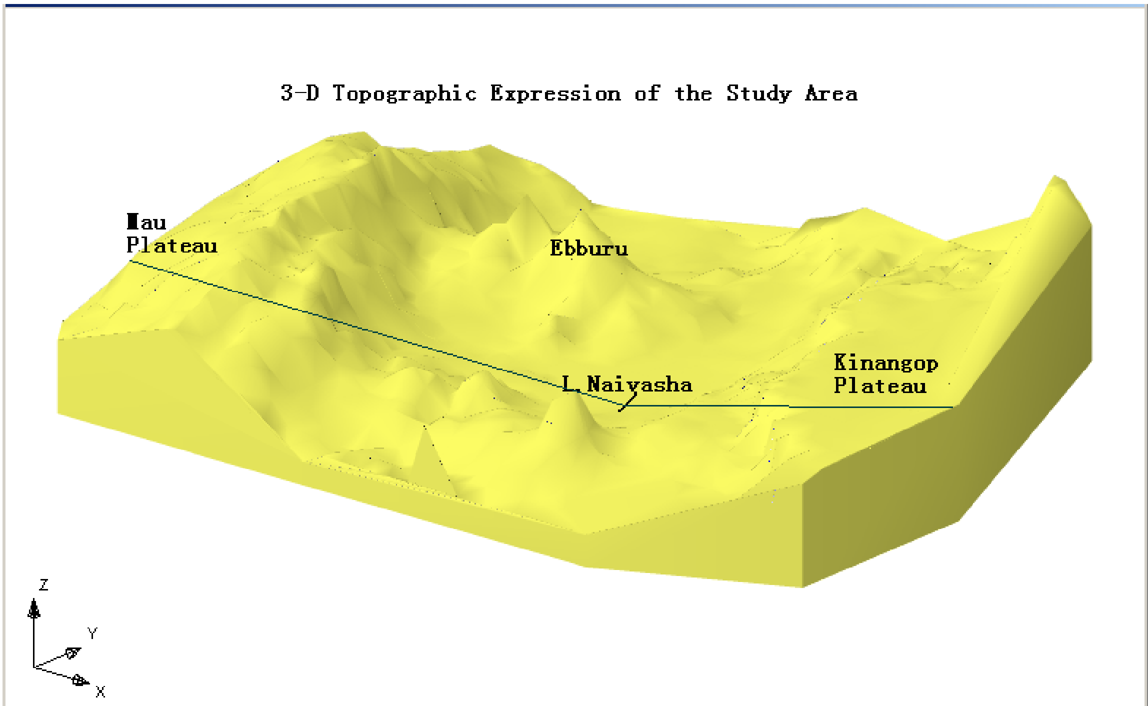

Figure 7.3.1a. Solid extruded to from TIN representing Surface Topography of the study Area. Line Traversing the Solid is the Approximate Position of section shown below.

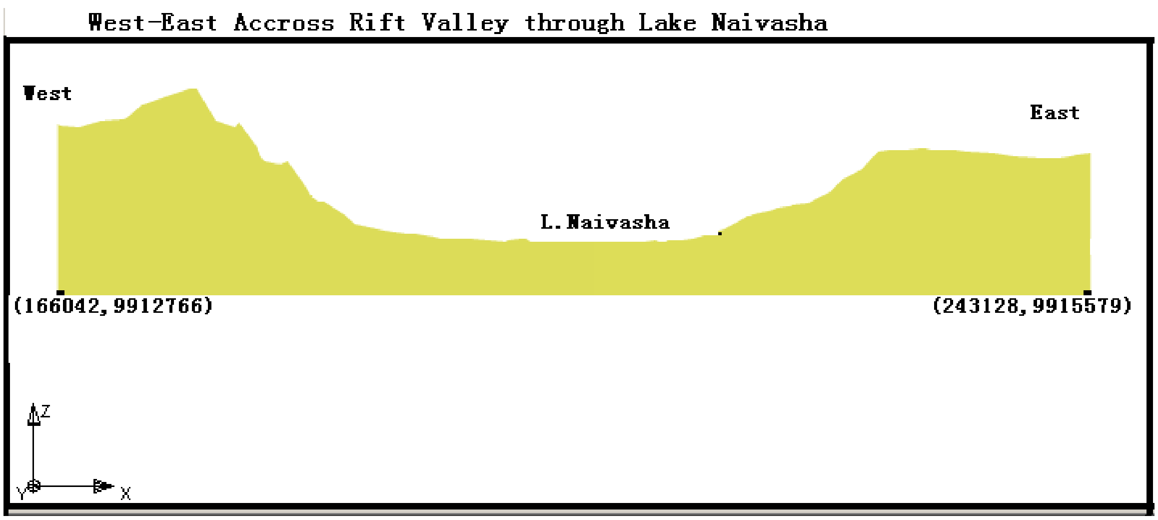

Figure 7.3.1b. West-East Section The Mau and Kinangop Plateaus tilt away from the Valley bottom indicating that scenario 5.3.3b holds in the area of study and hence the role of the rainfall in the highlands to the regional groundwater recharge is minimal as it flow away from the rift floor.

7.3.2 2.5-D Visualization of Geology

The rasterized geologic map of the study area was imported from ILWIS software into GMS3.1 Software as an image. This was then draped over the TIN representing the topographic surface of the study area. The resulting 2.5D expression of the surface area is as shown below in figure 7.3.2 below.

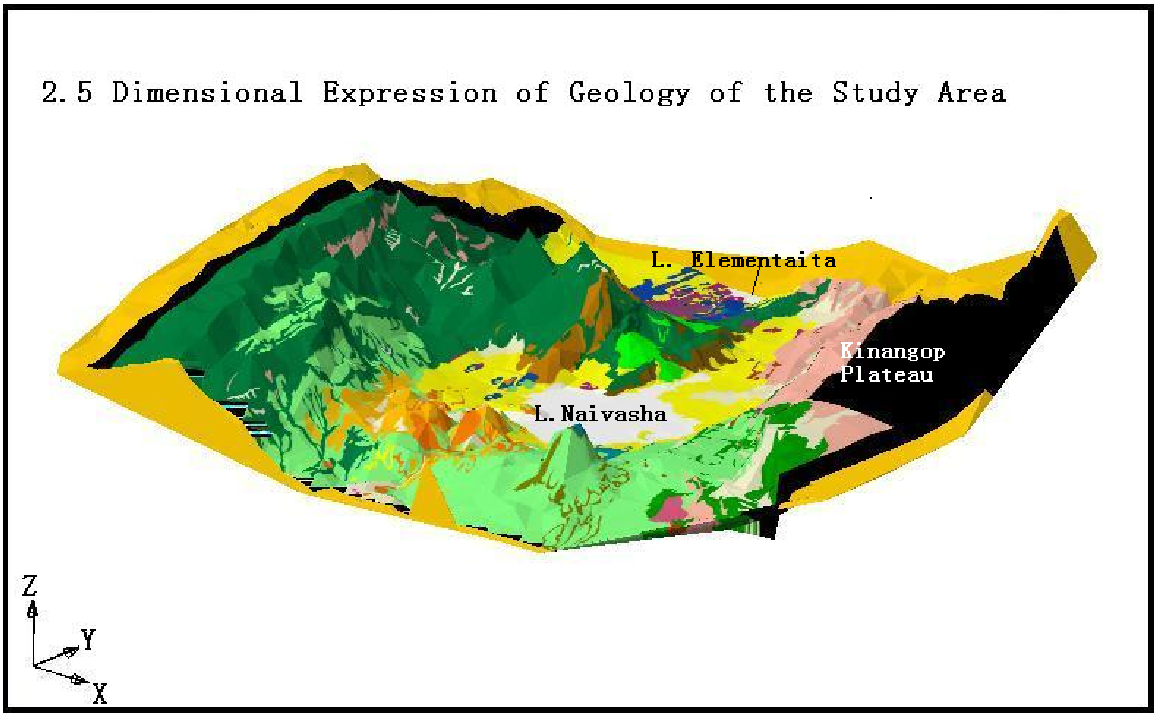

Figure 7.3.2: 2.5D expression of the geology of the area. While pumices mostly cover Mau Plateau, while the Kinangop Tuffs are mostly exposed in Kinangop Plateau. This means that more infiltration occurs in the former than in the later.

7.3.3 3-D Representation of Geology

This is attainable through two approaches, the Additive and subtractive approach.

7.3.3.1 Additive Approach

The bottom and top contacts of the different formations were separately selected and triangulated to constitute the bottom and top TINs of respective different formations. Solids representative of the material were then filled between these TINs and named accordingly. To appreciate the 3-D spatial relationship between these formations, six sections were cut through the study area; three along the Rift Valley and three across the Rift valley. The solid and the sections are as shown in Figure 7.3.3.1a and Figures 7.3.3.1b respectively.

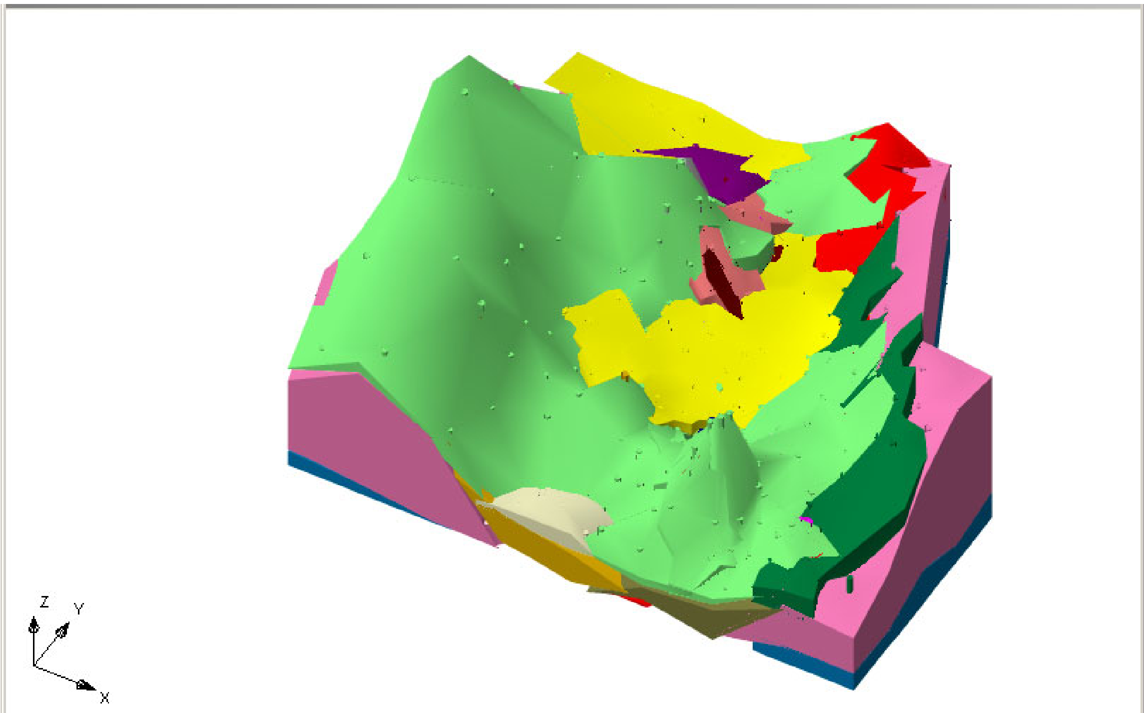

Figure 7.3.3.1a 3-D expression of geology of Area of Study constructed using the additive approach. A lot of empty space exists between different formations and there is a lot of overlapping between different adjacent formation

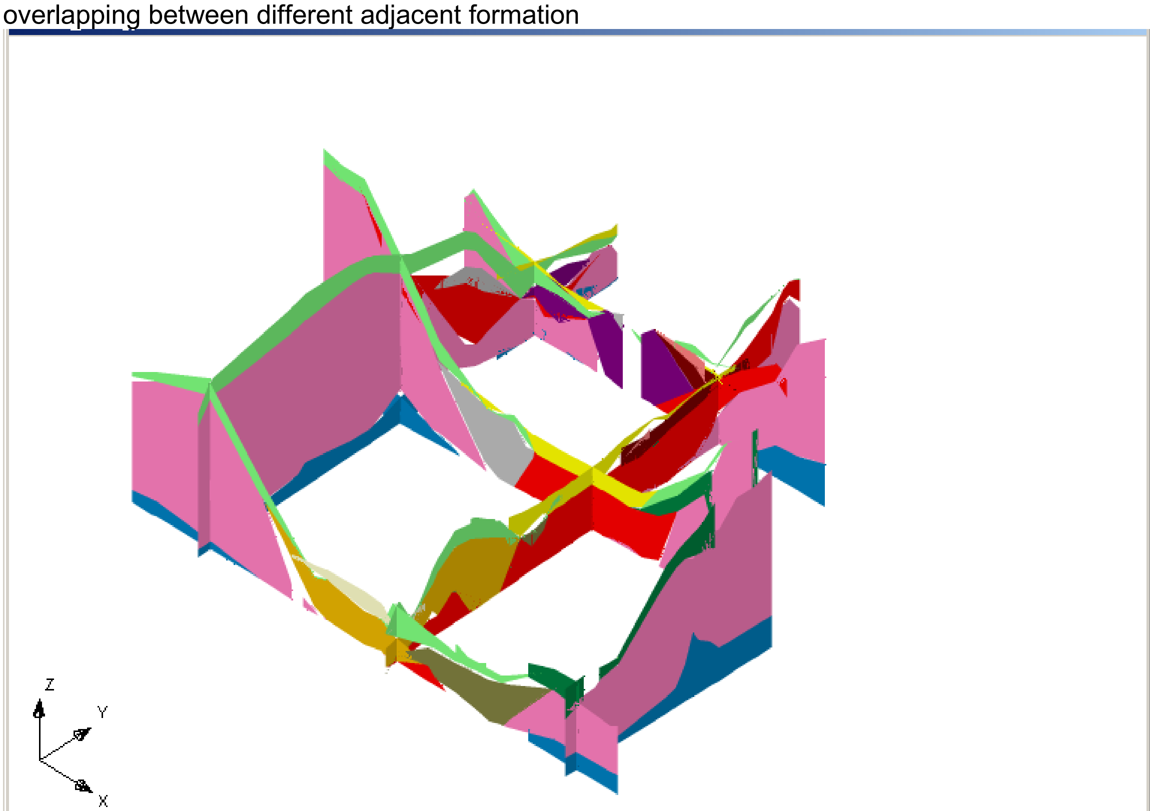

Figure 7.3.3.1b Sections through the model. There is a lot of empty space in the model. Besides, there is a lot of overlapping between different formations.

Legend

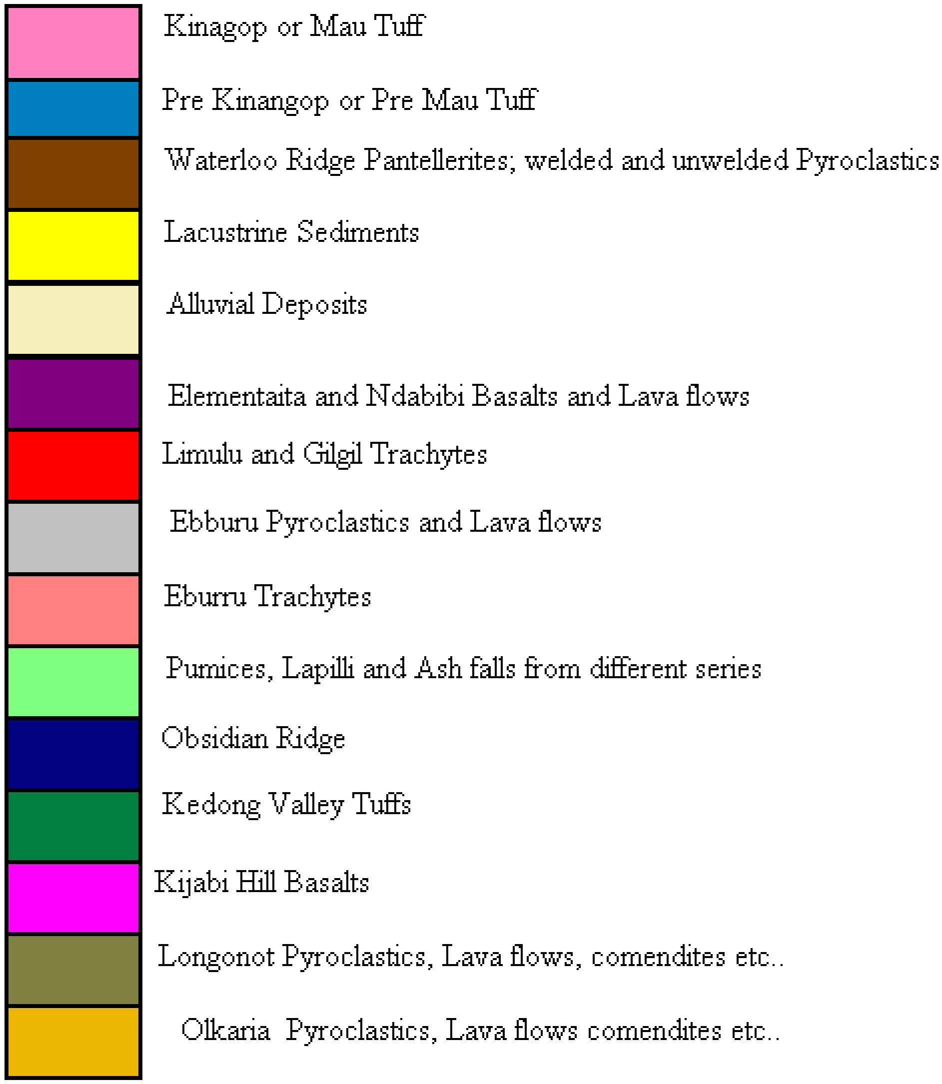

7.3.3.2 Subtractive Approach

In this approach, the topographic surface TIN was extruded into a solid to an elevation of 1500m above sea level to represent the topmost or outermost formation. The TIN representing the top surface of the next formation was also then extruded into a solid to an elevation of 1500m to representative of that layer. Since the upper most layer occupies even the space occupied by the lower layer, subtracting the lower solid from the upper larger solid while deleting the upper solid where they overlap, gives the solid that represents the upper layer and the lower solid layer(s). This process is repeated for each individual layers until all the formations are modeled. While this operation is theoretically possible and is meant to be executed with “set operations” in the GMS software, it could not be done at any level as the computer was continually “crushing”

The developer of the Software in the USA are yet to come up with ways of overcoming this problem.

7.4 Calibration

Due to the shortage of time and insufficient data, the model has not been calibrated. The model is still course and will be refined as more data become available and when the scale of modeling is increased. As more data become available In the future, attempts should be made to calibrate the model as a way of verifying its validity. The calibration exercise will entail assigning of hydraulic properties to the different formation and simulating the steady state hydraulic heads of the area before proceeding with the Transient state calibrations.

Chapter 8 Conclusions and Recommendations

8.1 Conclusions

Besides the faults that were responsible for the genesis of Mau and Satima escarpment on the western and Eastern side of the lake, there are three other major faults (system) that have been responsible for the evolution for the geology of the study area. These also greatly influence the regional flow pattern. Besides, the surface drainage in the area is dependent upon the fault system. The down throw of the eastern block along fault B accounts for the difference in depth of sedimentary formation on the different sides of that fault.

The smaller faults on the eastern and western escarpment impede the flow of water from the escarpment to the lake. This accounts for the low transmissivities along these flow direction that are evidenced by the high piezometric gradients that exist on the escarpments. Along the Rift Valley floor, however, these faults constitute preferential flow paths of out flow. The major southeastward outflow coincides with the fault C.

With reference to its relevance to its role in hydrogeology, the extent of the lacustrine sedimentary formation in the study area is exaggerated. This is evident from the driller’s log of borehole ITC183. While from the geological map this well is located in the lacustrine sediments, the information gathered from the driller’s log does not bear testimony to that. According to hydro geological principals, an aquifer in a sedimentary formation without confining layer must be unconfined. However, while no confining sedimentary formation is evidenced in this location, information from the driller’s log indicates that the water struck was under confined conditions in volcanic rocks. Consequently, from a hydro geological point of view would, the geology of this location should be more appropriately classified as Volcanic than sedimentary.

The sedimentary formations are more represented in the Northern and Northeastern part of the study area where its thickness goes as high as 120m in some locations. This formation clearly constitutes two-layered aquifer in this part: the shallow one to the depth of 60m and a second one between 80 m to 120m. Most wells in the area exploit only the first aquifer. In the southern, eastern or western side of lake Naivasha, the depth of the sedimentary formation at a distance beyond a distance of 500m from the lake rarely exceeds the depth of 20m.

The simple two-end member is appropriate in areas where the waters are a mixture of various ratios of the two end members along the mixing line which are the lake water and the direct recharge from rainfall in this case. However in the Northern and northeastern parts of the study area where besides lake water and direct recharge from rainfall, there is an evident recharge due to infiltration from rivers, this simple model is inappropriate.

The depression in the piezometric contour map on the northeastern side of the study area is as a result of abstraction of ground water in that part of the study area. Sustained increase in the abstraction from the well fields there will result to increased hydraulic gradient in that direction which will increase in the amount of water drawn from the lake to the well field.

The lack of significant lake water isotopic signature in the well field is as a result of two reasons. The fall of water level in the well field below the lake water level is a recent development, which started after 1980. Consequently insufficient time has elapsed for the water to migrate from lake to he well field. Besides, the dilution effect due to infiltration from Karati River will delay further the detection of lake water isotopic signature in the well field. This means that besides the lake and direct recharge from the rainfall, infiltration from Karati River is another major source of water to the well.

The plot of yield and depth against EC indicate that there is neither a correlation between yield and EC nor between Depth and EC. Therefore the deterioration of water quality with time is a consequence of radial interception of cone of depression with salt lenses caused by sustained high rate pumping rather than human induced up coning

The sedimentary formations are more represented in the Northern and Northeastern part of the study area where its thickness goes as high as 120m in some locations. This formation clearly constitutes two-layered aquifer in this part: the shallow one to the depth of 60m and a second one between 80 m to 120m. Most wells in the area exploit only the first aquifer. In the southern, eastern or western side of lake Naivasha, the depth of the sedimentary formation at a distance beyond a distance of 500m from the lake rarely exceeds the depth of 20m.

The Mau and Kinangop plateaus tilt away from the rift valley floor. Consequently rainfall in the plateaus contributes minimally to the regional groundwater recharge as most of it flows away from the valley bottom.

8.2 Recommendations

Given the enormous variations in the conductivity over very short distances, there is a need to study the hydrogeology of the area at a higher resolution. This will enable to study and understand the spatial variation of hydrogeology and its causes.

There seem to be areas of localized high conductivity channels. The possibility of underground flow channels is evident. This could be the explanation of localized high conductivity zones as evidenced by high very high yielding wells in close vicinity to totally dry wells or very low yielding wells. This phenomenon is observable at Ndabibi wheat farm and Three Point farm

Given the enormous variations in the conductivity over very short distances, there is a need to study the hydrogeology of the area at a higher resolution. This will enable to study and understand the spatial variation of hydrogeology and its causes.

A lot of activities related to water resources have taken place over the last couple of year. Consequently, this has resulted into an enormous amount of data being collected. However, the level of organization of this data and information leaves a lot to be desired. There is no unified labeling of sampling points. Besides, in some instances more that one-observation points bare the same label/code. To arrest this situation, there is a need to study, formulate and establish a well-organized database for the project area research. This will not only eradicate the confusion but also prevent them in the future as more data continue being gathered. The quality, state and for some locations the quantity of the hydrologic& hydro geologic data is wanting. There is hence a need to strengthen the existing environmental monitoring arrangement in the area so as to address the shortfall in data on water levels, wellheads elevations, groundwater abstraction and water quality.

A good number drilled in the area in the years 1996 and 1997 were drilled by Mowlem Construction. The driller and the geologists have logged most of these wells differently. While the driller based his classifications on field observations, the geologist based his classification on the published geological map of the area. Where there is a diversion in their classification, I recommend that the classification according to this particular driller be given preference over the geologist's log.

Complete Isotopic analysis should be done for wells in Northeastern portion of the study area. Plot of the dD against $d^{18}O$ values would clearly indicate whether water lies on the Direct Recharge _Lake Naivasha mixing line of off that line.

Given the enormous variations in the conductivity over very short distances, there is a need to study the hydrogeology of the area at a higher resolution. This will enable to study and understand the spatial variation of hydrogeology and its causes.

There are very few wells in the northern and eastern side of the lake. As a consequence of which the area being less understood as compared to the southern and western part of the lake, which have a number of wells. There is hence a need to drill some wells for the purposes of the studying the hydrogeology.

References

Anderson, M.P., and W.W. Woessner, 1992. Applied Groundwater modeling; Simulation of flow and Advective Transport. Academic Press, San Diego.

Appelo, C. A. J. and Postma, D., 1993, Geochemistry, groundwater and pollution.

Behar, H. A., 1999; Surface Water- Groundwater Interaction, Lake Naivasha, Kenya, MSc Thesis, ITC. Enschede, The Netherlands.

Clarke A.C.G., D. Allen, G. Darling. 1990. Geological, Volcanological and Hydrogeological Controls on the Occurrence of the Geothermal Activity in the Area Sorrounding Lake Naivasha, Kenya. Ministry of Energy, Republic of Kenya.

Domenico, P. A., and Schwartz, F. W.1990; Physical and Chemical Hydrogeology (Second Edition); John Wiley & Sons, Inc., NewYork.

Fetter, C.W., 1994. Applied Hydrogeology. Prentice Hall, Upper Saddle River, New Jersey.

Freeze, R. A., and J.A. Cherry. 1979. Groundwater. Prentice Hall, Englewood Cliffs, New Jersey.

Githae, I. T., 1998, Groundwater Flow Modeling as Tool For Water Balance Assessments, Case Study Nakuru-Elementaita Basin Within the Kenyan Rift Valley System.Thesis, ITC, Enschede, The Netherlands.

Graham, A., 1998. Groundwater Recharge Estimation of the Malewa Catchment, Naivasha, Kenya. M.Sc. Thesis, ITC, Enschede, The Netherlands.

Gressando, Y., 1999, Application of Geophysical Techniques for Groundwater Investigation in Lake Naivasha area, Kenya. M.Sc. Thesis, ITC, Enschede.

Groundwater Survey (Kenya) LTD. 1998. Borehole Site Investigations Naibor Ajijik, Report No. 98/547, Nairobi.

Hounslow, A. W., 1995, Water Quality Data (Analysis and Interpretation).

IAEA-1979, Isotope Hydrology, Proceedings of a symposium in Neuherberg,

ITC 2001. The Integrated Land and Water Information System 3.0. User's Guide Manual. ITC, Enschede, The Netherlands.

ITC, Water Resources Surveys. 1996. Water Resources Assessment Project Phase v, Mission Report, (WRAP). Water Resources modelling of the Rift valley lake Basins and Laikipia (Groundwater Component).

Lake Naivasha Riparian Owners Association, 1993; A Three Phase Environmental Impact Study of Recent Development around Lake Naivasha – Phase I.

McCann, D. L., 1972, **A** preliminary hydro geologic evaluation of the long-term yield of catchments related to geothermal prospect areas in the Rift valley of Kenya.Unpubl.UN geoth.proj.Report.

Mmbui, S. G., 1999*;* Study of Long-term Waterbalance of Lake Naivasha, Kenya, MSc Thesis, ITC, Enschede, The Netherlands.

Mook, W. G., 2000, Environmental Isotopes in the hydrological cycle (Principles and Applications). Centre for Isotope research, University of Groningen, The Netherlands.

Morgan, N. E., 1998; Groundwater Chemistry and Quality Assessment of the Lake Naivasha Area, Kenya, MSc Thesis, ITC, Enschede, The Netherlands.

Ojiambo, B. S., 1992, Hydrogeologic, Hydrochemical and Stable Isotopic Study of Possible Interactions Between Lake Naivasha, Shallow Subsurface and Olkaria Geotherma.

Ojiambo, B. S., 1996, Characterization of Subsurface Outflow from a closed-basin freshwater tropical lake, Rift Valley, Kenya.

Omenda, P. A., 1998, The Geology and Structural Controls of the Olkaria Geothermal System, Kenya. Journal of Geothermic, vol. 27, No.1.

Oppong-Boateng, R, 2001, Assessment of Groundwater for Irrigation in the Southern Part of Lake Naivasha, Kenya. M.Sc. Thesis, International Institute for Aerospace survey and Earth Sciences, Enschede.

Owor, M., 2000, The long term interaction of groundwater with Lake Naivasha, a numerical simulation of the relationship between groundwater and lake level allowing for fluctuation. M.Sc. Thesis, International Institute for Aerospace survey and Earth Sciences, Enschede.

Ramirez, 1999; Groundwater Flow Modeling of Lake Naivasha, Kenya, MSc Thesis, ITC, Enschede, The Netherlands.

Thompson, A.O. and R. G. Dodson. 1963. Geology of the Naivasha Area. Geological Survey of Kenya, Report. No. 55.

Trottman, D. K., 1999; Modeling Groundwater Storage Change in response to Fluctuations of Lake Naivasha, Kenya, MSc Thesis, ITC.

Viak Ltd, 1975; Naivasha Water Supply Project, Ministry of Agriculture, Republic of Kenya.

Wiberg,I. 1976, Naivasha Water Supply Project, Groundwater Investigation, VIAK EA Ltd., Consulting Engineering and Mapping Services.

Appendices

Appendix 1: Water Chemistry Analysis Results

Code	Location	X	Y	EC	Cl-	Fl-	Li [mg/l]	Ca [mg/l]	K [mg/l]	Mg [mg/l]	Na [mg/l]	$^{18}\delta O(^{o}/_{oo})$
NIK 1	Del B/H 1	213159	9922182	1254.00	33.50	4.80	0.04	21.84	28.24	3.38	208.07	-4.14
NIK 3	TPF Green House BH G	214004	9925600	810.00	22.20	8.55	0.12	15.42	20.17	0.92	138.48	
NIK 4	Brixia Dug well 1	203493	9924226	851.00	22.30	3.60	0.04	38.50	18.98	29.95	72.34	
NIK 5	Del B/H 5	212262	9924292	1036.00	107.25	1.95	0.01	75.75	23.65	7.14	81.79	-3.94
NIK 6	Karagita Dispensary	214065	9914362	1396.00	86.00	6.30	0.13	14.79	20.46	2.24	276.28	1.08
NIK 8	Del B/H 10	213825	9923256	528.00	7.90	2.70	0.08	20.00	12.27	1.35	78.88	-3.70
NIK 9	KWS Well	216083	9918162		15.90	9.00	0.11	6.65	16.27	0.27	153.71	-5.20
NIK 10	TPF BH M	213049	9924682	484.00	9.05	2.37	0.02	29.31	20.10	4.46	45.67	-4.00
NIK 49	TPT B/H E	213399	9924799	557.00	9.65	2.50	0.08	32.08	15.56	1.48	66.96	-3.16
NIK 13	Golf Course 2	201555	9926480	1160.00	20.00	10.90	0.20	6.79	26.25	0.83	264.00	-0.44
NIK 16	Green Park	201898	9925450	801.00	9.80	10.40	0.12	5.70	16.38	1.03	159.08	
NIK 17	Rose Wairimu's Farm C11307	216386	9914430	740.00	11.50	4.85	0.08	15.09	22.90	2.06	126.42	
NIK 19	Beuty Line	208279	9931280	755.00	23.30	3.60	0.08	27.26	22.50	4.53	102.63	
NIK 20	Del B/H 6	211668	9924646	1136.00	71.50	4.88	0.02	25.85	20.25	2.96	194.05	
NIK 21	Hospital	214843	9920716		44.50	9.10	0.10	14.84	25.29	1.98	172.60	
NIK 25	Point 52	215546	9915380	1100.00	56.50	7.10	0.07	17.11	29.68	2.86	194.05	
NIK 26	Israelite	208314	9931186		17.50	3.30	0.08	30.24	25.26	4.21	101.56	
NIK 27	TPF B/H B	213713	9924977	560.00	14.30	2.70	0.11	25.03	15.02	1.44	73.50	
NIK 28	TPF B/H A	213707	9925500	780.00	20.25	5.75	0.13	14.10	24.29	0.43	140.91	
NIK 29	La Bella Inn	214153	9920718		113.50	3.70	0.22	61.65	60.84	6.81	410.38	
NIK 31	Del B/H 4	211756	9922022	1274.00	88.00	2.20	0.02	70.60	25.02	9.80	165.92	

NIK 35	Lodia Well 1	200459	9922216	744.00	12.20	5.60	0.08	9.55	17.57	4.22	139.97	
NIK 36	Lodia Well 2	200459	9922216	745.00	12.60	5.80	0.10	10.23	19.99	1.46	144.43	
NIK 38	Del B/H 3	211874	9922902	483.00	10.10	2.25	0.02	22.17	13.57	3.37	61.60	-4.41
NIK 40	Kongoni AIC	194853	9909876	941.00	30.00	8.50	0.16	21.26	3.43	12.05	157.74	3.67
NIK 48	Pt 48 Karati Area	217823	9920176	677.00	15.90	6.40	0.02	6.13	19.78	3.15	123.41	
NIK 50	TPT B/H c	213409	9924916	620.00	13.00	5.50	0.10	39.99	15.56	1.68	71.43	-3.70
NIK 52	Point 49	219199	9920256	663.00	9.00	6.40	0.04	5.61	18.40	1.62	125.82	
NIK 54	TPF B/H D	213392	9924848	556.00	11.10	2.60	0.09	34.09	13.16	1.73	65.70	-3.46
NIK 55	Marula Farm	203808	9938988	613.00	14.80	5.75	0.07	19.12	18.89	3.21	89.27	-3.02
NIK 57	Del B/H 2	211733	9923434	1145.00	95.00	1.40	0.01	103.34	28.04	13.92	74.28	-3.87
NIK 58	Brixia well 2	203833	9924136	499.00	23.30	3.80	0.03	22.05	13.86	16.25	39.39	-1.05
NIK 59	Brixia well 3	203924	9923924	770.00	20.00	3.30	0.04	37.12	19.19	27.77	65.62	-0.20
NIK 60	Elementaita	194748	9948036	>3300	4100.00	420.00	0.39	2.17	366.88	0.65	1996.33	-1.34

Appendix 1A: Chemical Data Used in Studying Chemical Trends

B/H 1															
Year	ECus/cm	Cl^- mg/l	F^- mg/l	Li^+mg/l	Ca^{2+} mg/l	K^+ mg/l	Mg^{2+}mg/l	Na^+ mg/l	HCO3 -	CO3 2-	SO42-	TDS	Analysis By:	Depth	Yield
21-Nov-73	550	20.6			21.6	14.5	1.7	100	324.6	0	14.4	497	NAL	42.7	72
22-Apr-96	591	14.8	4.5						266	0	18		EWT	42.7	72
21-Nov-00	640	16			23.8	16.8	3.2	100.9	335.6	0	21.1	517	CNS	42.7	72
22-Sep-01	1254.00	33.50	4.80	0.04	21.84	28.24	3.38	208.07					itc	42.7	72
B/H 2														42.7	72
Year	ECus/cm	Cl^- mg/l	F^- mg/l	Li^+mg/l	Ca^{2+} mg/l	K^+ mg/l	Mg^{2+}mg/l	Na^+ mg/l	HCO3 -	CO3 2-	SO42-	TDS	Analysis By:	Depth	Yield
21-Nov-73	500	30.1			58.7	21.1	7.5	52.4	319.7	0	28.8	518	NAL	76.8	189
22-Apr-96	989	107	1.6		120.9		10.2		346	0	66		EWT	76.8	189
21-Nov-00	1060	85.4			173.5	27.4	14.2	69.9	445.4	0	62.9	694	CNS	76.8	189
21-Sep-01	1145.00	95.00	1.40	0.01	103.34	28.04	13.92	74.28					itc	76.8	189
B/H 3														76.8	189
Year	ECus/cm	Cl^- mg/l	F^- mg/l	Li^+mg/l	Ca^{2+} mg/l	K^+ mg/l	Mg^{2+}mg/l	Na^+ mg/l	HCO3 -	CO3 2-	SO42-	TDS	Analysis By:	Depth	Yield
21-Nov-73	450	18.8			29.7	14.9	3.8	74.9	294.1	0	4.3	440	NAL	82.3	171
22-Apr-96	460	9.8	1.3		27.23		3		214	0			EWT	82.3	171
21-Nov-00	490	9.9			33.7	16.8	4	54.5	268.5	0	9.1	338	CNS	82.3	171
21-Sep-01	483.00	10.10	2.25	0.02	22.17	13.57	3.37	61.60					itc	82.3	171
B/H 4														82.3	171
Year	ECus/cm	Cl^- mg/l	F^- mg/l	Li^+mg/l	Ca^{2+} mg/l	K^+ mg/l	Mg^{2+}mg/l	Na^+ mg/l	HCO3 -	CO3 2-	SO42-	TDS	Analysis By:	Depth	Yield
21-Nov-73	1100	69.8			28.3	17.2	3.2	242.3	595.5	0	262.3	1218	NAL	61	nk
22-Apr-96		10.3	1.1		26.4		2.9		214				EWT	61	nk
26-Jun-00	1494	99.4			174.4	19.5	26.7	239	379	16.3	149	1105	KSS	61	nk
21-Nov-00	1555	8.5			67.1	25.4	7.7	249	835.9	0	69.2	1263	CNS	61	nk
21-Sep-01	1274.00	88.00	2.20	0.02	70.60	25.02	9.80	165.92					itc	61	nk
B/H 5														61	nk
Year	ECus/cm	Cl^- mg/l	F^- mg/l	Li^+mg/l	Ca^{2+} mg/l	K^+ mg/l	Mg^{2+}mg/l	Na^+ mg/l	HCO3 -	CO3 2-	SO42-	TDS	Analysis By:	Depth	Yield
21-Nov-73														91.4	148.5

22-Apr-96	761	84	1.6		72.1		6.8		204	0	49		EWT		
21-Nov-00	960	95			99.2	25.8	7.7	75.4	353.9	0	69.2	625	CNS	91.4	148.5
22-Sep-01	1036.00	107.25	1.95	0.01	75.75	23.65	7.14	81.79					itc	91.4	148.5
B/H 6															
Year	ECus/cm	Cl^- mg/l	F^- mg/l	Li^+mg/l	Ca^{2+} mg/l	K^+ mg/l	Mg^{2+}mg/l	Na^+ mg/l	HCO3 -	CO3 2-	SO42-	TDS	Analysis By:	Depth	Yield
21-Nov-73	700	25.5			14.4	16	0.9	174.7	428	0	53.3	713	NAL	91.4	6
22-Apr-96	737	18.2	5.8		5.606		2		318	0	29		EWT	91.4	6
26-Jun-00	1098	97.5			105.6	14	12.3	188.5	585	19	54.8	1077	KSS	91.4	6
21-Nov-00	1080	60.6			34.3	19.2	3.3	176.1	445.4	0	72	698	CNS	91.4	6
21-Sep-01	1136.00	71.50	4.88	0.02	25.85	20.25	2.96	194.05					itc	91.4	6
B/H 7															
Year	ECus/cm	Cl^- mg/l	F^- mg/l	Li^+mg/l	Ca^{2+} mg/l	K^+ mg/l	Mg^{2+}mg/l	Na^+ mg/l	HCO3 -	CO3 2-	SO42-	TDS	Analysis By:	Depth	Yield
21-Nov-73	800	32.6			14.6	19.9	0.5	247.4			82.1	868	NAL	72.5	168
1976	850	42			14	16	1.3	178			52	771	GSK	72.5	168
Apr-81	990	90			23	19	1.4	218			19	790	GSK	72.5	168
22-Apr-96	1151	68.5	4.4						382	0	100		EWT		
18-Jun-05	1151	68.5	4.4		26.43		49.57		466.04	0	100		LU	76.2	168
1-Nov-99	1200	82			36	43	4.9	210			96	879	LVDS	72.5	168
26-Jun-00	1025	81.5			64.7	14.9	8.6	188.5	307.5	27	39.4	733	KSS	72.5	168
21-Nov-00	1190	80.6			34.3	21.9	2.8	205.1	445.4	0	96.1	784	CNS	72.5	168
Nov-01														72.5	168
B/H 10														79	9.1
Year	ECus/cm	Cl^- mg/l	F^- mg/l	Li^+mg/l	Ca^{2+} mg/l	K^+ mg/l	Mg^{2+}mg/l	Na^+ mg/l	HCO3 -	CO3 2-	SO42-	TDS	Analysis By:	Depth	Yield
21-Nov-73														64	204
9-Apr-96	600	11			28	12	2.4	100	280	0	48	524	LVDS	64	204
22-Apr-96	519	8.1	3.9		28.83		53.17		368	0	1		EWT	64	204
26-Jun-00	526	21.3			84.8	10.2	7.4	77	203.2	21.6	18.7	445	KSS	64	204
21-Nov-00	540	13.1			32.1	14.9	1.9	74.7	299	0	6.2	356	CNS	64	204
21-Sep-01	528.00	7.90	2.70	0.08	20.00	12.27	1.35	78.88					itc	64	204

Appendix 1.2: Results of Linearity Tests

Fluoride analysis HACH DR/2010 spectrophotometer
0-2 mg/l   SPADNS method

Standard solution (mg/l)	Measured (mg/L)			Average	standard deviation	% relative error
0	0	-0.01	0.01	0.00	0.01	-
0.5	0.52	0.51	0.54	0.52	0.02	2.9
1	1.01	1	0.96	0.99	0.03	2.7
2	1.9	1.91	1.96	1.92	0.03	1.7

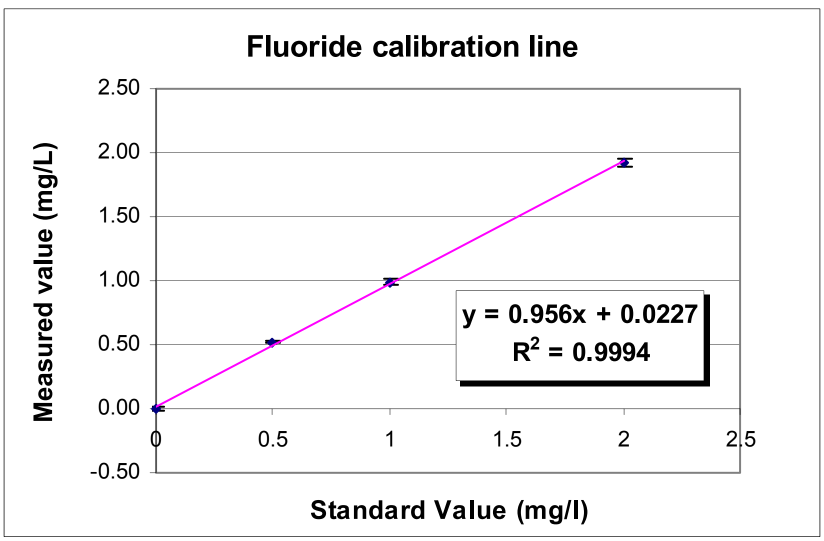

Chloride analysis DACH 2010 spectrometer
0-20 mg/l   SPADNS method Mercuric Thiocyanate method

Standard solution (mg/l)	Measured (mg/L)			Average	standard deviation	% relative error
0	0	0	0.1	0.03	0.06	-
3	3	3.1	3.1	3.07	0.06	1.9
9	9.9	9.6	8.4	9.30	0.79	8.5
15	15.3	15.5	15.2	15.33	0.15	1.0

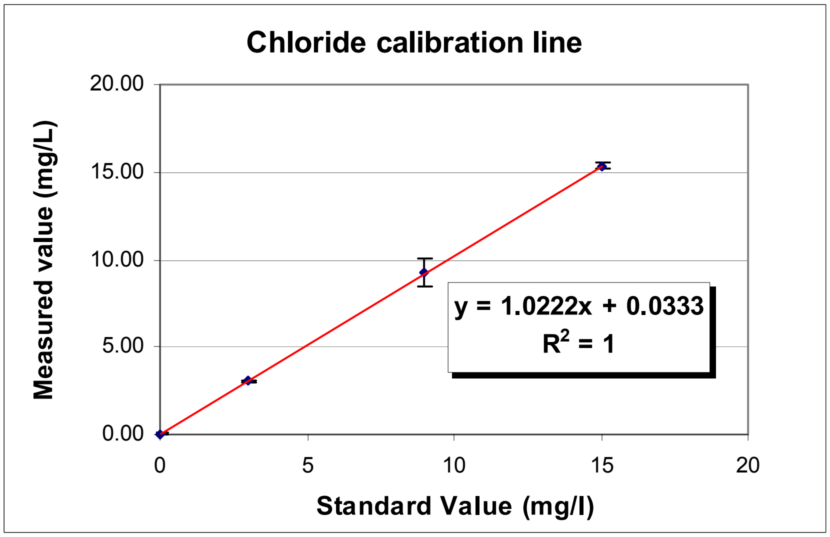

Na 589

525154	20
235686	10
108618	5
40068	2
19744	1
10311	0.5
1163	0

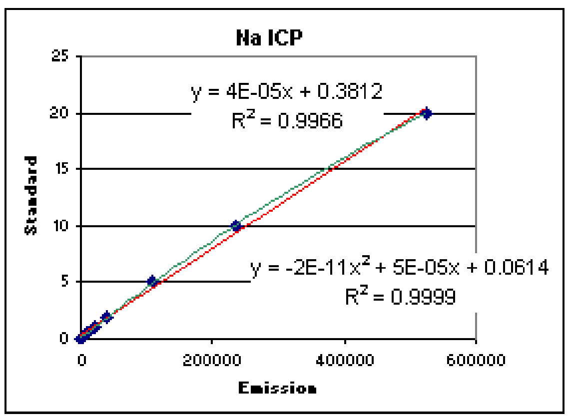

Mg 285

277594	20
139180	10
68874	5
27702	2
13911	1
7206	0.5
72	0

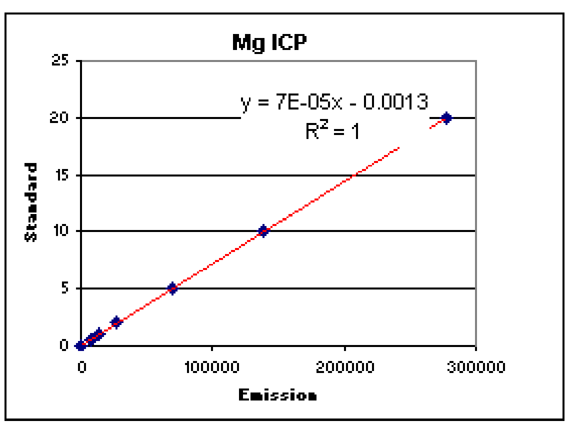

K 769

22360	20
9826	10
4515	5
1452	2
961	1
469	0.5
230	0

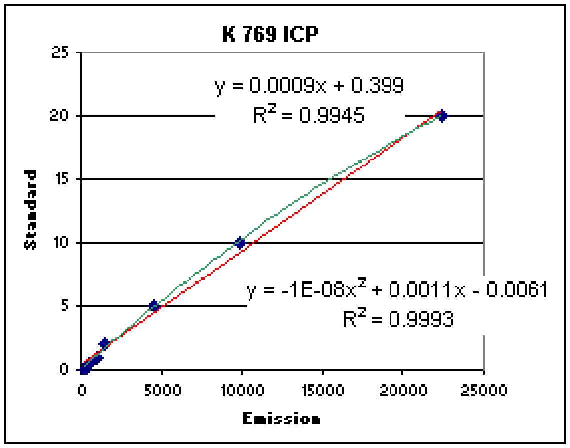

Ca 422

958045	20
452741	10
214102	5
83353	2
41329	1
28172	0.5
1209	0

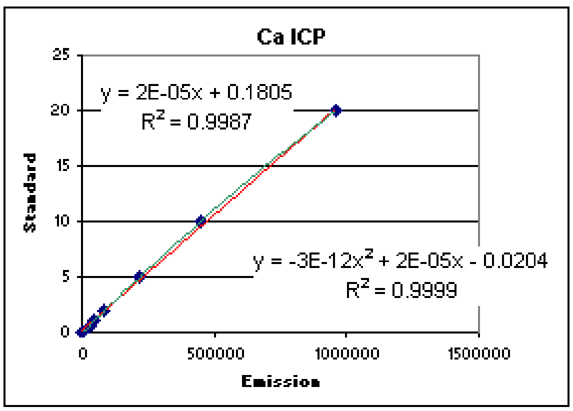

Li (A) 670.784

0.5	35330
1	75732
2	151307
5	371372

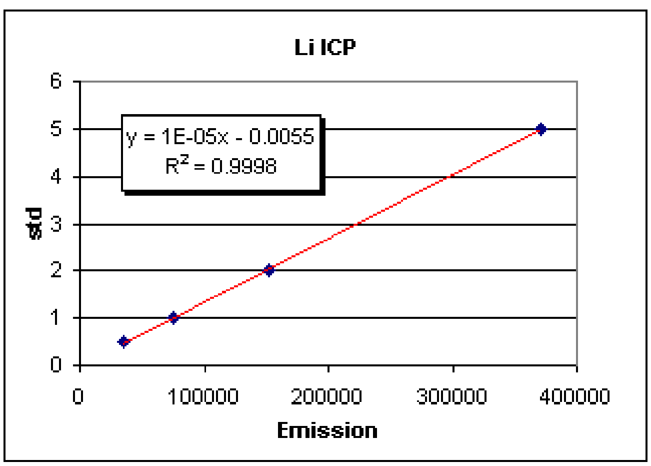

Appendix 2: Isotopic Analysis Results

Sample code	Location	X	Y	EC	Temp	Elevation	Depth	WRL	Sampled By	dD	^{18}dO
IS1	Eburru Steam Harv	195595	9928618			2542			Isah		-3.93
IS2	Lake Elementeita	194748	9948036	3300	40.1	1795			Isah		-1.34
IS3	Njawu's Well	215546	9915380	1100	27.8	1958	300	57	Isah		-3.89
IS4	Rose's Farm	216386	9914430	740	25		70		Isah		-4.51
IS5	Marula Farm							*	Isah		-3.02
IS6	Kinangop area							*	Isah		-3.7
IS7	Karagita Disp	214065	9914362	1396	23.5	1951			Isah		1.08
IS8	TPF B/H E	213399	9924799	557	23.6	1913	60	29.02	Isah		-3.16
IS9	Del BH 1	213159	9922174	1249	23.5	1917			Isah		-4.14
IS13	Del BH 10	213825	9923256	528	19.4				Isah		-3.7
IS14	Brixia Farm BH2	203833	9924136	499	20.1		40	6.1	Isah		-1.05
IS15	Del BH 6	211690	9924612	1136	23.5	1919			Isah		-4.05
IS16	La Bella inn	214842	9920718			1921			Isah		-2.07
IS19	Del BH 5	212262	9924292	1036	24.4	1948			Isah		-3.94
IS20	KSW	216083	9918162			2026			Isah		-5.2
IS21	hospital	214843	9920716			1949			Isah		-4.69
IS22	Israelite's well	208315	9931192	755	20.4	1916			Isah		-3.35
IS23	TPF B/H M	213049	9924682	484	22.7		58	22	Isah		-4
IS24	Kongoni AIC	194853	9909876	941	18.9	1918			Isah		3.67
IS25	Del BH 3	211874	9922902	483	23.6	1895			Isah		-4.41
IS26	TPF B/H D	213392	9924848	556	22.8	1907	52	29.15	Isah		-3.46
IS27	Brixia Farm BH3	203929	9923972	770	20.3	1922	6	3.15	Isah		-0.2
IS28	Del BH 2	211733	9923434	1145	24.4	1939			Isah		-3.87
IS29	Lodiya Farm	200459	9922216	744	18.7	1941			Isah		2.38
IS30	Del BH 4	211756	9922022	1274	22.2	1929			Isah		-3.62
IS32	Golf Course 2	201555	9926480	1160	23.6	2111			Isah		-0.44

Appendix 3: Wells used to Draw Piezometric Contours

STATION	UTM_X	UTM_Y	PIEZOMETRI
ITC001	213518	9924527	1881
ITC002	213735	9925528	1885
ITC003	213713	9924977	1886
ITC004	213459	9924929	1882
ITC007	214004	9925600	1884
ITC008	213544	9925720	1884
ITC009	211437	9921386	1886
ITC010	211914	9924455	1884
ITC011	213101	9928951	1887
ITC012	214504	9926572	1913
ITC013	212603	9923764	1883
ITC015	210473	9928944	1867
ITC020	211231	9924924	1881
ITC021	211822	9923166	1880
ITC022	212334	9922728	1885
ITC025	212267	9923041	1883
ITC026	208752	9928952	1886
ITC029	204034	9928849	1886
ITC031	211769	9924324	1882
ITC035	215467	9917087	1903
ITC036	214224	9919179	1886
ITC038	203516	9924230	1886
ITC040	201591	9926461	1885
ITC042	207165	9925364	1886
ITC043	210769	9920726	1887
ITC045	209462	9928455	1889
ITC047	208988	9937384	1934
ITC048	212459	9931771	1958
ITC052	214316	9917024	1883
ITC054	197600	9929926	2333
ITC055	214375	9916225	1889
ITC056	213900	9916550	1882
ITC057	216171	9926241	2037
ITC058	218032	9922558	1999
ITC059	216171	9924404	2006
ITC060	216175	9918873	1984
ITC063	210602	9924401	1883
ITC066	199466	9920700	1877
ITC070	195752	9928078	2523
ITC071	205035	9920703	1884

ITC072	197605	9920698	1886
ITC073	199465	9922547	1903
ITC077	208741	9926237	1887
ITC080	212469	9913339	1877
ITC081	195762	9911480	1886
ITC082	206306	9931350	1886
ITC084	214313	9920708	1895
ITC085	212995	9923310	1885
ITC087	211625	9927400	1906
ITC088	213350	9921550	1885
ITC092	219888	9911496	2135
ITC093	195763	9909632	1885
ITC101	214318	9913340	1931
ITC102	199473	9909635	1878
ITC104	205043	9907802	1844
ITC105	210608	9915174	1801
ITC106	212469	9913339	1870
ITC107	212412	9903826	1899
ITC110	210612	9907806	1936
ITC121	210619	9898578	2070
ITC130	214317	9915176	1908
ITC134	210610	9911490	1920
ITC136	219659	9902553	1872
ITC140	213885	9912005	1884
ITC141	194855	9909913	1898
ITC144	213038	9914522	1891
ITC145	212664	9915091	1887
ITC146	212469	9926230	1914
ITC147	213850	9921800	1885
ITC149	217150	9918100	1929
ITC151	212675	9918025	1879
ITC152	201200	9910050	1909
ITC153	218100	9930525	2165
ITC154	211200	9912475	1886
ITC156	214009	9917763	1888
ITC158	202435	9909675	1890
ITC159	195974	9908951	1887
ITC160	196851	9915861	1888
ITC161	197660	9918954	1888
ITC162	215784	9912357	1884
ITC180	203360	9925256	1886
ITC183	208323	9931189	1884
ITC185	194375	9919316	1885
N12	215200	9913100	1907
N52	219411	9926765	2064
N54	219848	9929261	2168

N40	216441	9913361	1910
C2709	186474	9907789	2114
C0466	190189	9917009	1907
C1404	190190	9915161	1894
C2300	190500	9909750	1914
V301	193940	9902400	1774
C2557	195300	9912500	1892
EW1	196900	9930575	1852
C2586	198500	9905140	1842
V26	200130	9902275	1594
C733	202750	9940250	1819
ITC_ked1	214204	9907097	1904
ITC_ked2	208867	9909074	1883
ITC_sher	207857	9908376	1884
ITC186	194608	9918650	1885
ITC187	193160	9951043	1777
NIK16	201898	9925450	1886

Appendix 4: Leveled Wells

Owner/ Location	UTM_X	UTM_Y	Source	Altitude	WRL	Measured by/Year	Piez_ele.
Three Point Ostrich	213518	9924527	Differential GPS fieldwork 1999	1910.00	29.49	Isah 2001	1880.51
Three Point Ostrich	213735	9925528	Differential GPS fieldwork 1999	1915.00	30.39	Kibona 1999	1884.61
Three Point Ostrich	213713	9924977	Differential GPS fieldwork 1999	1911.00	25.18	Kibona 1999	1885.82
Three Point Ostrich	213459	9924929	Differential GPS fieldwork 1999	1909.00	26.69	Kibona 1999	1882.31
Three Point Ostrich	214004	9925600	Differential GPS fieldwork 1999	1918.00	33.65	Kibona 1999	1884.35
Three Point Ostrich	213544	9925720	Differential GPS fieldwork 1999	1917.00	33.21	Kibona 1999	1883.79
Manera Farm	211437	9921386	Differential GPS fieldwork 1999	1891.00	5.40	Opiyo (averaged)1999	1885.60
Milk factory	211914	9924455	Differential GPS fieldwork 1999	1904.00	20.08	Opiyo (averaged)1999	1883.92
DTI Insitute (BH103)	213101	9928951	Differential GPS fieldwork 1999	1940.00	52.70	Nairobi Data base 1960	1887.30
BH107	214504	9926572	Differential GPS fieldwork 1999	1940.01	27.00	Opiyo 1975	1913.01
Kobil station	212603	9923764	Differential GPS fieldwork 1999	1902.00	19.05	Kibona 1999	1882.95
Marula Farm (Irish artist)	210473	9928944	Differential GPS fieldwork 1999	1894.00	27.11	Kibona 1999	1866.89
C11954	203360	9925256	Geodetic leveled (1999)	1938.30	52.00	Opiyo (averaged)1999	1886.30
BH2 Manera Farm	211323	9922533	Geodetic leveled (2001)	1892.58	15.30	Ochieng/Sipul and Isah	1877.28
BH7 Manera Farm	211231	9924924	Geodetic leveled (2001)	1903.32	22.07	Ochieng/Sipul and Isah	1881.25
BOINEETBH1 (Brig Farm)	194375	9919316	Geodetic leveled (2001)	1927.12	42.20	Ochieng/Sipul and Isah	1884.92
BOINEETBH2 (Brig Farm)	194608	9918650	Geodetic leveled (2001)	1922.20	37.20	Ochieng/Sipul and Isah	1885.00
GOLFCOURSEBH2 (up)	201561	9926470	Geodetic leveled (2001)	2075.75	191.00	Ochieng/Sipul and Isah	1884.75
ISRAELBH1/Beauty Line	208323	9931189	Geodetic leveled (2001)	1899.15	15.05	Ochieng/Sipul and Isah	1884.10
KEDONGBH	214204	9907097	Geodetic leveled (2001)	2022.93	119.00	Ochieng/Sipul and Isah	1903.93
KONGONIAICBH	194827	9909902	Geodetic leveled (2001)	1902.99	5.21	Ochieng/Sipul and Isah	1897.78
New sher well	207857	9908376	Surveyed with respect to sher peg level(sipul)=1905.88	1905.74	21.57		1884.17
Kedong C210	208867	9909074	Surveyed with respect to sher peg level(sipul)=1905.88	1899.13	16.25		1882.88
Hearther	214281	9909564	Sipul	1975.50	90.12		1885.38

Appendix 5A: Format of Project File **“modelfinal.gpr”**

```
PROJECT
MAT         "modelfinal.mat"
BHOLE "modelfinal.bor"
SOLID "modelfinal.sol"
MAP         "modelfinal.map"
TIN         "modelfinal.tin"
STNGS "modelfinal.ini"
```

Appendix 5: Format of TIN File `"modelfinal.tin"`

```
TIN
BEGT
ACTIVETIN
HIDDEN
ID  7596
TNAM "top_mau_tuff"
MAT 1
VERT 112
1.743410000000000e+005  9.949570000000000e+006  1.800000000000000e+003                 1
1.732490000000000e+005  9.943477000000000e+006  1.860000000000000e+003                 1
1.732520000000000e+005  9.900129000000000e+006  2.550000000000000e+003                 1
1.733430000000000e+005  9.890443000000000e+006  2.330000000000000e+003                 1
1.975860000000000e+005  9.890261000000000e+006  1.500000000000000e+003                 1
1.882930000000000e+005  9.890989000000000e+006  2.015000000000000e+003                 1
1.807530000000000e+005  9.890534000000000e+006  2.440000000000000e+003                 1
…..
…..
TRI 169
      45          48          89
       5         112          97
       7          20          21
      17          69          95
       4           7           3
…..
ENDT
```

Appendix 6: Format of Borehole File "modelfinal.bor"

```
BHOLE
DISW 6.696410000000000e+002   8.705330000000000e+002
DSETS 0
BEGH
BNAM "Ok1"
ID 1
CONT 3
  1.893890000000000e+005      9.910380000000000e+006  2.019690000000000e+003  7
  1.893890000000000e+005      9.910380000000000e+006  1.919690000000000e+003  5
  1.893890000000000e+005      9.910380000000000e+006  1.500000000000000e+003  5
SAMPPTS 0
ENDH
BEGH
BNAM "W5"
ID 102
CONT 4
  2.281080000000000e+005      9.913274000000000e+006  2.550000000000000e+003  8
  2.281080000000000e+005      9.913274000000000e+006  2.450000000000000e+003  1
  2.281080000000000e+005      9.913274000000000e+006  1.700000000000000e+003  2
  2.281080000000000e+005      9.913274000000000e+006  1.500000000000000e+003  2
SAMPPTS 0
ENDH
```

Appendix 7: Format of Material File "modelfinal.mat"

```
MAT
MN    1     "kinangop_tuff_or_mau_tuff"
MS    1     0
OPAQ  1     1.000000
MC    1     255   128   192
MN    2     "pre_kinangop_tuff_or_mau_tuff"
MS    2     0
OPAQ  2     1.000000
MC    2     0     128   192
MN    3     "sedimentary_formation"
MS    3     0
OPAQ  3     1.000000
MC    3     255   255   0
MN    4     "limulu_or_gilgil_tranchytes"
MS    4     0
OPAQ  4     1.000000
MC    4     255   0     0
MN    5     "olkaria_pyroclastics_lava_flow_comendites_etc"
MS    5     0
OPAQ  5     1.000000
MC    5     234   182   2
MN    6     "longonot_pyroclastics_lava_flow_comendites_etc"
MS    6     0
OPAQ  6     1.000000
MC    6     128   128   64
MN    7     "pumice_or_lapili"
MS    7     0
OPAQ  7     1.000000
MC    7     128   255   128
MN    8     "kedong_valley_tuff"
MS    8     0
OPAQ  8     1.000000
MC    8     0     128   64
MN    9     "ebburru_pyroclastic_lava_flows_comendites_etc"
MS    9     0
OPAQ  9     1.000000
MC    9     192   192   192
MN    10    "ebburru_tranchytes"
MS    10    0
OPAQ  10    1.000000
MC    10    255   128   128
MN    11    "waterloo_ridge_pyroclastics"
MS    11    0
OPAQ  11    1.000000
MC    11    128   0     0
MN    12    "kijabe_basalts"
MS    12    0
OPAQ  12    1.000000
MC    12    255   0     255
MN    13    "obsidian_ridge"
MS    13    0
OPAQ  13    1.000000
MC    13    0     0     128
```

```
MN    14    "elementaita_and_eburru_basalts"
MS    14    0
OPAQ  14    1.000000
MC    14    128   0     128
MN    15    "water"
MS    15    0
OPAQ  15    1.000000
MC    15    0     0     255
MN    16    "alluvia_deposits"
MS    16    0
OPAQ  16    1.000000
MC    16    250   250   200
```

Appendix 8: Format of Logged wells

```
BHOLE
DSETS 0
BEGH
BNAM "ITC1"
ID 1
WTE 1880.53
CONT 7
213518.00   9924527     1910  1
213518.00   9924527     1908  2
213518.00   9924527     1892  11
213518.00   9924527     1848  2
213518.00   9924527     1840  11
213518.00   9924527     1786  6
213518.00   9924527     1780  6
SAMPPTS 0
ENDH
BEGH
BNAM "ITC147"
ID 2
WTE 1905
CONT 5
213850.00   9921800     1920  1
213850.00   9921800     1918  2
213850.00   9921800     1904  11
213850.00   9921800     1864  6
213850.00   9921800     1860  6
SAMPPTS 0
ENDH
BEGH
BNAM "ITC155"
ID 7
WTE 1872
CONT 5
213700      9920850     1895  1
213700      9920850     1893  6
213700      9920850     1871  5
213700      9920850     1825  4
213700      9920850     1805  4
SAMPPTS 0
ENDH
BEGH
BNAM "ITC191T"
ID 8
WTE 1910
CONT 5
213940.00   9921486     1920  1
213940.00   9921486     1918  2
213940.00   9921486     1905  11
213940.00   9921486     1883  6
213940.00   9921486     1880  6
SAMPPTS 0
ENDH
```

```
BEGH
BNAM "ITC151"
ID 12
WTE 1866.23
CONT 4
212675.00   9918025     1886.9      1
212675.00   9918025     1884.0      11
212675.00   9918025     1808.9      7
212675.00   9918025     1785.9      7
SAMPPTS 0
ENDH
BEGH
BNAM "ITC149"
ID 13
WTE 1929
CONT 9
217150      9918100     2023.5      1
217150      9918100     2020.5      2
217150      9918100     2009.5      5
217150      9918100     2000.5      8
217150      9918100     1989.0      7
217150      9918100     1926.0      5
217150      9918100     1893.0      6
217150      9918100     1867.0      11
217150      9918100     1847.0      11
SAMPPTS 0
ENDH
BEGH
BNAM "pt18"
ID 14
WTE 1888
CONT 5
212545.00   991852      1888.00     10
212545.00   991852      1886.82     11
212545.00   991852      1826.82     7
212545.00   991852      1821.82     6
212545.00   991852      1816.82     6
SAMPPTS 0
EN
```

Annex

Annex 1: Steps Followed in Generation of Topographic and Geologic Profiles

1. Segment map "section2" was created. With the aide of the DEM of the study area, 10 segments were digitized on the screen.

2. These were then separated into individual 10 segment maps each with one segment through a masking process using the script shown below.

Different sections of enlarged study area.

sec1:=SegmentMapMask(Section2,"sec1")
sec2:=SegmentMapMask(Section2,"sec2")
sec3:=SegmentMapMask(Section2,"sec3")
sec4:=SegmentMapMask(Section2,"sec4")
sec5:=SegmentMapMask(Section2,"sec5")
sec6:=SegmentMapMask(Section2,"sec6")
sec7:=SegmentMapMask(Section2,"sec7")
sec8:=SegmentMapMask(Section2,"sec8")
sec9:=SegmentMapMask(Section2,"sec9")
sec10:=SegmentMapMask(Section2,"sec10")

3. Four georeferences were created, isane, isanw, isase and isasw so as resample the dem into portions of sizes comparable to those of the individual segments.

4. The DEM was then resampled using georeferences created in 3 above to have areas of sizes comparable to the sizes of the segment maps. To effect this, the script shown below was created

Resampling and hence enlarging the DEM

isademne:=MapResample(try3, isane, BiCubic)
isademnw:=MapResample(try3, isahnw, BiCubic)
isademse:=MapResample(try3, isase, BiCubic)
isademsw:=MapResample(try3, isasw, BiCubic)

5. The geological Map was also resampled using georeferences created in 3 above so as to have areas corresponding to the segment in size. To effect this, the script shown below was created

Resampling and hence enlarging the Geological Map

isageolne:=MapResample(geo2, isane, NearestNeighbour)
isageolnw:=MapResample(geo2, isahnw, NearestNeighbour)
isageolse:=MapResample(geo2, isase, NearestNeighbour)
isageolsw:=MapResample(geo2, isasw, NearestNeighbour)

6. The segments were then rasterized using the georeferences of the area in which the fall. To effect this, the script shown below was created

Rasterization of Segments

secr1:=MapRasterizeSegment(sec1,isahnw)
secr2:=MapRasterizeSegment(sec2,isahnw)
secr3:=MapRasterizeSegment(sec3,isane)
secr4:=MapRasterizeSegment(sec4,isane)
secr5:=MapRasterizeSegment(sec5,isane)
secr6:=MapRasterizeSegment(sec6,isase)
secr7:=MapRasterizeSegment(sec7,isasw)
secr8:=MapRasterizeSegment(sec8,isasw)
secr9:=MapRasterizeSegment(sec9,isane)
secr10:=MapRasterizeSegment(sec10,isase)

7. Map calculation was performed so as to DEM for the individual segments.Each individual pixel of the rasterized segments now has an altitude valvue attributed to it.. To effect this, the script shown below was created

Mapcalculations to get altitude values attributed to the section segments. To effect this, the script shown below was created

secdm1:=ifnotundef(secr1,isademnw)
secdm2:=ifnotundef(secr2,isademnw)
secdm3:=ifnotundef(secr3,isademne)
secdm4:=ifnotundef(secr4,isademne)
secdm5:=ifnotundef(secr5,isademne)
secdm6:=ifnotundef(secr6,isademse)
secdm7:=ifnotundef(secr7,isademsw)
secdm8:=ifnotundef(secr8,isademsw)
secdm9:=ifnotundef(secr9,isademne)
secdm10:=ifnotundef(secr10,isademse)

8. The Dem sections were then vectorised to get point maps.

Vectorization of the dem section into point maps

secpt1:=PointMapFromRas(secdm1)
secpt2:=PointMapFromRas(secdm2)
secpt3:=PointMapFromRas(secdm3)
secpt4:=PointMapFromRas(secdm4)
secpt5:=PointMapFromRas(secdm5)
secpt6:=PointMapFromRas(secdm6)

secpt7:=PointMapFromRas(secdm7)
secpt8:=PointMapFromRas(secdm8)
secpt9:=PointMapFromRas(secdm9)
secpt10:=PointMapFromRas(secdm10)

9. Map calculation was performed so as to get the geology for the individual segments. Each individual pixel of the rasterized segments now has an altitude valvue attributed to it. To effect this, the script shown below was created

Mapcalculations to get geology type attributed to the section segments.

secgeol1:=ifnotundef(secr1,isageolnw)
secgeol2:=ifnotundef(secr2,isageolnw)
secgeol3:=ifnotundef(secr3,isageolne)
secgeol4:=ifnotundef(secr4,isageolne)
secgeol5:=ifnotundef(secr5,isageolne)
secgeol6:=ifnotundef(secr6,isageolse)
secgeol7:=ifnotundef(secr7,isageolsw)
secgeol8:=ifnotundef(secr8,isageolsw)
secgeol9:=ifnotundef(secr9,isageolne)
secgeol10:=ifnotundef(secr10,isageolse)

10. The geology sections were then vectorised to get point maps from the geology rasterized section.

Vectorization of the geology rasterized sections into point maps

secgeolpt1:=PointMapFromRas(secgeol1)
secgeolpt2:=PointMapFromRas(secgeol2)
secgeolpt3:=PointMapFromRas(secgeol3)
secgeolpt4:=PointMapFromRas(secgeol4)
secgeolpt5:=PointMapFromRas(secgeol5)
secgeolpt6:=PointMapFromRas(secgeol6)
secgeolpt7:=PointMapFromRas(secgeol7)
secgeolpt8:=PointMapFromRas(secgeol8)
secgeolpt9:=PointMapFromRas(secgeol9)
secgeolpt10:=PointMapFromRas(secgeol10)